CHARACTERIZATION OF NOVEL *C. ELEGANS* KAINATE RECEPTORS AND THEIR CONTRIBUTION TO GRADIENT NAVIGATION

by

Jann W. Gardner

A dissertation submitted to the faculty of
The University of Utah
in partial fulfillment of the requirements for the degree of

Doctor of Philosophy

Department of Biology

The University of Utah

August 2013

The University of Utah Graduate School

STATEMENT OF DISSERTATION APPROVAL

The dissertation of **Jann W. Gardner**

has been approved by the following supervisory committee members:

Andres Villu Maricq	, Chair	**6/04/13** Date Approved
Katharine Ullman	, Member	Date Approved
Markus Babst	, Member	**6/13/13** Date Approved
David Blair	, Member	**6/13/13** Date Approved
Erik Jorgensen	, Member	**6/04/13** Date Approved

and by **Neil Vickers** , Chair of the Department of **Biology**

and by Donna M. White, Interim Dean of The Graduate School.

ABSTRACT

Behavior is a complex and poorly understood result of nervous system function. How do molecules, cell, and circuits function in response to sensory input to achieve a behavioral response? This remains a fundamental question in the field of neurobiology. My thesis work addressed this question by undertaking a functional, genetic and electrophysiological analysis of a defined neuronal circuit in the nematode *Caenorhabditis elegans.* The *C. elegans* nervous system functions to allow animals to sense and navigate a wide variety of gradients. Worms use thermotactic behavior to maintain a favorable internal temperature, a fundamental component of worm behavior and survival. Chemotactic behavior is used to sense or avoid various stimuli. We describe the role of glutamate receptors in these circuits and provide insight into the molecular control of circuit function and behavior.

The thermotaxis circuit is a well-defined circuit that directs worm movement in response to previous temperature experiences. One neuronal pair, RIA, functions as the major integrating and decision-making neuron within the circuit. Specific chemotactic behavior shares common circuitry with the

thermotaxis circuit–including RIA. Understanding how RIA functions at the molecular level up to the level of circuit communication is vital to determining how these circuits control behavior. We show the characterization of two classes of glutamate receptors, kainate and AMPA, within RIA and the fundamental differences found at the levels of localization, channel kinetics and behavior during gradient taxis behaviors. Within RIA, the AMPA receptor GLR-1 is expressed at high levels and mediates the majority of glutamate-gated current. Alternatively, kainate receptors–composed of GLR-3 and GLR-6 subunits are expressed exclusively in RIA, show limited expression, and contribute a fraction of the glutamate-gated current. However despite these differences, *glr-1* mutants show only subtle thermotaxis and chemotactic defects while *glr-3, glr-6* mutants are severely impaired. AMPA and kainate receptors also localize to independent synapses in RIA. We show input from upstream neurons common to both circuits signal primarily through kainate receptors at specific synaptic inputs. We took advantage of this unique opportunity to study a highly conserved family of receptors within a single neuron and the behaviors that they regulate.

TABLE OF CONTENTS

ABSTRACT ……..…....iii

LIST OF FIGURES ……..…....viii

ACKNOWLEDGMENTS …… x

Chapters

1. INTRODUCTION ……..…..1

Overview….. ……....1
Behavior and the Nervous System……..……2
Intercellular Signaling Between Cells of the Nervous System…….....3
Vertebrate Excitatory Neurotransmission……..……....6
Vertebrate Ionotropic Glutamate Receptors…….……7
Desensitization of iGluRs…….……11
iGluR Localization and Regulation……..……...14
Vertebrate Kainate iGluRs……17
Systems Neuroscience Approach to Studying Neuronal Circuits…..……19
Factors in Model System Choice in Studying Neurobiology…….…..……20
Caenorhabditis elegans as a Model System…….20
Glutamate Signaling in *C.elegans* Behaviors..……..24
Gradient Behaviors……26
Chemotactic Behavior and Neuronal Circuitry in *C. elegans*…..……26
Thermotactic Behavior…….……....28
Thermotactic Behavior and Neuronal Circuitry in *C. elegans*……..…29
Movement in *C. elegans* and the Function of the Interneuron RIA……32
Significance of Research…….....34
Figures……37
References …….....42

2. NOVEL ROLES FOR KAINATE RECEPTORS IN *C.ELEGANS* GRADIENT NAVIGATION……....49

Abstract ……..……....49
Introduction …….……..50

Results ……..…….53
The interneuron RIA is essential for efficient gradient navigation……..53
RIA expresses multiple classes of glutamate receptors……..……..57
GLR-3 and GLR-6 are sufficient to reconstitute a functional iGluR in *Xenopus* ooctes ……..…...58
GLR-3 and GLR-6 mediate a portion of the fast glutamate gated current in RIA……..……..63
GLR-3, GLR-6 receptors and GLR-1 receptors have distinct expression patterns in the interneuron RIA…..……65
AIZ signaling occurs specifically through GLR-3, GLR-6 receptors…….....66
glr-3, glr-6 and *glr-1* mutants show defect in chemotaxis and warm thermotaxis…….……69
glr-3, glr-6 mutants perform decreased short reversals and increased long reversals during gradient behavior……73
Chemotaxis disruption by the artificial activation of AIZ is blocked by *glr-3* mutants…….……74
AIZ activation signals short reversals through kainate receptors…….……..76
Discussion ……..……..……..……...78
Experimental Procedures ..……..……....84
General methods and strains……84
Deletion alleles……84
Molecular biology……85
Electrophysiology……85
Microscopy……86
Behavioral assays……86
Figures ……..……..……88
References ……..……..……..……...111

3. IDENTIFYING NOVEL KAINATE-SPECIFIC ACCESSORY PROTEINS USING GAIN-OF-FUNCTION RECEPTOR SUBUNITS……114

Abstract……..……..……..114
Introduction……..……..……..115
Results……...……....117
Expression of GLR-6 A/T induces behavioral and neuronal defects ……..……..……..…117
Gain of function mutations in kainate receptor subunits alter channel kinetics……..……..……..…119
Activated kainate receptor suppressor screen……..……...120
sup1 and *sup2* suppress RIA morphological and electrophysiological defects……..……..……..…121
Discussion……..…122

Experimental Procedures……126
General methods and strains……...126
Electrophysiology……...127
Microscopy……..127
Mutagenesis and screening……..127
Behavioral assays……..128
Figures……..……129
References……..…….....136

4. SUMMARY AND CONCLUSIONS……...138

Introduction……138
GLR-3, GLR-6 Channels Function as Kainate Type Receptors..……140
GLR-1 AMPA and GLR-3, GLR-6 Kainate Receptors in RIA are Functionally Different…..……142
Activated Kainate Receptors in the Interneuron RIA……144
Concluding Remarks……...145
References……....……..146

Appendices……147

LIST OF FIGURES

Figure Page

1.1 The chemical synapse……..……...……37

1.2 iGluR subunit topology……..……..…….....38

1.3 Desensitization of ionotropic glutamate receptors and mutations that affect desensitization……..……..……..…..39

1.4 Thermotaxis and Chemotaxis neuronal circuit…….……..…...40

2.1 RIA functions in navigating chemotaxis and thermotaxis gradients……...88

2.2 GLR-3 and GLR-6 are expressed exclusively in RIA and localize to distinct synapses from AMPA receptors……..……..90

2.3 *C. elegans* GLR-3 and GLR-6 are distantly related to vertebrate kainate receptor subunits……..…….....92

2.4 GLR-3, GLR-6 receptors functionally resemble vertebrate kainate receptors... ……94

2.5 GLR-3 and GLR-6 mediate a portion of iGluR in RIA……...96

2.6 AIZ input signals through GLR-3, GLR-6 receptors and modifies short reversal behavior……..…….....97

2.7 *glr-1* and *glr-3, glr-6* show different defects in behavioral taxis……..99

2.8 Model for kainate receptor function during gradient behaviors……101

2.S1 Worms lacking RIA neurons as well as glutamate receptor mutants exhibit normal behavior under baseline conditions……102

2.S2 RIA lacking worms show minor defects in food migration ……104

2.S3 Knockout alleles of *glr-3* and *glr-6* genes……105

2.S4 GLR-3 and GLR-6 mediate a portion of iGluR Current in RIA……106

2.S5 *glr-3, glr-6* mutants show distinct defects from *glr-1* in warm thermotaxis…… ….107

2.S6 Thermotaxis defects in RIA null and *glr-3, glr-6* mutant worms……....108

2.S7 iGluR mutants show defects during taxis behaviors…….....110

3.1 Activating mutations in GLR-6 cause neuronal morphological defects in RIA…….....129

3.2 Gain of function kainate receptors are defective in thermotactic behavior……..……...…...131

3.3 Gain of function mutations in kainate receptor subunits alter channel kinetics……133

3.4 *sup1* mutants suppress activated kainate receptor defects ……..……..134

3.5 *sup1* and *sup2* mutants suppress neuronal morphological defects in RIA…….……..135

A.1 AWC synapses through kainate receptors in RIA……..149

B.1 GLR-6 expression in RIA……153

B.2 GLR-3 expression in RIA……154

B.3 GLR-1 expression in RIA……155

B.4 Co-expression of GLR-6 and GLR-1 in RIA……156

B.5 Analysis of GLR-1 and GLR-6 localization and expression……..157

B.6 Split-GFP puncta between AIZ and GLR-6 subunits……..158

B.7 Split-GFP expression between GLR-1 subunits and AIZ……..…159

ACKNOWLEDGMENTS

I would like to express my great appreciation to my advisor, Dr. A. Villu Maricq, for all his support, encouragement and enthusiasm for both my personal and scientific success. His commitment and dedication to science pushed me to expand my abilities and seek answers to difficult questions. Also, I would like to thank my committee members, Dr. Markus Babst, Dr. Katharine Ullman, Dr. Erik Jorgensen, and Dr. David Blair, for all of their support, encouragement and enthusiasm throughout my graduate career.

I have a great appreciation for the members in the Maricq laboratory, both past and present. Encouragement and helpful suggestions over the years were invaluable for the completion of my graduate work. I would like to thank Jerry Mellem, Penny Brockie, Fred Hörndli, Dave Madsen, Dane Maxfield, Craig Walker, Kathy Phan, and Angy Kallarackal.

Finally, I would like to thank my husband Spencer and our four children for always being there when I needed them and for their never-ending support.

CHAPTER 1

INTRODUCTION

Overview

The survival of an animal is dependent on its ability to incorporate sensory information from the environment and in turn process that information into an appropriate response. Dynamic and complex environments necessitate the ability of an animal to sense and respond quickly and appropriately to many different situations. These types of behavior are mediated by the nervous system. Animals equipped with even the simplest of nervous systems allow for significant advantages in survival and reproductive fitness. The nervous system controls all these types of behaviors, from simple animal responses up to human thought, creativity and memory.

The nervous system facilitates behavior as a function of its components. The basic unit of the nervous system, the neuron, possesses specialized characteristics that are determined by the molecular machinery expressed within each cell. Neurons function together as a network of interconnected cells that respond to stimuli, integrate information, and in response, directly generate behaviors. Understanding the molecular, cellular and circuit components of the

nervous system and how they function together will contribute to a fundamental goal of neuroscience: understanding how behavior is controlled by the nervous system.

Vertebrates, with complicated behaviors and complex nervous systems, have hindered progress in understanding how the nervous system facilitates behavior at the molecular, cellular and circuit levels. Many of these hurdles have been overcome by taking advantage of model organisms such as the soil nematode *C. elegans*. Manipulation of this simple nervous system can be used to uncover how molecules, cells, and neuronal circuits function together to sense and modulate behavior.

The aim of this study was to uncover the molecules, neurons and neuronal circuits that allow *C. elegans* to integrate and respond to distinct types of sensory input. Additionally, we sought to understand how these components function together to achieve behavior. To study this, we have used genetic, molecular and electrophysiological techniques to: 1) characterize *C. elegans* neurons required for gradient behavior responses (temperature and chemosensory); 2) identify and characterize molecules required in these cells for efficient gradient responses; and 3) determine the mechanism by which these molecules affect behavioral responses.

Behavior and the Nervous System

A primary function of the nervous system is to process information from the external environment and direct an appropriate behavioral response. How is

behavior generated from neural activity? What critical underlying molecular and cellular differences exist that regulate and control neuronal responses? Furthermore, how are these responses modified in response to experience and different sensory inputs? Unraveling the answers to these questions remains a daunting task in the study of the nervous system. "Behavior is the result of a complex and ill-understood set of computations performed by nervous systems…" (Brenner et al., 1974). One of the most fundamental questions facing neurobiology today is that of understanding how behavior is generated by the nervous system. The vertebrate brain contains on the order of 10^{11} neurons, with each neuron making thousands of synaptic contacts. These contacts inter-connect neurons into a complex network of neural circuits that collectively function to somehow regulate the thought processes and behavioral abilities of an animal. Within this complex network lie individual circuits, whose function is defined by the contributing neurons as well as the types of connections they make and the specific molecules they express. Thus, understanding the generation of behavior requires a knowledge not only of the circuit components at cellular and molecular levels, but also how those components function to acquire, store, and process information.

Intercellular Signaling Between Cells of the Nervous System

The fundamental idea that neurons function as discrete, individual cells that can transmit information was pioneered by Cajal in the late 19th century and described as the "Neuron Doctrine" (Cajal, 1894). This theory was in stark

contrast to the prevailing ideology, which focused on the idea that the nervous system was composed of a syncytium connected by membranous bridges. The invention of the electron microscope revealed that the anatomy of neurons was in fact made up of distinct individual cells bound by a continuous plasma membrane. Additionally, it was evident that many of these cells have morphological endings that terminated without physically fusing to the neighboring neurons. Instead, they ended in close proximity to the neighboring cell, indicating that the transfer of information to the next cell would require some specialized method. This specialized method was resolved by the discovery of two types of signaling: gap junctions (Furshpan et al., 1959), which provide direct connections that allowed the electrical coupling of the interior of cells, and the discovery of chemical synapses (Palade et al., 1954). In contrast to the direct coupling of gap junctions, the chemical synapse contains a gap, referred to as the synaptic cleft, that separates the presynaptic and postsynaptic cells. This separation prevents the direct passage of current from one cell to another. Electrical activity in presynaptic nerve terminals results in the rapid fusion of synaptic vesicles with the plasma membrane. Consequently, neurotransmitters contained within the synaptic vesicles are released into the synaptic cleft and diffuse across the cleft and bind receptors found on the postsynaptic cell (Figure 1.1).

Neurotransmitter receptors come in varying types, including G-protein coupled receptors and ionotropic receptors. Upon the binding of neurotransmitter to G-protein coupled receptors, activation results in the

regulation of downstream signaling pathways within the cell (Nakanishi et al., 1994). Ionotropic receptors are ligand-gated channels that are found in the plasma membrane of the cell. Ionotropic receptors are typically found in a closed state. However the binding of neurotransmitter to a neurotransmitter receptor results in the activation of the ion channel, inducing a conformational change of the receptor. This change allows the passage of ions through the channel's pore, changing the electrical state of the postsynaptic cell. This change can be either excitatory or inhibitory, depending on the type of neurotransmitter receptor present as well ion selectivity (for review, see Dingledine et al., 1999; Hollmann et al., 1999; Ozawa et al., 1998).

Studies of the neuromuscular junction have contributed much of our understanding of ion channel activation in postsynaptic cells during excitatory neurotransmission (Katz, 1966). Neuromuscular junction synapses are formed between a presynaptic motor neuron and a postsynaptic muscle cell. Excitation of the presynaptic neuron triggers the release of the neurotransmitter acetylcholine (ACh), which diffuses across the synaptic cleft and binds to ACh receptors on the postsynaptic muscle cell. Upon binding, cations flow into the postsynaptic cell through the receptor pore, causing depolarization of the membrane and subsequent calcium entry into the cell. This action drives the contraction of the muscle fiber. Inhibitory synaptic activation is primarily mediated by the neurotransmitters y-aminobutyric acid (GABA) and glycine. Fast inhibition is achieved through the activation of postsynaptic anion channels, which induces the hyperpolarization of the postsynaptic cells.

Vertebrate Excitatory Neurotransmission

The neurotransmitter glutamate mediates the vast majority of fast excitatory neurotransmission in the vertebrate nervous system. The importance of glutamatergic neurotransmission is evident by the range of neurological processes it influences as well as the variety of disorders that arise from improper function. Glutamate receptors play important roles in development, learning and memory (Chen and Tonegawa, 1997). The disruption of glutamate receptor function manifests itself in a variety of neurological disorders including schizophrenia, Parkinson's disease, Alzheimer's disease, and amyotrophic laternal sclerosis (ALS) (Montastruc et al., 1997; Ulas et al., 1994). Neuronal cell death caused by glutamate receptor induced excitotoxicity is also associated with epileptic seizures and ischemic brain damage (Meldrum et al., 1994; Mody et al., 1998).

Studies have revealed that glutamate functions in the CNS via separate receptor pathways. These glutamate-induced pathways are activated by glutamate receptors that can be separated into two categories, defined by the receptor signaling mechanism. Metabotropic glutamate receptors (mGluRs), function as G-protein coupled proteins and regulate downstream cascades and molecules on a slower timescale. Alternatively, ionotropic glutamate receptors (iGluRs) are ligand-gated channels that respond rapidly to glutamate by opening and allowing the passage of ions, resulting in rapid electrical changes (Dingledine et al., 1999; Hollmann et al., 1999; Ozawa et al., 1998).

.

Vertebrate Ionotropic Glutamate Receptors

As part of a highly diverse family of ion channels, vertebrate ionotropic glutamate receptors co-assemble to form functional receptors with highly varying properties. Eighteen iGluR subunits have been identified in the rat. These subunits can be separated into subtypes based on pharmacological and molecular characteristics (Table 1.1). The major division of iGluR subunits separates those that are sensitive to the drug NMDA (N-methyl-D-aspartate) from those that are not. Non-NMDA receptors can be separated further into additional pharmacological classes: those sensitive to α -amino-3-hydroxy-5-methyl-4isoxazole propionic acid (AMPA), those sensitive to kainate (KA), and those that belong to the delta class of iGluRs (reviewed Watkins, 2006; Watkins et al., 2006). Delta receptors are orphan subunits that, while showing molecular identity with other iGluR subunits, fail to respond to known iGluR agonists (Zuo et al., 1997; Mayer et al., 2006; Lomeli et al., 1998; Yamazaki et al., 1992).

Following the identification of the first iGluR cDNA (Lomeli et al., 1993), vertebrate genes encoding iGluRs that fall into each subtype were discovered. Sequence comparisons between the iGluR subunits showed up to 80% similarity as well as the conservation of intron and exon structures (Suchanek et al., 1995; Wenthold et al., 1992). Of the eighteen subunits identified, the NMDA subtype contains seven subunits while there are five in the kainate, four in the AMPA, and two in the delta class (Lipsky et al., 2003).

Despite the high sequence and structure conservation across iGluR subunits, a functional receptor is formed only when subunits from the same class

coassemble to form a ligand-gated ion channel (Puchalski et al., 1994; Ayalon et al., 2001). However despite this limitation, the assembly of receptors using different combinations of subunits provides an extensive range of receptors that differ in kinetics, ion permeability and pharmacological specificity. Posttranscriptional splice variants as well as posttranscriptional RNA editing allow for further molecular diversity among iGluRs (reviewed, Seeburg et al., 1998). Some subunits are also capable of forming homomeric receptors as well as heteromeric receptors, adding additional possible combinations. These mechanisms result in a complex and extensively diverse family of receptors capable of regulating a wide range of neurological functions (reviewed, Dingledine et al., 1999).

iGluRs exist as integral membrane proteins. Their structure is determined by four large subunits, each around 900 residues, which together form an ion channel pore. Based on the high sequence similarly conserved between all known glutamate receptor subunits, all iGluRs are considered to share the same architecture and topology (Figure1.2A). Each receptor subunit contains discrete domains: an extra cellular N-terminal domain, two extra cellular domains, S1 and S2, that form a ligand binding domain involved in agonist binding and receptor desensitization (Sternbach et al., 1994), four hydrophobic transmembrane domains (three true transmembrane domains and a re- entrant loop), and an intracellular C-terminal domain important in receptor clustering and regulation (Daw et al., 2000; Osten et al., 2000). Detailed crystallographic descriptions of glutamate receptors as well as functional and biochemical data show that iGluRs

form as tetrameric channels (Laube et al., 1998; Rosenmund et al., 1998; Armstrong et al., 1998; Armstrong et al., 2000; Sobolevsky et al., 2009). Chimeric experiments performed using AMPA and kainate subunits showed that interactions within the N-terminal domain control the dimerization between subunits of the same subtype. AMPA subunit interactions are dictated by hydrophobic interactions and the kainate subtype by electrostatic interactions (Ayalon et al., 2001; Ayalon et al., 2005). These and single particle electron microscopy images showed data consistent with the mechanism that iGluRs assemble as a dimer of dimers, and thus function as tetrameric channels (reviewed Dingledine et al., 2010; Safferling et al., 2001).

Upon proper assembly and localization of receptors to the post-synaptic site, iGluRs are capable to receive and transduce glutamate-mediated signals from the pre-synaptic cell. Activation and thus opening of the channel requires that one glutamate molecule binds directly to each receptor subunit. A glutamate-binding site is formed in each subunit by two protein domains, S1, an extra-cellular region near the N-terminus, and S2, a domain located in a large extra-cellular loop separated from S1 by M1, the re-entrant loop, and M3. (Figure 1.2A) The binding of glutamate requires the interaction between residues from both S1 and S2 –regions that are highly conserved within the different glutamate subtypes (Armstrong et al., 1998; Stern-Bach et al., 1994). Kainate receptors however do not show full conservation of the residues lining the agonist binding cavity, allowing for subunit selective agonists (Mayer et al., 2005). In order to facilitate ligand binding, the S1 and S2 domains adopt a clamshell-like formation,

with each domain forming half of the clamshell. Within the cleft formed between the two lobes lies the agonist-binding pocket (reviewed Dingledine, 2010). Glutamate binding within the pocket induces a conformational change that results in moving the S1 and S2 domains in closer proximity to one another. However how this conformational change induces channel opening is not well understood. The activation gate blocks the flux of ions while the receptor is in the closed state and therefore is altered upon ligand binding to allow channel opening. The three transmembrane domains M1, M3 and M4 as well as the re-entrant pore are directly coupled to the ligand-binding domain and thus can affect the gating of the receptor. A region of importance for receptor gating was identified due to a spontaneous mouse mutation in the GluD2 iGluR. A single alanine to threonine point mutation in the C-terminal portion of M3 caused mice to experience ataxia and a lurching gait, a behavior leading to the mutant name “lurcher.” This single residue change led to the apoptotic death of cerebellar Purkinje neurons in mice expressing the mutant receptor. Closer analysis of the A/T substitution placed it in the most highly conserved motif (SYTANLAAF) within vertebrate glutamate receptor subunits (Kuner et al., 2003) and rendered the ion channels constitutively active (Zuo et al., 1997). Further studies have shown the M3 segment to be a key determinant of gating in iGluRs (reviewed Dingledine, 2010).

The ion pore of the iGluR is formed by the amino acids from the M2 re-entrant loops that line the inner cavity of the pore. One re-entrant loop is contributed by each of the four subunits to form the pore of the receptor (Figure

1.2B). These amino acids found in the inner cavity of the pore determine the ion selectivity of an iGluR to Na^+, K^+ and in some cases Ca^{2+} ions. While all iGluRs are permeable to Na^+ and K^+, the Ca^{2+} permeability is tightly regulated due to the role of calcium in intracellular signaling. As such, the Ca^{2+} permeability is largely dependent on the subunit composition and on the specific amino acid at the Q/R site located at the mouth of the pore. AMPA and kainate receptor subunits that encode a glutamine (Q) at this site maintain a high permeability to Ca^{2+}. Alternatively, RNA editing can modify this site post-transcriptionally to an arginine (R) residue, resulting in decreased Ca^{2+} permeability (Dingledine et al., 1999; Sommer et al., 1991; Bass et al., 2002).

Desensitization of iGluRs

The closing of the iGluR channel after activation is an essential step in terminating the glutamatergic response. This process can occur in one of two ways. In the event of the agonist becoming dissociated from the receptor, the conformational changes that initially opened the channel can be reversed, restoring the closed, inactive state. Alternatively, the receptor can become desensitized–where an additional conformational change occurs which closes the channel despite the presence of bound glutamate (Figure 1.3A) (Jones et al., 1996). AMPA and kainate receptors desensitize rapidly, achieving more than a 90% decrease in current within 20 ms. In contrast, NMDA receptors desensitize slower and to a lesser extent, with some receptors showing almost no

desensitization (reviewed Dingledine, 2010). Receptor channels can recover from the desensitized state and again become capable of activation. Desensitization of AMPA and kainate receptors occurs upon the continuous application of glutamate. However the kinetic parameters between the two classes of receptors vary considerably. One key difference is the extent of receptor desensitization as a result of agonist activation. For example, the drug kainate, after which the kainate receptor class is named, produces a completely desensitizing current in kainate receptors while AMPA receptors show non-desensitizing currents in response to application (Mott et al., 2009). A second difference that distinguishes AMPA and kainate desensitization kinetics is that of the time course for desensitization recovery. Desensitization in kainate receptors has a time course ~50 times slower than that of AMPA receptors (review Dingledine, 2010). Finally, AMPA and kainate receptors show different sensitivity to allosteric modulators. Differential selectivity by some allosteric modulators allows the discrimination between AMPA and kainate receptor function by modifying the receptor desensitization rate (Sternbach et al., 1998). The drug cyclothiazide effectively blocks the desensitization of a subset of AMPA receptors (Partin et al., 1993; Johansen et al., 1995) but has no effect on the kainate subtype of receptors (Bettler et al., 1995). Conversely, Concanavalin A (ConA) is a plant lectin that effectively blocks the desensitization of kainate receptors by binding to extra-cellular glycosylation sites found in the N-terminal domain, but is much less potent when blocking AMPA receptor desensitization. ConA irreversibly potentiates agonist-evoked currents in kainate receptors by

increasing agonist affinity and reducing receptor desensitization when interacting with the receptor in the non-desensitized state (Everts et al., 1999; Huettner., 1990; Partin et al., 1993; Wong et al., 1994). Thus, the kinetic differences as well as the use of allosteric modulators provide useful information for characterizing and discriminating kainate and AMPA type receptors.

Mutagenesis studies have led to the identification of specific amino acids and domains within iGluR subunits important for desensitization. Site-specific mutagenesis within the ligand-binding domain revealed that the amino acids that contribute to agonist binding are also important for desensitization. Replacement of a specific amino acid (L507Y) located between two residues in a highly conserved region that forms the glutamate-binding site results in a completely nondesensitizing channel in AMPA receptors (Figure 1.3B). Conversely, kainate receptors, which do not express the conserved leucine, show no kinetic difference when the analogous site is mutated. These experiments suggest the site is specific for AMPA desensitization, but not kainate, and remains a key feature difference in non-NMDA receptors (Stern-Bach et al., 1998).

The desensitization of receptors is an integral step in the proper function of iGluRs. This step provides the elimination of receptor signaling in the event that glutamate clearance from the synaptic cleft is not achieved. The accumulation of glutamate may occur in the event of high frequency release, multiple presynaptic inputs at a synapse, or spillover from nearby synapses (Stern-Bach et al., 1998; Trussell et al., 1989; Otis et al., 1996B; reviewed Jones, 1996). Desensitization therefore ensures the proper synaptic signal from a

receptor is achieved. Differential desensitization rates and the rate of receptor recovery from desensitization may determine the extent and duration of the postsynaptic response (Dingledine et al., 1999).

iGluR Localization and Regulation

Within the vertebrate central nervous system, iGluR expression is found in almost all neurons as well as some glial cells. A subset of the peripheral nervous system also shows iGluR expression and function (Petralia et al., 1999). Throughout the vertebrate brain, each iGluR subunit shows a unique pattern of expression as well as varying expression levels. Expression patterns can differ from nearly widespread and abundant, as is the case for some AMPA and NMDA subunits, while others show restricted expression–as in other AMPA and kainate receptor subunits. Some NMDA receptor subunits even show low-level expression found in only one or a few brain structures. The co-expression of receptor subunits within cells suggests the possibility of heteromeric receptors between subunits. However most cells express several receptor class subunits. The postsynaptic response is therefore defined by the iGluR composition expressed within a particular cell and how those iGluRs are arranged at individual synapses.

Due to the high level of iGluR subunit diversity, the iGluR composition of any given neuronal cell could contain a variety of distinct receptors. Neurons are also capable of expressing both excitatory and inhibitory neurotransmitter receptors within in the same cell. Proper positioning of receptors in the post-

synaptic cell is critical to ensure that receptors are located across from functional neurotransmitter release sites. Additionally, controlling the insertion and removal of iGluRs at the synapse can alter the sensitivity of the synapse by adjusting the response to a signal (Bliss et al., 1973). Altering the sensitivity of synaptic neurotransmission is thought to be the underlying mechanism of learning and memory.

To ensure the proper localization of iGluRs, intracellular scaffolding proteins interact with an iGluR to regulate the localization and insertion into the membrane. Intracellular interactions of both NMDA and non-NMDA receptors occur at a consensus PDZ binding motif located at the C-terminal end of the receptors. PDZ domain containing proteins can interact with the iGluR-binding motif via a small protein-protein interaction domain. Several glutamate receptor-associated proteins containing PDZ domains have been identified, including PSD-95 family members, GRIP, and ABP (AMPA receptor-binding protein) (reviewed Tomita et al., 2001; Scannevin et al., 2000). Further studies have shown that insertion or stability of iGluRs in the membrane can be regulated by the interaction with PDZ domain containing proteins (Daw et al., 2000; Osten et al., 2000). These studies suggest that protein levels and their localization to post-synaptic regions function to regulate glutamate receptor localization and insertion specific to the synaptic response required.

In addition to the regulation of localization and insertion of iGluRs via PDZ domain containing proteins, the regulation of iGluR activity by auxiliary molecules has also been discovered. A spontaneous mouse mutation led to the

identification of the first iGluR regulatory transmembrane protein (Sweet et al., 1993). The mutated gene encoded a multitransmembrane protein, stargazin. Recordings from cerebellar granule cells expressing the stargazin mutation revealed a significant loss of AMPA receptor currents, while retaining normal NMDA mediated currents. Stargazin was found to belong to a family of proteins that interact with AMPA receptor subunits, transmembrane AMPA receptor regulatory proteins (TARPS), which direct the proper expression and localization of AMPA iGluRs (Letts et al., 1998; Hashimoto et al., 1999; Chen et al., 2000; Chen et al., 1999B; Schnell et al., 2002) . In addition to the role of TARPS in the localization of AMPA receptors, they were further shown to affect the functional properties of iGluRs. AMPA receptors associated with TARPS showed an increase in single channel conductance, an increase in open probability, increased activation rate, reduced desensitization and a slowed deactivation time course (reviewed Dingledine, 1999; Yamazaki et al., 2004). In response to the activation of glutamate, the effects of TARP regulation on AMPA receptors significantly increase the AMPA receptor current (reviewed Nicoll, 2006).

Recently, accessory proteins for NMDA and kainate receptors have also been discovered. NMDA receptors have been found to interact with the extra-cellular domain of a single transmembrane, C1r/C1sk, Uefg, Bmp1 (CUB) domain containing protein, Neto1 (neuropilin tolloid-like 1). Loss of Neto1 in transgenic mice resulted in the decrease of NMDA receptor expression, leading to impaired LTP, learning and memory (Ng et al., 2009; Zhang et al., 2009). In addition to interacting with NDMA receptors, Neto1 has been shown to modulate

kainate receptor kinetics. Expression of Neto1 enhances glutamate-evoked currents from kainate receptors. A second protein belonging to the same family, Neto2 (neuropilin tolloid-like 2) modulates kainate receptors to a higher degree. Neto2 functions to increase the peak amplitude as well as the open probability and slow the receptors decay time course. Interestingly, Neto2 has been shown to have no impact on the expression of kainate receptors. Rather, kainate receptors enhance Neto2 expression in a dose-dependent manner (reviewed Dingledine, 2010; Zhang et al., 2009).

Vertebrate Kainate iGluRs

Since the cloning of glutamate receptors in the early 1990s, in depth study into the synaptic functions of NMDA and AMPA receptors has provided a strong knowledge base for these types of receptors. Conversely, the physiological roles of kainate receptors have remained elusive and have distinguished themselves as unconventional members of the iGluR family. Distinct from NMDA and AMDA receptors, kainate iGluRs are found to function presynaptically with a crucial role in neurotransmitter release (Pinheiro et al., 2008; Contractor et al., 2008) as well as postsynapitcally in the regulation of activity of synaptic networks (Yue et al., 1995). Kainate receptors have also been found to link to nonconventional metabotropic signaling pathways as well as functioning as conventional iGluRs (Rodriguez-Moreno et al., 1998).

A major discrepancy in the study of kainate receptors is that of vastly different kinetics between heterologously expressed recombinant kainate

receptors and native receptors. *In vitro* recordings show relatively fast kinetics and strong desensitization, similar to AMPA receptors. Conversely, *in vivo* studies reproducibly show slow kinetics as a predominant feature of kainate receptors throughout the CNS (Cossart et al., 1995; Frerking et al., 1998; Bureau et al., 2000; Miyata et al., 2006). Furthermore, the over expression of kainate receptors *in vivo* shows no enhancement of kainate receptor mediated excitatory postsynaptic currents (EPSCs) (reviewed Contractor, 2010). These findings suggest that native kainate receptors may require additional modulatory proteins to achieve proper functionality. The discoveries of vertebrate modulatory proteins that interact with kainate receptors support this hypothesis but do not fully resolve kinetic discrepancies (Ng et al., 2009; Zhang et al., 2009).

The physiological roles of kainate receptors are beginning to emerge as a critical component of vertebrate neurotransmission. Kainate iGluRs are now thought to function as regulators of synaptic networks using diverse mechanisms such as postsynaptic depolarization, presynaptic modulation, enhancement of neuronal excitability, and by the refinement of synaptic strength during development (reviewed Contractor, 2010). Despite the progression of vertebrate kainate receptor understanding, a number of difficult neurobiological questions have remained elusive. The challenge of bridging the gap between a receptor's synaptic mechanism to how the signaling properties contribute to behavior now challenges the field of vertebrate iGluRs.

Systems Neuroscience Approach to Studying Neuronal Circuits

Previous strategies to understanding behavior have focused on identifying and understanding individual elements that contribute to behavior. This includes breaking down a behavior to identify not only the contributing neurons within the neuronal circuit, but also specific proteins and the genes that encode them. However many times these studies focus solely on the single element being studied. In recent years, a new subdiscipline of neurobiology known as Systems Neuroscience has evolved (reviewed Kohl, 2010). This type of study broadly focuses on the analysis of neural circuits as well as how these circuits analyze sensory information, form decisions, and in turn execute appropriate behaviors. Furthermore, it aims to understand the relationship between molecular and cellular levels within a neuronal circuit and how they work together to achieve a behavioral response. Systems Neuroscience aims to understand neural circuits not only on the levels of genes, molecules, cells and circuits, but also to understand how each of these levels function together to achieve behavior. Observations across these different levels provide insight into understanding how molecules and neuronal circuits function to shape complex behaviors.

To fully address behavior using a systems approach, a carefully selected biological problem must be chosen. In order to be successful, both the behavior as well as the scientific system must be amenable to analysis from individual genes up to the neuronal circuits and consequential behavioral output.

Factors in Model System Choice in Studying Neurobiology

The highly complex vertebrate nervous system makes a systems approach to understanding behavior nearly impossible. To get around this, model organisms with vastly simpler nervous systems have been utilized. Each model system comes equipped with its own strengths and weaknesses. Model systems were themselves chosen because of the advantages and opportunities available to scientific research. Thus each problem must be evaluated and a model system chosen that is amenable to the questions being asked. The task of studying any neurobiological problem requires careful selection of not only a model organism that has a simplified nervous system, but also one that is capable of performing tractable behaviors. Additionally, in many animals small perturbations to the nervous system result in lethal or severely detrimental phenotypes. Selection of a model organism capable of not only surviving but also reproducing despite nervous system dysfunction is vital to the successful dissection of neuronal function. Finally genetic, molecular, electrophysiological and behavioral tools must be available to allow for the manipulation and dissection of the nervous system and the subsequesent evaluation of relevant behaviors.

Caenorhabditis elegans as a Model System

As a model system, *C. elegans* provides several significant advantages that aid in breaking down complex questions. Due to its simplicity compared to other multicellular organisms, *C. elegans* was chosen as a model organism by

Sydney Brenner in 1963. As a small roundworm, it possesses not only a simple, condensed nervous system, but is also capable of responding to environmental signals and executing a variety of behaviors. As a simple metazoan species, the adult hermaphrodite is composed of a total of 959 somatic cells, and a bilaterally symmetric nervous system of 302 neurons. Relative to other model systems used in neurobiological studies, the size of the nervous system in *C. elegans* is extraordinarily small, roughly an order or magnitude smaller than Drosophila and vastly smaller than the mouse or rat. Importantly, the nervous system is also made up of different neuronal cell types. Primarily, they can be classified as sensory neurons, interneurons, or motorneurons. However based on morphologies, positions, and cellular connections they make up 118 different neuronal types. Within these 302 neurons, approximately 600 gap junctions and 500 chemical synapses exist that allow either the direct or indirect communication between them, respectively. Additionally, the neuronal lineage and development is largely invariant from animal to animal, making reproducible identification of individual neurons possible. Since the initial use of *C. elegans* by Sydney Brenner as a model organism, large advances in information and techniques have continually increased the usefulness in scientific research. Presently, it is the only animal in which serial section electron microscopy has identified the connections between all neurons in the nervous system (White et al.,1986). Anatomically, this wiring diagram provides not only information regarding neurons that assemble into circuits, but also provides detailed information regarding the inputs and outputs of each neuronal cell.

To understand how neuronal circuits regulate behavior, one must determine the role of individual neurons or groups of neurons. Techniques that enable individual neurons to be identified and killed by a laser microbeam are routinely used to assay the resultant behavioral phenotypes (Bargmann and Avery, 1995). Optogenetic assays have also been implemented in *C. elegans* that allow for the monitoring of neuronal activity as well as manipulating their activity directly using light-activated ion channels. Improved variants of light-activated channels now allow precise temporal control of depolarization. Improved Channelrhodopsin (called ChIEF) accelerates the rate of channel closure over previous versions and exhibits more consistent responses (Lin et al., 2009). Understanding the way in which molecules function within neurons requires ways of directly assaying molecules and their actions. The availability of the complete genomic sequence of *C. elegans* as well as closely related species and mutant genetic sequencing provides genetic mapping, de novo gene prediction and mutant gene identification. Both forward and reverse genetic manipulation within the *C. elegans* genome provides powerful and relatively easy genetic study. Often, disruption of nervous system function or impairment of critical molecules functioning within the nervous system severely impairs the survival and propagation of an animal. *C. elegans*, however, survives as a self-fertilizing hermaphrodite. As such, the worm is capable of surviving and propagating without requiring movement or mating behaviors in order to reproduce. This increases the likelihood of survival despite highly detrimental nervous system defects. While the worm exists primarily as a hermaphrodite,

males can be produced and utilized for cross-fertilization. This aids in genetic manipulation and provides a simple way to achieve specific genetic backgrounds. In addition to direct genetic manipulation, transgenic methods have been developed that allow further manipulation of genes and the nervous system. Genes of interest can be tagged directly using reporter molecules and imaged to identify the protein localization and sites of function. The transparent cuticle of the worm allows imaging to occur directly within the live animal.

In order to effectively study the function of the nervous system and its critical components, methods to access and monitor the electrical response of individual neurons are crucial. Electrophysiological methods have been developed that circumvent the hurdles surrounding neuronal access within the worm (Francis et al., 2003). As an adult, the worm measures only approximately 1 mm in length, with neurons measuring between 1-3μm in diameter. In addition to the overall small size of the worm, methods to penetrate the durable cuticle that forms the exterior of the worm have led to new dissection and electrophysiological techniques. These methods allow neuronal access to be achieved by splitting the cuticle near the neuron of interest where electrical activity can then be monitored (Goodman et al., 1998; Richmond et al., 1999; Richmond et al., 1999B; Francis et al., 2005). The *C. elegans* nervous system spans the length of the worm. However, the largest neuropil (called the nerve ring) resides as a large bundle of many axons that form numerous synapses and is regarded as the central nervous system or brain of the worm.

Electrophysiological procedures have been modified that allow a live worm to be immobilized and a slit made along the anterior portion of the worm. This slit is done proximally to neurons found in the nerve ring and allows electrical access to head neurons. Individual neurons can then be tested for their responses to agonists as well as the effect of mutations on neuronal function (Brockie et al., 2001; Mellem et al., 2002).

C. elegans provides not only a system containing the appropriate behaviors and neuronal circuitry, but also a set of powerful tools that allows the manipulation and in depth study of the nervous system. Thus, *C. elegans* may provide a system in which a comprehensive understanding sensory input and behavioral responses can be achieved.

Glutamate Signaling in *C. elegans* Behaviors

Similar to the vertebrate nervous system, *C. elegans* also requires glutamatergic signaling as a critical component of nervous system function (Brockie et al., 2006). Glutamate signaling is used as the primary excitatory neurotransmitter in invertebrates as well as vertebrates. *C. elegans* also uses two types of glutamate receptors: metabotropic glutamate receptors and ionotropic glutamate receptors. Of the ionotropic glutamate receptors, both inhibitory and excitatory receptors exist in the worm (Brockie et al., 2003). Within its genome, ten genes that encode excitatory iGluR subunits have been identified. These genes are homologous to vertebrate iGluRs and as such can be separated into the vertebrate receptor classes based on pharmacological

properties. Of the 10 receptor subunits, NMR-1 and NMR-2, show the most similarity to the NMDA class of receptors and are the only NMDA-like receptors in the worm. In the non-NMDA classes, the receptor subunits GLR-1-GLR-8 resemble either the AMPA or Kainate classes. Of these, the subunits GLR-1 and GLR-2 are the closest AMPA type receptors, and GLR-3 is the most similar to the Kainate class. The final subunit, GLR-8, is divergent from the other non-NMDA worm subunits (Brockie et al., 2001). Similar to vertebrate glutamate receptors, the large iGluR subunit family found in *C. elegans* provides the potential to express a diverse population of functional receptors.

The expression of GFP-fused iGluR subunits revealed a detailed expression pattern for each of the individual subunits. Distribution for all *C. elegans* subunits is restricted to the animals' nervous system, but with varying and sometimes overlapping patterns of expression. Overlapping expression of receptor subunits suggest that subunits may function together to form heteromeric receptors in these neurons. Two receptor subunits, GLR-3 and GLR-6, exemplify this overlapping expression. These subunits show exclusive expression of both subunits in a single interneuron, RIA, a neuron that functions control movement in response to temperature. GLR-3 and GLR-6 are the only receptor subunits to show exclusive expression to a single neuron, the remaining eight subunits show a broader expression pattern. The non-NMDA receptor subunits GLR-1, GLR-2, GLR-4, and GLR-5 as well as the NMDA subunits NMR-1 and NMR-2 show expression in many of the command interneurons, a set of neurons that control forward and backward movements in the worm. Finally, the

remaining two subunits, GLR-7 and GLR-8, are expressed in neurons in the pharyngeal nervous system, with partially overlapping expression patterns (Hart et al., 1995; Maricq et al., 1995). The wide distribution of iGluRs found in the *C. elegans*. nervous system suggests that homomeric or heteromeric glutamate-gated ion channels may mediate a diverse range of behaviors.

Gradient Behaviors

Animals possessing the simplest of nervous systems up to the complex system found in humans exhibit a variety of behaviors that require the proper navigation of some kind of gradient. These types of behavior require not only proper sensing and interpretation of concentrations or levels of the stimulus, but also appropriate movement and orientation resulting in locating or avoiding the source. These types of navigating behaviors are central to a wide variety of critical behaviors including locating food sources, identifying a mate or seeking out a hospitable environment. Therefore, many species have evolved mechanisms allowing for the detection and orientation to a wide variety of stimuli (Bell, 1991; Schone, 1984).

Chemotactic Behavior and Neuronal Circuitry in *C. elegans*

Chemotaxis in *C. elegans* is the ability to orient and navigate a gradient in response to chemical concentration. Remarkably, this nematode has the ability to detect and discriminate an impressive range of chemical compounds including water-soluble chemicals (i.e., cyclic nucleotides), anions, cations (Cl^-, Na^+, and

K^+), amino acids (lysine and histidine), biotin, basic pH, and volatile chemicals (i.e., aromatic compounds, pyrazines, thiazoles, esters, alcohols, and ketones) (Ward, 1973; Bargmann et al., 1997; 1993; 1991). Within its natural environment, these chemotactic behaviors enable the worm to locate food sources and escape unfavorable environments. In a laboratory setting, these responses can be observed by exposing the animals to a concentration gradient of a substance, and evaluating attractive or repellent movement.

Through a series of laser ablation experiments, the chemosensory neurons required for chemotaxis have been identified. *C. elegans* possesses 32 chemosensory neurons, of 14 different types. Twenty-two of these chemosensory neurons are components of the most complicated sensory organ, located at the tip of the head, the amphid sensilla (White et al., 1986). The ablation of individual chemosensory neurons has demonstrated that most detect either volatile or water-soluble chemicals and either direct attraction or aversion. However, some compounds have been shown to act in an attractive manner at low concentrations and repellent at high levels (Bargmann et al., 1993; Bargmann & Horvitz, 1991; Troemel et al., 1995; 1997). Of the chemosensory neurons, two, AWA and AWC mediate chemotaxis to volatile attractants while AWB neurons mediate volatile avoidance behavior. ADF, ASE, ASG, ASI and ASK have been shown to mediate chemotaxis to water-soluble attractants. Additional chemosensory neurons have been identified having roles in sensing mechanical cues, dauer regulation and dauer suppression (Bargmann & Horvitz, 1991; Schackwitz et al., 1996).

One of the numerous chemotactic behaviors in *C. elegans*, attraction to the volatile odorant diacetyl has proven useful as a tool in the laboratory setting. Diacetyl sensation is mediated by the chemosensory neuron AWA (Bargmann & Horvitz, 1991). In addition to other outputs, AWA synapses heavily onto both the second order neurons AIY and AIZ, two neurons also heavily involved in *C.elegans* thermotactic behavior (see Thermotactic Behavior and Neuronal Circuitry in *C. elegans*) (White et al., 1986). Robust and reproducible attraction to a range of diacetyl concentrations provides an unambiguous behavioral output, useful in the evaluation of nervous system function.

Thermotactic Behavior

Another critical gradient behavior found in all animals is that of maintaining an internal body temperature within physiological range. At extreme levels, both heat and cold can directly damage tissue by compromising cellular integrity as well as denaturing critical cellular components. However outside of extreme levels, even subtle yet suboptimal temperatures can alter biochemical processes. Thus, while cellular integrity is not being immediately compromised, everything from enzymatic reactions to the flow of ions through channels is affected. The optimal temperature range allows the internal biochemistry and physiology of the animal to remain fully functional and also dictates the nature of the environment that an animal can inhabit. This task is accomplished in varying ways across species, and varies dramatically between warm-blooded and cold-blooded animals. Warm-blooded animals, or endotherms, control their internal

temperature homeostasis using changes in physiology, such as regulation of autonomic nervous system functions. Additional regulation uses mechanical means such as sweating or panting (Hensel et al., 1973; Simon et al., 1986). These mechanisms allow endotherms to maintain a constant body temperature independent of the ambient temperature. Conversely, cold-blooded or exothermic animals' body temperature varies with the ambient temperature. This requires behavioral strategies to be used as the primary method for maintaining optimal internal temperatures (Stevenson et al., 1985; Huey et al., 2003). To achieve this, exothermic animals control their exposure to temperature sources as a means of regulating internal body temperature. This behavior, composed of movement toward or away from a particular temperature, is referred to as thermotaxis. The behavior of thermotaxis requires an animal to constantly monitor its current temperature, compare it to the desired temperature, and in turn, execute the proper movements to achieve that temperature. The ability of an animal to maintain its body temperature within a narrow optimum range is not only vital to the overall survival, but also for maximizing fitness in the wild. Critical temperature monitoring and behavioral computations to achieve this are accomplished via the complex processing of the nervous system.

Thermotactic Behavior and Neuronal Circuitry in *C. elegans*

Like other cold-blooded animals, *C. elegans* also performs thermotaxis in an effort to maintain a favorable body temperature. Due to its small mass, and thus small heat capacity, the internal structures of the worm will rapidly

equilibrate to the temperature of the surrounding environment (Stevenson et al., 1985; Heinrich et al., 1993). This rapid equilibrium dictates that behavioral strategies for seeking out and maintaining appropriate environmental temperatures are critical for the animals' body temperature control. *C. elegans* thrives at temperatures ranging from 15 to 25 degrees Celsius, but quickly deteriorates at temperatures outside of this temperature span. Of the many behaviors *C. elegans* is capable of, very few have been studied as in depth as that of thermotaxis. In addition to characterizing the basic temperature-response behavior, the major components of the neuronal circuit have been elucidated and even some critical, individual proteins have been identified.

Early observations of *C. elegans* showed a robust reaction in response to temperature. When animals were cultivated in the presence of food at particular temperature within their physiological range (15-25) and then placed on a temperature gradient, the animals reproducibly migrate to the previous cultivation temperature. Upon reaching or nearing the cultivation temperature, worms track isothermally (Hedgecock et al., 1975; Mori et al., 1995). This temperature pairing also shows plasticity in that a cultivation time of 2-4 hours at a new temperature will reset the worms' temperature preference (Mori et al., 1999). In an effort to identify the neuronal network responsible for thermotactic behavior, ablations of individual and specific subsets of neurons in live animals was performed using a laser microbeam, and the consequential effects on thermotactic behavior evaluated (Mori et al., 1995; Biron et al., 2008). This approach, in conjunction with analysis of thermotaxis defective mutants, led to a proposed neural circuit

responsible for thermotaxis (Figure 1.4). In brief, the environmental temperature is directly sensed by the major thermosensory neuron AFD and to a lesser degree the sensory neuron AWC. Thermal signals from these neurons are transmitted downstream to the interneurons AIY and AIZ, and sent further downstream to the major integrating neuron RIA. Functionally, the circuit can be divided into two halves: cryophilic and thermophilic. Disruption of AFD or AIY signaling results in the migration of worms to temperatures below that of cultivation, known as cryophoilic behavior. Thus the AFD and AIY-mediated pathways drive warm directed movement. Conversely, AIZ defects resulted in worms migrating to temperatures higher than that of cultivation, or thermophilic behavior. AWC defects also result in mild thermophilic defects. Thus, AWC and AIZ-mediated pathways drive cold directed movement. Functionally, RIA connects the two halves of circuit, and when disrupted shows a mixture of both cryophilic and thermophilic behavior. Consequently, RIA integrates signals from AIY and AIZ and transmits the outcome of these neural computations to motorneurons located in the head of the worm. These signals result in the control of the worms' movement by in turn regulating the body wall muscles. Thus, RIA functions to integrate the input from AIY and AIZ and compute the appropriate behavioral output based on experience and the worms current environmental temperature. As such, RIA plays a key role in thermotactic execution.

Movement in *C. elegans* and the Function of the Interneuron RIA

The ability of the worm to properly navigate through its environment requires the integration of environmental information into movement. To achieve this, environmental information is initially sensed directly by sensory neurons before information is relayed into interneurons. Information is integrated by interneurons and the appropriate response further relayed to motor neurons, responsible for dictating the corresponding movement. The RIA interneurons reside in the head of the worm as a bilaterally symmetric pair of cells. Thought to function as a major integrating interneuron in the worm, RIA receives input from a large number of sensory neurons as well as other interneurons. With the exception of synapses in nerve cords used to control body movement, the RIA neurons have the largest number of chemical synapses within the *C. elegans* nervous system. In turn, RIA sends output almost exclusively to the head and neck motor neurons, RMD and SMD, two neurons that function in the movement of the worm. (White et al.,1986)

In addition to the proposed role of RIA in thermotaxis behavior, the role of RIA in general worm movement has also been investigated. Worm movement through a nonaqueous environment is composed of a series of dorsal and ventral body bends, which propel the animal forward in the form of a sinusoidal trajectory. Occasional changes in direction occur by either transient reversals, turning of the head during forward movement, or Ω bends–a reorientation resembling the Greek letter omega, and used by the worm to randomly reorient in a new direction. Typical worm movement is characterized by extended

periods of forward runs, interrupted by reversals and omega turns–resulting in a biased random walk. However, worm movement behavior differs immediately following the removal of a food source. Immediately following the removal of food, worms exhibit a limited local search before dispersing. This behavior is characterized by a high number of reversals and omega turns as well as short forward runs. The ablation of RIA and its primary postsynaptic partners SMD and RMD revealed a role in local search behavior (Gray et al., 2005). Loss of RIA results in a minor decrease in reversal frequency. The loss of the SMD neurons resulted in a reduction in the frequency of Ω turns and the loss of either the SMD or RMD neurons increased the worms' reversal frequency. The movement defects resulting in the loss of RIA and its postsynaptic partners suggest that this neuronal circuit may function in regulation of reversals and turns involved in worm taxis. However, the role of RIA during gradient behaviors remains unknown.

Gradient behavior requires worm taxis to be modified in such a way that it enables the worm to bias its movement. Lengthening runs in the correct direction and decreasing runs in the inappropriate direction achieve a worm's bias toward or away from a stimulus. Decreasing runs occur by disrupting forward movement by a reversal, or more typically, a pirouette (a bout of turns including reversals and Ω turns). Analysis during water-soluble attraction showed that the frequency of pirouettes occurred more often as the chemoattractant concentration decreased compared to increasing or no change in concentration (Pierce-Shimomura et al., 1999). Reversals function as an effective way for rapid

reorientation. Reversal length can be used to distinguish short reversals from long reversals. Long reversals have been defined as backward movement comprised of three or more head swings (Gray et al., 2005). An additional movement strategy, known as the weathervane strategy, demonstrates that animals also gradually curve during forward movement to higher concentrations of an attractant (Iino & Yoshida, 2009).

Significance of Research

The aim of this study was to comprehensively understand how a specific behavior is controlled by the nervous system: from molecules to neuronal circuits to behavior. This work utilized the relatively simple nervous system and powerful tools *C. elegans* offers as a model organism to understand how a worm's behavioral response to stimuli is mediated differentially through ionotropic glutamate receptors. To truly dissect the role of specific iGluRs in response to sensory behavior, this work took advantage of the well-studied gradient behaviors of thermotaxis and chemotaxis and focused specifically on the major integrating interneuron RIA.

This work describes the study of thermotactic and chemotactic behavior at the level of cells and molecules. The expression of kainate receptor subunits, GLR-3 and GLR-6, is found exclusively in the interneuron RIA. In addition to the exclusive expression of these two subunits, they are the only kainate class subunits expressed in *C.elegans*. We took advantage of the unique expression of *glr-3* and *glr-6* to investigate how kainate receptors modulate cell, circuit, and

whole animal behavior–an outstanding problem in the field of neuroscience. Here we show that in addition to kainate receptors, the interneuron RIA also expresses GLR-1 AMPA type receptors. This is the first example of AMPA and kainate channels functioning within a single neuron in *C. elegans*. This expression allows the study of individual receptor localization as well as differential function within the same neuron. We show GLR-1 AMPA receptors are found at many more synapses throughout the neuronal process compared to those containing GLR-3, GLR-6 heteromeric channels, and those synapses appear to be distinct from one another.

To understand the role of AMPA and kainite receptors in RIA, we performed electrophysiological recordings from both heterologous cells and native, *in vivo* RIA cells. The reconstitution of GLR-3 and GLR-6 receptor subunits in a heterologous system revealed that unlike GLR-1 AMPA channels, GLR-3 and GLR-6 did not require auxiliary subunits for expression. However, a functional iGluR channel did require the expression of both GLR-3 and GLR-6 subunits. This work shows for the first time the reconstitution of an invertebrate kainate type receptor in a heterologous system. Here, we also show the first *in vivo* electrophysiological recordings of the interneuron RIA, and the current contributions from AMPA and kainate receptor populations. By generating *glr-3* and *glr-6* deletion alleles, we found that similar to the differences in receptor expression, AMPA receptors mediate the vast majority of glutamate-gated current within RIA while kainate receptors contribute only a small fraction of

current. However this fractional current yields major and specific defects in gradient behavior distinct from perturbation of AMPA-type receptors.

RIA plays a critical role in the gradient behaviors of the worm. Here we show the differential roles of GLR-1 and GLR-3, GLR-6 receptors in the ability of the worm to migrate to warm temperatures as well as chemotax to a known attractant. We show that neither AMPA nor kainate receptors in RIA affect temperature sensation or chemical sensing, but rather modulate the movement of the worm as it migrates up a temperature or chemical gradient. Furthermore, we show the synaptic input of upstream thermotactic and chemotactic neurons specifically through kainate, but not AMPA, receptors.

Together this work provides insight into the role of kainate receptors as modulators of finely tuned behavior, an area of kainate receptor function presently unknown in vertebrates. Additionally, this work focuses on the genes *glr-3* and *glr-6* and shows how their gene products form functional heteromeric receptors that work differentially from AMPA receptors to mediate gradient navigation. These findings provide insight into the function of kainate and AMPA receptors and will aid in further understanding how a nervous system functions to control an animal's behavior.

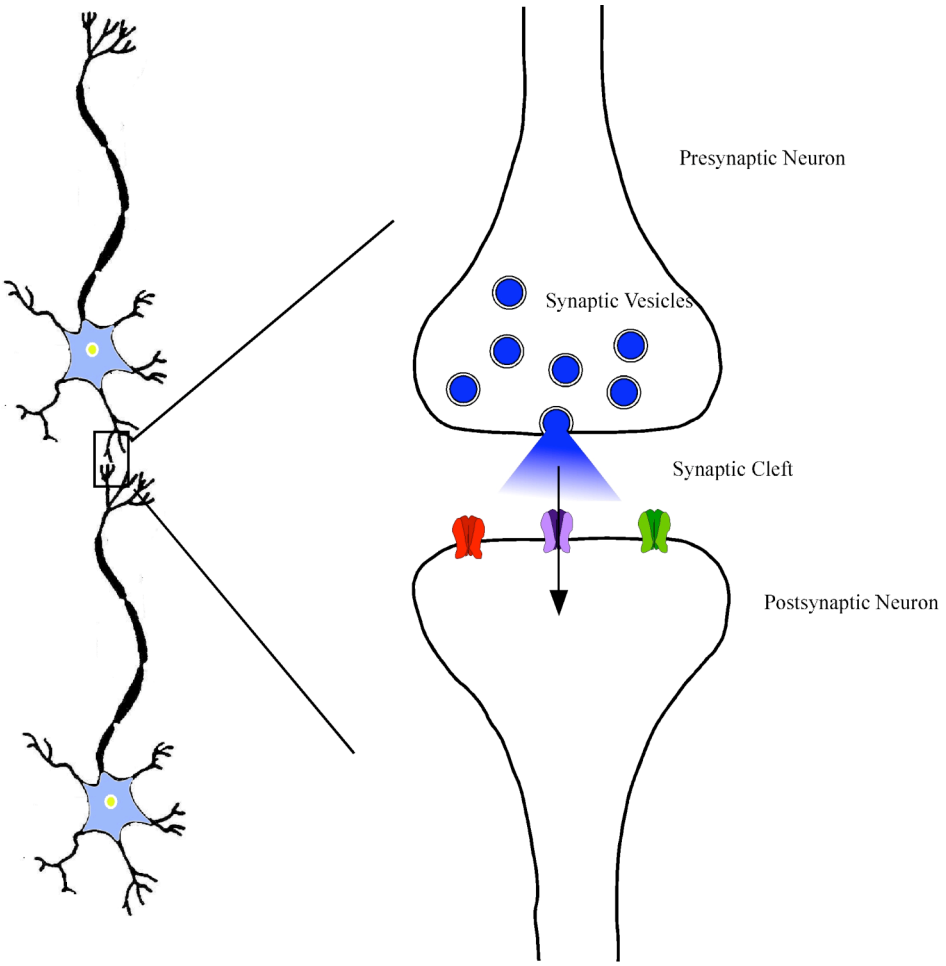

Figure 1.1 The chemical synapse. Figure showing two neurons forming a synaptic contact. Boxed region shows a blown up view of the synapse. Depolarization of the presynaptic neuron triggers neurotransmitter filled vesicles to fuse with the presynaptic plasma membrane releasing the neurotransmitter. Neurotransmitter diffuses across the synaptic cleft where it binds to receptors located in the postsynaptic membrane. Upon binding, postsynaptic receptors undergo a conformational change resulting in ion flow into the postsynaptic cell. During excitatory neurotransmission, cations flow into the postsynaptic cell causing depolarization of the cell membrane. Inhibitory neurotransmission results from the flow of anions into the postsynaptic cell, hyperpolarizing the membrane.

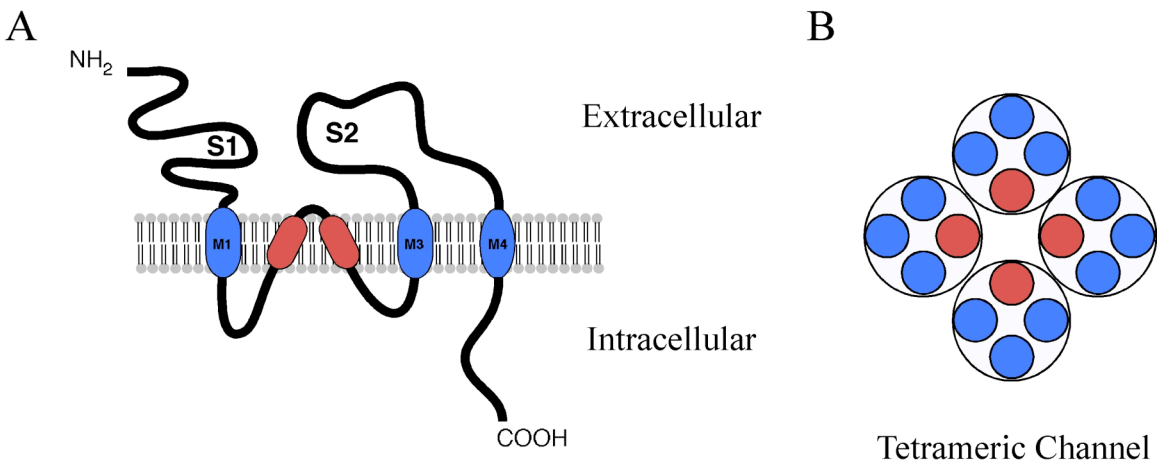

Figure 1.2 iGluR subunit topology. A) Ionotropic glutamate receptor subunits contain three transmembrane domains(blue) and a re-entrant loop(red). The binding site for glutamate is formed by the S1 domain in the extra-cellular N-terminus and S2 domain in the extracellular loop between M3 and M4. B) The channel is formed by a tetrameric assembly of subunits with the re-entrant loop lining the pore of the receptor (top view).

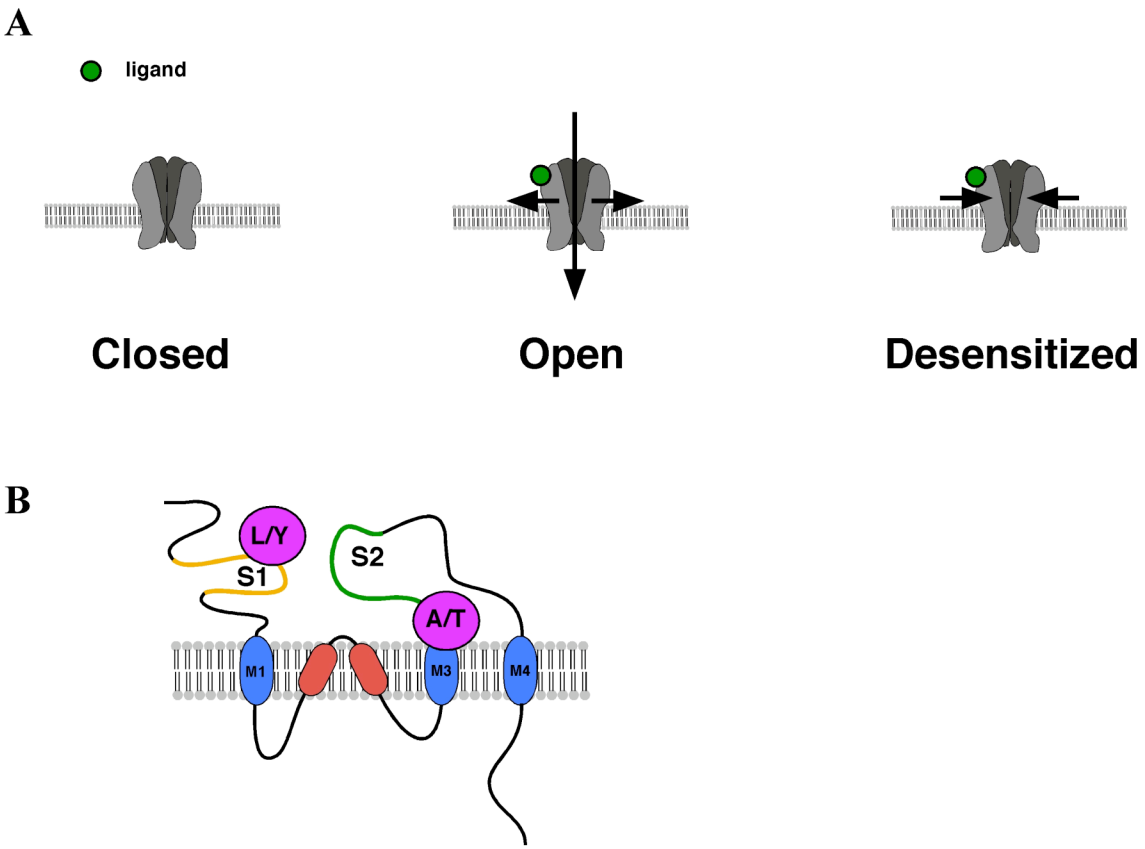

Figure 1.3 Desensitization of ionotropic glutamate receptors and mutations that affect desensitzation. A) The binding of ligand (green) to a closed receptor causes a conformational change, opening the receptor and allowing ions to flow through. The receptor rapidly closes in the presence of ligand entering a desensitized state. Removal of the ligand returns the receptor to the closed state, available for activation. B) Mutations effecting desensitization. A L to Y mutation within the S1 ligand binding domain and an A to T mutation near M3 drastically alter receptor desensitization.

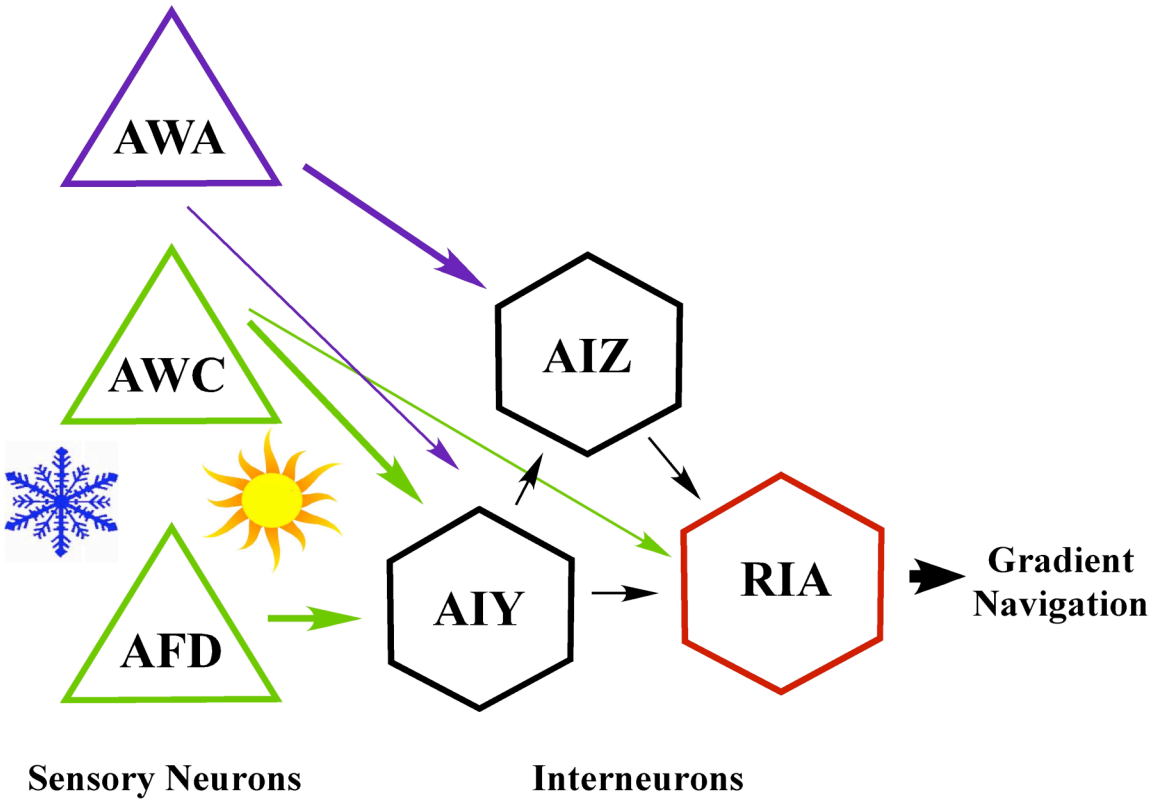

Figure 1.4 Thermotaxis and chemotaxis neuronal circuit. Temperature information is sensed by AFD and to a lesser degree AWC and is transmitted to the AIY and AIZ interneurons. Information is further relayed to the interneuron RIA and integrated into motor output. Chemotaxis to diacetyl is sensed by the chemosensory neuron AWA. Chemotaxis uses common interneurons AIY, AIZ and potentially RIA. Arrows indicate chemical synapses. Large arrows indicate a larger synaptic input. Purple arrows show chemosensory outputs; green arrows indicate thermosensory output.

Table 1.1 Vertebrate Ionotropic Glutamate Receptor Subunits

Family	Subunit
NMDA	GluN1
	GluN2A
	GluN2B
	GluN2C
	GluN2D
	GluN3A
	GluN3B
AMPA	GluA1
	GluA2
	GluA3
	GluA4
Kainate	GluK1
	GluK2
	GluK3
	GluK4
	GluK5
	GluK6
Delta	GluD1
	GluD2

References

A., Lee, L. M. & Ziff, E. B. (2000) *Neuron* 27, 313-25.

Ames, G. F. (1986) *Annu Rev Biochem* 55, 397-425.

Armstrong, N. & Gouaux, E. (2000) *Neuron* 28, 165-81.

Armstrong, N., Sun, Y., Chen, G. Q. & Gouaux, E. (1998) *Nature* 395, 913-7.

Armstrong, N., Sun, Y., Chen, G. Q. & Gouaux, E. (1998) *Nature* 395, 913-7.

Ayalon, G. & Stern-Bach, Y. (2001) *Neuron* 31, 103-13.

Ayalon, G., Segev, E., Elgavish, S. & Stern-Bach, Y. (2005) *J Biol Chem* 280, 15053-60.

Bargmann, C.I. & Horvitz, H.R. (1991) *Science*. 251:1243-46.

Bargmann, C.I. & Horvitz, H.R. (1991) *Neuron.* 7:729-42.

Bargmann, C.I., Hartwieg, E., Horvitz, H.R. (1993) *Cell* 74:515-27.

Bargmann, C.I., & Avery, L. (1995) *Methods in Cell Biololgy* 48 (Academic Press, San Diego).

Bargmann, C.I. & Mori, I. (1997) *C. elegans II*. Cold Spring Harbor NY: Cold Spring Harbor Lab Press. pp.717-37.

Bartlett, F.S, Mori, Y., Campbell, K.P., & Frankel, W.N. (1998) *Nat Genet* 19, 340-347.

Bass, B.L. (2002) *Annu Rev Biochem* 71, 817-846.

Bell, W.J. (1991) *Searching Behavior: The Behavioral Ecology of Finding Resources.* Chapman and Hall.

Bettler, B. & Mulle, C. (1995) *Neuropharmacology* 34, 123-39.

Biron, D., Wasserman, S., Thomas, J.H., Samuel, A.D., & Sengupta, P. (2008) *Proc Natl Acad Sci USA* 105, 11002-11007.

Bliss, T. V. & Lomo, T. (1973) *J Physiol* 232, 331-56.

Brenner, S. (1974) *Genetics* 77, 71-94.

Brockie, P. J. M., A. V. (2006) in *WormBook, ed.* (The C.elegans Research Community, WormBook 10.1895.

Brockie, P. J., Madsen, D. M., Zheng, Y., Mellem, J. & Maricq, A. V. (2001) *J Neurosci* 21, 1510-22.

Brockie, P. J., Mellem, J. E., Hills, T., Madsen, D. M. & Maricq, A. V. (2001) *Neuron* 31, 617-30.

Bureau, I. et al. (2000) *Proc Natl Acad Sci USA* 97, 6838-6843.

Cajal, S.R. (1984) *Proc R Soc (London)* 55, 444-68.

Chen, C., & Tonegawa, S. (1997) *Annu Rev Neurosci* 20, 157-84.

Chen, L., Bao, S., Qiao, X. & Thompson, R. F. (1999) *Proc Natl Acad Sci U S A* 96.

Chen, P. E. & Wyllie, D. J. (2006) *Br J Pharmacol*.

Collingridge, G. L. & Isaac, J. T. (2000) *Neuron* 28, 873-86.

Contractor, A. & Swanson, G.T. (2008) *The Glutamate Receptors.* Humana Press.

Contractor, A., Mulle, C., & Swanson, G.T. (2011) *Trends Neurosci* 1-10.

Cossart, R. et al. (1998) *Nat Neurosci* 1, 470-478.

Daw, M. I., Chittajallu, R., Bortolotto, Z. A., Dev, K. K., Duprat, F., Henley, J. M.,

Dingledine, R., Borges, K., Bowie, D. & Traynelis, S. F. (1999) *Pharmacol Rev* 51, 7-61.

Everts, I., Petroski, R., Kizelsztein, P., Teichberg, V. I., Heinemann, S. F. & Hollmann, M. (1999) *J Neurosci* 19, 916-27.

Francis, M. M., Evans, S. P., Jensen, M., Madsen, D. M., Mancuso, J., Norman, K. R. & A.V. Maricq. (2005) *Neuron* 46(4): 581-594.

Francis, M. M., Mellem, J. E. & Maricq, A. V. (2003) *Trends Neurosci* 26, 90-9.

Frerking, M., et al. (1998) *Nat Neurosci* 1, 479-486.

Furshpan, E. J. & Potter, D. D. (1959) *J. Physiol* 145, 289–325.

Goodman, M. B., Hall, D. H., Avery, L. & Lockery, S. R. (1998) *Neuron* 20, 763-72.

Gray, J.M., Hill, J.J., Bargmann, C.I. (2005) *Proc Natl Acad Sci USA* 102, 3184-91.

Hart, A. C., Sims, S. & Kaplan, J. M. (1995) *Nature* 378, 82-5.

Hedgecock, E. M. & Russell, R. L. (1975) *Proc Natl Acad Sci U S A* 72, 4061-5.

Heinrich, B. (1993) *The Hot-blooded Insects.* Harvard University Press, Cambridge, MA.

Hensel, H. (1973) *Physiol Rev* 53, 948-1017.

Hogner, A., Kastrup, J. S., Jin, R., Liljefors, T., Mayer, M. L., Egebjerg, J., Larsen, I. K. & Gouaux, E. (2002) *J Mol Biol* 322, 93-109.

Huettner, J.E. (1990) *Neuron* 5, 255-266.

Huey, R.B., Hertz, P.E., Sinervo, B. (2003) *Am Nat* 161, 357-366.

Iino, Y. & Yoshida, K. (2009) *J Neurosci.* 17:5370-5380.

Jin, R., Banke, T. G., Mayer, M. L., Traynelis, S. F. & Gouaux, E. (2003) *Nat Neurosci* 6, 803-10.

Johansen, T. H., Chaudhary, A. & Verdoorn, T. A. (1995) *Mol Pharmacol* 48, 946-55.

Jones, M. V. & Westbrook, G. L. (1996) *Trends Neurosci* 19, 96-101.

K. (2004) *Neurosci Res* 50, 369-374.

Kalia, L.V., Joo, D., McKerlie, C. (2009) *PLoS Biol* 7, 41.

Katz, B. (1966) *Nerve, Muscle and Synapse* (New York: McGraw-Hill).

Kohl, P., Crampin, E.J., Quinn, T.A., & Noble, D. *Clin Pharm Thera* 88, 25-33.

Kuner, T., Seebur, P.H., & Guy, H.R. (2003) *Trends Neurosci* 26, 27-32.

Kuusinen, A., Arvola, M. & Keinanen, K. (1995) *Embo J* 14, 6327-32.

Laube, B., Kuhse, J. & Betz, H. (1998) *J Neurosci* 18, 2954-61.

Letts, V.A., Felix, R., Biddlecome, G.H., Arikkkath, J., Mahaffey, C.L., Valenzuela, A., Barlett, F.S., Mori, Y., Campbell, K.P., Frankel, W.N. (1998) N*at Genet* 19(4): 340-7.

Lipsky, R. H. & Goldman, D. (2003) *Ann N Y Acad Sci* 1003, 22-35.

Lin, J.Y., Lin, M.Z., Steinbach, P., Tsien, R.Y. (2009) *Biophys J.* 96:1803-14.

Lomeli, H., Sprengel, R., Laurie, D. J., Kohr, G., Herb, A., Seeburg, P. H. & Wisden, W. M. (1999) *J Neurosci* 19, 916-927.

M., Kim, K.S., Straub, C., Burlingame, A.L., Hower, R.J., & Tomita, S. (2009) *Neuron* 61, 385-396.

Maricq, A. V. (2005) *Neuron* 46, 581-94.

Maricq, A. V., Peckol, E., Driscoll, M. & Bargmann, C. I. (1995) *Nature* 378, 78-

Mayer, M. L. (2006) *Nature* 440, 456-62.

Mayer, M.L. (2005) *Neuron* 45, 539-552.

Meldrum, B.S. (1994) *Neurology* 44, S14-23.

Mellem, J. E., Brockie, P. J., Zheng, Y., Madsen, D. M. & Maricq, A. V. (2002) *Neuron* 36, 933-44.

Miyata, M. & Imoto, K. (2006) *J Physiol* 575, 161-174.

Mody, I. (1998) *Int Rev Neurobiol* 42, 199-226.

Montastruc, J.L., Rascol, O., & Senard, J.M. (1997) *Neurosci Biobehav Rev* 21, 477-80.

Mori, I. & Ohshima, Y. (1995) *Nature* 376, 344-8.

Mori, I. (1999) *Annu Rev Genet* 33, 399-422.

Mott, D., Rojas, A., Fisher, J., Dingledine, R.J., & Benveniste, M. (2009) *J Phys* 588, 683-700.

Nakanishi, N., Shneider, N. A. & Axel, R. (1990) *Neuron* 5, 569-81.

Nakanishi, S. (1994) *Neuron* 13, 1031-8.

Ng, D., Pitcher, G.M., Szilard, R.K., Sertie, A., Kanisek, M., Clapcote, S.J., Lipina, T., Kalia, L.V., Joo, D., McKerlie, C., Corez, M., Roder, J.C., Salter, M.W., McInnes, R.R. (2009) *PLos Biol* 24;7(2).

Nicoll, R. A., Tomita, S. & Bredt, D. S. (2006) *Science* 311, 1253-6.

O'Hara, P. J., Sheppard, P. O., Thogersen, H., Venezia, D., Haldeman, B. A., McGrane, V., Houamed, K. M., Thomsen, C., Gilbert, T. L. & Mulvihill, E. R. (1993) *Neuron* 11, 41-52.

Osten, P., Khatri, L., Perez, J. L., Kohr, G., Giese, G., Daly, C., Schulz, T. W., Wensky, A., Lee, L.M., & Ziff, E.B. (2000) *Neuron* 21 1:99.

Otis, T. S., Wu, Y. C. & Trussell, L. O. (1996) *J Neurosci* 16, 1634-44.

Otis, T., Zhang, S. & Trussell, L. O. (1996) *J Neurosci* 16, 7496-504.

Ozawa, S., Kamiya, H., & Tsuzuki, K. (1998) *Prog Neurobiol* 54, 581-618.

Palade, G. E. & Palay, S. L. (1954) *Anat. Rec* 118, 335.

Partin, K. M., Patneau, D. K., Winters, C. A., Mayer, M. L. & Buonanno, A. (1993) *Neuron* 11, 1069-82.

Petralia, R. S., Esteban, J. A., Wang, Y. X., Partridge, J. G., Zhao, H. M., Wenthold, R. J. & Malinow, R. (1999) *Nat Neurosci* 2, 31-6.

Pierce-Shimomura, J.T., Morse, T.M., Lockery, S.R. (1999) *J Neurosci.* 19:9557-69.

Pinheiro, P.S. & Melle, C. (2008) *Nat Rev Neurosci* 9, 423-436.

Puchalski, R. B., Louis, J. C., Brose, N., Traynelis, S. F., Egebjerg, J., Kukekov, V., Quiocho, F. A. & Ledvina, P. S. (1996) *Mol Microbiol* 20, 17-25.

Richmond, J. E. & Jorgensen, E. M. (1999) *Nat Neurosci* 2, 791-7.

Richmond, J. E., Davis, W. S. & Jorgensen, E. M. (1999) *Nat Neurosci* 2, 959-64.

Rodriguez-Moreno, A. & Lerma, J. (1998) *Neuron* 20, 1211-1218.

Rosenmund, C., Stern-Bach, Y. & Stevens, C. F. (1998) *Science* 280, 1596-9.

Safferling, M., Tichelaar, W., Kummerle, G., Jouppila, A., Kuusinen, A., Keinanen, K., & Madden, D.R. (2001) *Biochem* 40, 13948-13953.

Scannevin, R. H. & Huganir, R. L. (2000) *Nat Rev Neurosci* 1, 133-41.

Schackwitz, W.S., Inoue, T., Thomas, J.H. (1996) *Neuron*. 17:719-28.

Schnell, E., Sizemore, M., Karimzadegan, S., Chen, L., Bredt, D. S. & Nicoll, R.A. (2002) *Proc Natl Acad Sci U S A* 99, 13902-7.

Schone, H. (1984). *Spatial Orientation.* Princeton University Press. Princeton, NJ.

Seeburg, P.H., Higuichi, M., & Sprengel, R. (1998) *Brain Res Rev* 26, 217-29.

Simon, E., Pierau, F.K., Taylor, D.C. (1986) *Physiol Rev* 66, 235-300.

Sobolevsky, A.I., Rosconi, M.P., & Gouauz, E. (2009) *Nature* 462, 745-756.

Sommer, B., Kohler, M., Sprengel, R. & Seeburg, P.H. (1991) *Cell* 67, 11-19.

Stern-Bach, Y., Bettler, B., Hartley, M., Sheppard, P.O., O'Hara, P.J., & Heinemann, S.F. (1994) *Neuron* 41:367-378.

Stern-Bach, Y., Bettler, B., Hartley, M., Sheppard, P.O., O'Hara, P.J., & Heinemann, S.F. (2004) *Neuron* 13:1345-57.

Stern-Bach, Y., Russo, S., Neuman, M. & Rosenmund, C. (1998) *Neuron* 21, 907-18.

Stevenson, R.D. (1985) *Am Nat* 126, 362-386.

Suchanek, B., Seeburg, P. H. & Sprengel, R. (1995) *J Biol Chem* 270, 41-4.

Tomita, S., Nicoll, R. A. & Bredt, D. S. (2001) *J Cell Biol* 153, F19-24.

Troemel, E.R., Chou, J.H., Dwyer, N.D., Colbert, H.A., Bargmann, C.I. (1995) *Cell.* 83:207-18

Troemel, E.R., Kimmel, B.E., Bargmann, C.I. (1997) *Cell*. 91:161-69.

Trussell, L. O. & Fischbach, G. D. (1989) *Neuron* 3, 209-18.

Ulas, J., Weihmuller, F.B., Brunner, L.C., Joyce, J.N., Marshall, J.F., & Cotman, C.W. (1994) *J Neurosci* 14:6317-24.

Ward, S. (1973) *Proc.Natl.Acad.Sci. USA* 70:817-21.

Watkins, J. C. & Jane, D. E. (2006) *Br J Pharmacol* 147 Supl 1, S100-8.

Watkins, J. C. (2000) *Biochem. Soc. Trans* 28, 297–310.

Wenthold, R. J., Rogers, S. W., Lin, F., Moran, T. & et al. (1994) *Neuron* 13, 131-47.

Wenthold, R. J., Yokotani, N., Doi, K. & Wada, K. (1992) *J Biol Chem* 267, 501-7.

White, J. G., Southgate, E., Thomson, J. N. & Brenner, S. (1986) *Phil. Trans. R. Soc. Lond.* B 314, 1-340.

Wong, L.A., Mayer, M.L., Jane, D.E., & Watkins, J.C. (1994) *J Neurosci* 14, 3881-3987.

Yamazaki, M., Araki, K., Shibata, A., & Mishina, M. (1992) *Biochem Biophys Res Commun* 183, 886-92.

Yamazaki, M., Ohno-Shosakku, T., Fukaya, M., Kano, M., Watanabe, M., & Sakimure, K. (2004) *Neurosci Res* 50:369-74.

Yue, K. T., MacDonald, J. F., Pekhletski, R. & Hampson, D. R. (1995) *Eur J Pharmacol* 291, 229-35.

Zhang, W., St-Gelais, F., Grabner, C.P., Trinidad, J.C., Sumioka, A., Morimoto-Tomita,M., Kim, K.S., Straug, C., Burlingame, A.L., Howe, J.R. & Tomita, S. (2009) *Neuron* 61:385-396.

Zuo, J., De Jager, P. L., Takahashi, K. A., Jiang, W., Linden, D. J. & Heintz, N. (1997) *Nature* 388, 769-73.

CHAPTER 2

NOVEL ROLES FOR KAINATE RECEPTORS IN *C. ELEGANS* GRADIENT NAVIGATION

Abstract

All animals require the ability to quickly and efficiently navigate different types of gradients. For example, thermotaxis to a physiological temperature stabilizes a cold-blooded animals' internal temperature or chemotaxis to an odorant allows the location of a food source. Efficient navigation in these types of behaviors is crucial for the survival and fitness of an animal. Changes in the movement and navigation can provide an enormous advantage or disadvantage depending on the overall outcome. How a neural circuit computes the environmental information within a gradient and determines an appropriate behavioral response is a major outstanding question in neurobiology. The soil nematode *C. elegans* exhibits a wide variety of taxis behaviors. While neural circuits that contribute to these behaviors have begun to be identified, the molecular mechanisms that regulate circuit function are not well understood. Here we show that two types of gradient behaviors, thermotaxis and chemotaxis, depend on glutamatergic synaptic inputs mediated by the AMPA and kainate classes of ionotropic glutamate receptors (iGluRs). GLR-3 and GLR-6 kainate

and GLR-1 AMPA receptors (AMPARs) are expressed in the RIA pair of interneurons; these interneurons receive inputs from both thermal and chemical sensing circuitry. Deletion mutations in *glr-1*, or in either of the *glr-3* and *glr-6* genes, which are expressed exclusively in RIA, disrupt taxis and eliminate a portion of the glutamate-gated current. Reconstitution studies demonstrate that GLR-3 and GLR-6 form a heteromeric receptor that is gated by kainate or glutamate. We find that AMPARs and kainate receptors have different kinetics, are localized to distinct synapses and have distinct roles in mediating efficient gradient taxis.

Introduction

The ability of an animal to navigate effectively through its environment requires responses to a variety of environmental signals. A wide array of essential behaviors, including locating food sources, seeking out favorable environmental conditions or identifying a mate, all rely on the appropriate integration of sensory signals by the nervous system and navigation along a gradient of those signals. A major outstanding question in neurobiology is that of how the nervous system functions to receive, process, integrate and interpret these sensory signals and in turn generate an appropriate behavior. Complexities within the vertebrate nervous system have hindered the ability to dissect a behavior down not only to the neuronal circuit, but also to the individual cells, synapses and molecules that are required. In recent years, this problem has become more tractable with the realization that organisms with relatively

simple nervous systems can nonetheless sense, discern and navigate a wide repertoire of signals (Bargmann, 1993; Hedgecock, 1975; Mori, 1995). For example, the nematode *C. elegans*, with a nervous system consisting of only 302 neurons, exhibits many complicated behaviors. To achieve this, one could hypothesize that this simple and condensed nervous system has evolved to use individual neurons in a variety of different facets.

A particularly well-studied form of gradient navigation in *C. elegans* is thermotaxis. In this taxis assay, worms placed onto a linear temperature gradient will move to the temperature at which they were previously cultivated (Hedgecock et al., 1975; Mori et al., 1995). Laser ablation studies along with analysis of informative mutants have led to the identification of a core neural circuit for thermotaxis. This circuit contains the AFD and AWC sensory neurons, the second order interneurons AIY and AIZ, and the third-order interneuron RIA (Mori et al., 1995; Biron et al., 2008; Clark et al., 2006; Kuhara et al., 2008). Ablation of a single class of interneuron can lead to cryophilic (AIY), thermophilic (AIZ) or an intermediate phenotype (RIA). Based on electron-microscopic reconstructions, RIA receives synaptic inputs from AWC, AIZ and AIY, and provides outputs to a number of interneurons and motor neurons. These connectivity data are consistent with RIA having an integrative role in thermotaxis. Although there has been considerable progress in the identification of gene products that contribute to the differentiation of neurons in this circuit, far less is known about the molecular mechanisms of circuit function.

Another well-studied gradient behavior in *C.elegans* is that of chemosensory attraction to the volatile odorant, diacetyl. Laser ablation studies have shown the chemosensory neuron AWA to be specific for the sensation of diacetyl and pyrazine, while maintaining normal responses to other odorants (Bargmann et al., 1993). Among other connections, AWA provides synaptic output to both the second order interneurons AIY and AIZ (White et al., 1986). Ablation studies during taxis behaviors has suggested that AIY signals to promote forward movement (suppress reversals) while AIZ functions to trigger reversals (Gray et al*.,* 2005; Wakayabashi et al., 2004 ; Tsalik & Hobert, 2003). These behavioral pathways converge with input into AIY, AIZ and downstream into RIA. This connectivity data is consistent with RIA also playing a functional role in the execution of chemotaxis to diacetyl.

Most central nervous system synapses utilize glutamate as their major excitatory neurotransmitter. Signaling is mediated by activation of different classes of receptors, including iGluRs that are classified by molecular and pharmacological criteria into the AMPA, kainate and NMDA classes (Seeburg et al., 1993; Dingledine et al., 1999; Hollmann et al., 1999). *C. elegans* has proved to be a well-suited model system for the study of iGluRs. A particular focus has been on the GLR-1 AMPAR, which is required for certain avoidance responses. Study of GLR-1 has led to fundamental advances in our understanding of the AMPAR complex, the identity of auxiliary subunits, and the regulation of synaptic localization and receptor turnover (Zheng et al., 1999; 2006; Walker et al.,

2006). Also studied has been the NMDA receptor, but to date, kainate receptors have not been described in *C. elegans* (Brockie et al., 2001).

Here, we show that the bilateral interneuron pair, RIA, is essential in effectively navigating gradient behaviors. Furthermore, this behavior is dependent on the only kainate-type iGluR found in *C. elegans.* We show that two glutamate receptor subunits, *glr-3* and *glr-6,* expressed exclusively in RIA form a heteromeric receptor that shares characteristics with mammalian kainate receptors. These receptors are localized to a small number or RIA synapses and do not colocalize with GLR-1 AMPARs. We have generated deletion mutations in *glr-3* and *glr-6*. These mutants are viable with no overt visible phenotypes; however, they are defective in effectively navigating both thermal and chemical gradients. Interestingly, we find that kainate receptors and AMPARs have distinct kinetics, different ion permeabilities and distinguishable roles in gradient behaviors. Furthermore, we show that the upstream neuron, AIZ, signals specifically through kainate receptors to modulate animal movement up a gradient. Our genetic and electrophysiological analyses indicate that a single neuron selectively uses different classes of iGluRs for information processing.

Results

The interneuron RIA is essential for efficient gradient navigation

One of the most characterized taxis behaviors in *C. elegans,* chemotaxis to diacetyl, is mediated by the chemosensory neuron AWA (Bargmann & Horvitz,1991). Thermotaxis or taxis along a temperature gradient, on the other

hand, requires the thermosensory neuron AFD as the primary temperature sensing neuron, and AWC and as minor, secondary temperature sensing neuron (Mori et al., 1995; Biron et al., 2008). Both behavioral circuits share the downstream interneurons AIY and AIZ. Previous work has demonstrated that AIY functions to signal movement in forward directions (laser ablation experiments exhibit animals with increased reversals and turning), while AIZ stimulates reversals (ablations result in a decreased reversal rate) (Gray et al., 2005; Wakayabashi et al., 2004; Tsalik & Hobert, 2003). Both AIY and AIZ relay information primarily to RIA (White et al., 1986).(Figure 2.1A)

Since RIA is common and central to both sensory circuits one might expect to see severe defects in reversal behaviors when RIA is ablated. Surprisingly, however, previous laser ablation studies revealed only a minor reversal defect in animals lacking RIA (Gray et al., 2005). To test the role of animals lacking RIA neurons, we generated transgenic animals that over-express a caspase to generate cell death specifically in RIA. Examination of a soluble GFP marker coexpressed with the caspase in RIA showed high cell death in transgenic animals (Stetak et al., 2009). Our results confirmed that movement in transgenic animals expressing a caspase in RIA showed no obvious movement defects compared to that of wildtype animals (Supplemental Figure 2.1A). To further examine what role RIA may play in worm behavior, we examined animals lacking RIA on different types of gradients. Based on previous research, we looked at gradient behavior in response to temperature, chemotaxis to diacetyl, and food taxis.

In both warm thermotaxis and chemotaxis to diacetyl, RIA-caspase expressing worms were capable of appropriately navigating the different gradients; however this occurred on a much longer time scale compared to wild type animals. Over the course of an hour, most wildtype worms arrived at either the warm side of the gradient or the attractant. Conversely, animals lacking the interneuron RIA arrived with a statistically slower time course. Half of wildtype worms arrived by 30 minutes compared to worms lacking RIA, in which half of the worms took more than 45 minutes to arrive (Figure 2.1B). Taxis to food was also disrupted, but to a much lesser degree than chemotaxis or thermotaxis (Supplemental Figure 2.2). The ability of animals to arrive at the appropriate stimulus indicated that the worms were still capable of sensing the gradient; however, we hypothesized that perhaps the efficiency in navigating the gradient had been somehow impaired. To further examine the movement of animals during gradient behaviors, we filmed, tracked, and analyzed worm taxis during both chemotaxis and thermotaxis assays using published tracking software (Albreicht et al., 2011). This allowed us to not only track the worm, but to break down the movement into segments of forward runs, pausing, reversals (lacking an omega turn), and a final parameter that looks at the amount of forward time and reversal time overall associated with performing omega turns (termed reverse pirouette and forward pirouette). Visible differences were immediately apparent looking at the movement tracks during both chemotaxis and thermotaxis between wildtype and transgenic worms lacking RIA (Figure 2.1E). Further analysis of the tracks showed that worms lacking RIA spent an increased

amount of time tracking in incorrect directions (Figure 2.1C). Turning and reversal behavior was increased and average forward time was decreased (Figure 2.1D). These findings all indicate that RIA is critical for efficient signal integration and navigation of the gradient. However how RIA functions in this circuit and what molecules it utilizes is unknown. A critical component is to identify the neurotransmitter used within a neural circuit. To uncover important signaling molecules within this pathway, we took advantage of an observation from previous work on the circuitry of these two gradient behaviors.

Mutations in the *eat-4* gene disrupt glutamate-mediated avoidance behaviors (Berger et al., 1998; Lee et al., 1999). *eat-4* encodes a vesicular glutamate transporter, which is required to load glutamate into vesicles in glutamatergic neurons (Lee et al., 1999; Bellocchio et al., 2000). Therefore, *eat-4* mutants are predicted to release no glutamate from presynaptic neurons. It was observed by Yamada et al. (2003) that *eat-4* mutants are also defective in thermotaxis, suggesting that control of thermotaxis uses glutamatergic signaling. Individual chemotaxis behaviors are specifically mediated by individual neurons or groups of neurons (see Introduction). One of the many chemotaxis behaviors, the robust attraction to diacetyl, functions specifically through the chemosensory neuron AWA (Bargmann et al., 2003). An important downstream neuron from AWA, AIZ has also been shown to express *eat-4* (Ohnishi et al., 2011). This along with impaired chemotaxis behavior to diacetyl by *eat-4(ak75)* mutant animals led us to examine the role that glutamate receptors play in taxis behaviors mediated by RIA (Supplementary Figure 2.1B).

RIA expresses multiple classes of glutamate receptors

We previously showed that transgenic worms expressed partial GFP::GLR-3 and GFP::GLR-6 fusion proteins in RIA (Brockie et al., 2001a). Due to the potential importance of the receptor subunits to RIA physiology, we reexamined the distribution pattern using the upstream regions of *glr-3* and *glr-6* to drive expression of the fluorescent proteins GFP and mCherry (Figure 2.2C). We used confocal microscopy to examine GFP and mCherry expression in transgenic worms and found that expression was limited to the single pair of RIA interneurons. Additionally, strains expressing mCherry under the upstream region of the AMPA iGluR *glr*-1 showed overlapping expression with *glr-3::*GFP within RIA (Figure 2.2A). A previous study found that postsynaptic proteins were preferentially localized to the proximal RIA process, whereas presynaptic proteins were localized to the distal process (Colon-Ramos et al., 2007). To determine the subcellular distribution of GLR-6 and GLR-3 we expressed functional full-length GFP or mCherry::receptor fusion proteins in transgenic *glr-3* or *glr-6* mutants (Figure 2.2E,F). We found that GLR-3 and GLR-6 were both found to be expressed predominantly in the proximal portion of RIA. To evaluate the localization of GLR-6 with respect to presynaptic sites, we coexpressed mCherry::GLR-6 and the presynaptic protein RAB-3::GFP in RIA. We observed very little overlap of the two signals: the majority of the GLR-6 puncta were proximal to the region showing RAB-3 expression (Figure 2.2D). The RIA neuron extends a process ventrally to the ventral neuropil before forming a hairpin turn returning to the nerve ring. Fluorescence imaging of the GLR-6 full-length

protein fused to mCherry showed a limited number of discrete puncta in the process leading to the ventral neuropil (Figure 2.2E). This part of the process contains synaptic connections with many sensory neurons including those involved with sensing mechanical touch to the nose, dauer formation, osmotic stimuli, thermotaxis and chemotaxis (White et al., 1986). The number of mCherry puncta that are seen represent a fraction of those present on the RIA process as determined by electron microscopy (White et al., 1986), consistent with only a subset of glutamatergic neurons signaling through GLR-3 and GLR-6 in RIA.

GLR-3 and GLR-6 are sufficient to reconstitute a functional iGluR in *Xenopus* oocytes

As uncharacterized subunits, we sought to evaluate the glutamate receptors composed of the GLR-3 and GLR-6 proteins. From vertebrate literature, AMPA and kainate receptors possess identifying characteristics both structurally and functionally (see Introduction). Sequence analysis suggests *glr-3* and *glr-6* contain a mixture of kainate and AMPA receptor features. The major identifying feature in vertebrates to distinguish between AMPA and kainate subunits is the L/Y residue important for desensitization of the receptor (Stern-Bach et al., 1998). AMPA receptors require a leucine at this position, while vertebrate kainate receptors typically have a tyrosine or alanine. Sequence alignments of GLR-3 and GLR-6 with vertebrate kainate and AMPA receptors revealed that GLR-3 uses a tyrosine residue and GLR-6 an alanine residue

(Figure 2.3B). While this key residue indicates kainate-like characteristics, additional kainate specific residues do not show similar conservation in GLR-3 and GLR-6. It has also been shown that kainate receptors, but not AMPA receptors, have an absolute requirement for external ions to achieve channel activation and proper kinetics (reviewed Bowie, 2010). Several key residues required for ion binding are located in close proximity to one another in kainate subunits but are not conserved in AMPA subunits. One of these residues was identified as the molecular determinant of external cation effects. Vertebrate kainate receptors express a methionine or equivalent residue to confer external cation sensitivity, while AMPA receptors house a positively charge lysine at the homologous position (Paternain et al., 2003). Interestingly, GLR-3 and GLR-6 show conservation at this site with AMPA receptors. GLR-3 and GLR-6 also resemble AMPA residues at two additional sites that contribute to ion binding in kainate receptors (Plested & Mayer, 2007) (Figure 2.3C). The mixture of AMPA and kainate sequence characteristics failed to clearly place GLR-3 and GLR-6 in an iGluR class. Additionally, phylogenetic analysis of *glr-3* and *glr-6* compared to vertebrate NMDA and non-NMDA subunits does not clearly distinguish which subtype they belong to, but places them roughly the same the distance away from AMPA and kainate subunits (Figure 2.3A). Sequence analysis of *C. elegans* subunits *glr-3* and *glr-6* clearly characterizes both as non-NMDA subunits. However, further distinguishing between AMPA and kainate class subunits becomes unclear due to the mixture or absence of identifying features found in vertebrate subunits.

Based on their overlapping expression pattern and sequence similarity, we hypothesized that GLR-3 and GLR-6 form a hetereomeric functional receptor in the worm. To determine if GLR-3 and GLR-6 were sufficient to form a functional channel complex, cDNAs encoding the GLR-3 and GLR-6 were isolated and used to prepare cRNA for injection into *Xenopus laevis* oocytes. GLR-3 or GLR-6 injected alone produced no detectable current (Figure 2.4A). However, co-injection of GLR-3 and GLR-6 followed by application of glutamate resulted in a fast inward current that rapidly desensitized (Figure 2.4A,B).

To determine what type of iGluR GLR-3 and GLR-6 subunits belong to, we performed functional analyses using *in vivo* and *in vitro* methods. Functionally, AMPA and kainate receptors respond differently to various agonists and pharmacological agents (see Introduction). These differences can be useful in functionally identifying what class of receptors GLR-3 and GLR-6 may belong to. Vertebrate AMPA and kainate receptors respond differently to the agonist kainate. While AMPA receptors respond to kainate application, kainate receptors possess a much a higher affinity. Additionally, kainate receptors have a much higher affinity to kainate compared to that of glutamate. Another defining functional feature of kainate receptors is that of the response to Concanavalin A (ConA). Previous work has shown that application of the plant lectin ConA to vertebrate kainate type glutamate receptors causes large increases in peak currents and decreases in desensitization rates (Everts et al., 1999), while having only a small effect on AMPA receptors. Finally, one of the key distinguishing features between the function of AMPA and kainate receptors is the requirement

of TARPS for the trafficking and function of AMPA receptors in vertebrates (reviewed Dingledine, 2010). This feature is conserved in *C. elegans*, where the AMPA receptor GLR-1 requires the accessory subunits SOL-1 and STG-1 for proper function. We took advantage of these defining features to classify GLR-3 and GLR-6 using functional analysis in the heterologous system *Xenopus laevis*.

To determine if GLR-3, GLR-6 heteromeric receptors functioned as AMPA or kainate receptors, we tested the functional properties of the channel in response to kainate application and ConA treatment as well as testing for the requirement of accessory proteins. To establish the sensitivity of the GLR-3, GLR-6 channels to different agonists, we performed dose response experiments to glutamate and kainate. Vertebrate kainate receptors have been shown to have a higher sensitivity to kainate over glutamate and desensitize quickly after activation. However, the sensitivity to the agonist varies somewhat based on the subunit composition of the receptor (reviewed Dingledine, 2010). Dose response experiments indicated that GLR-3, GLR-6 receptors showed a higher sensitivity to kainate than glutamate (Figure 2.4C). Sensitivity levels of GLR-3, GLR-6 channels to glutamate and kainate were similar to the reported levels of vertebrate kainate receptors (reviewed Lerma et al., 2001), suggesting that GLR-3 and GLR-6 subunits may belong to the kainate class of receptor subunits.

Peak response measurements of the GLR-3/GLR-6 channel to increasing glutamate concentrations provided an EC50 measurement of 18+/-2.5uM, similar to the vertebrate Kainate receptor GluK2 EC50 31+/-2.5uM, which forms homomeric channels in ooctyes (Egebjerg et al., 1991). Individual receptor

subunits can influence the ions conducted by the ion channel. In order to better understand the characteristics of the GLR-3/GLR-6 iGluR we analyzed the current response at different holding potentials. Analysis of the current voltage relationship of the GLR-3/GLR-6 iGluR revealed a more positive reversal potential compared with vertebrate GluK2, which reverses near zero millivolts. These results are surprising and may indicate a novel functional difference between GluK2 and GLR-3/GLR-6. To understand the ion permeability of the GLR-3, GLR-6 channel, we performed ion substitution experiments and looked for changes in the current-voltage relationship of the agonist-gated currents. These experiments revealed that the GLR-3, GLR-6 channel is conductive primarily to sodium (Figure 2.4D).

To discern the effect of ConA treatment on GLR-3, GLR-6 receptors, GLR-3/GLR-6 expressing oocytes were treated with ConA, followed by application of glutamate, resulting in a >20 fold increase in peak current. ConA also prevented rapid desensitization (Figure 2.4A,B). ConA sensitivity of GLR-3, GLR-6 receptors further indicated the functional similarity to vertebrate kainate receptors.

Finally, a well-known requirement for the function of AMPA receptors is that of TARPs or auxiliary proteins that aid in the trafficking and function of the receptor. We have previously shown the requirement of SOL-1 and STG-1 in the receptor function of recombinant GLR-1 AMPAR (Zheng et al., 2004; Wang et al., 2008; Walker et al., 2006). The expression of GLR-1, SOL-1 and STG-1 in oocytes results in a rapid inward current with rapid desensitization kinetics, but is

dependent on the expression of all three proteins. To test for the requirement of accessory proteins in GLR-3, GLR-6 receptors, we coinjected oocytes with GLR-3, GLR-6 RNA as well as either SOL-1, STG-1 or a combination of both. Current size in response to glutamate application in each combination of RNAs showed no increase in current compared to that of GLR-3, GLR-6 receptors alone (Figure 2.4 E,F). These results suggest that GLR-3, GLR-6 receptors function alone, independent of known AMPA receptor accessory proteins and in a manner substantially different from that of *C. elegans* AMPA receptor GLR-1. GLR-3, GLR-6 receptors' high affinity for kainate, sensitivity to ConA treatment and the lack of a functional requirement for TARP-like proteins indicates the GLR-3, GLR-6 receptors function in a manner more similar to vertebrate kainate receptors than AMPA receptors.

GLR-3 and GLR-6 mediate a portion of the fast glutamate gated current in RIA

GLR-3 and GLR-6 are both expressed exclusively in RIA and form a functional channel in *Xenopus* oocytes. To determine the contribution of GLR-3 and GLR-6 to channel function *in vivo*, we generated deletion alleles in *glr-3* and *glr-6* by Tc1 insertion and subsequent imprecise excision (*glr-3(ak57)* and *glr-6(ak56),* respectively). In each case, lesions removed significant portions of the open reading frame encoding GLR-3 and GLR-6, including large portions of the N-terminal domain, transmembrane domains one and two, along with the region encoding the pore. As these regions are critical for function, the remaining coding

sequence is not predicted to form a functional subunit (Supplementary Figure 2.3A,B). In wildtype animals, when RIA was voltage clamped at -60mV followed by pressure application of glutamate, a rapid inward current was observed that quickly desensitized during glutamate or kainate application (Figure 2.5A). If GLR-3 and GLR-6 are functioning within RIA, elimination of channel subunit function is predicted to change the response of RIA to glutamate. *glr-3(ak57)* or *glr-6(ak56)* mutant animals did not have a complete loss of response when glutamate was applied, suggesting that there are additional iGluR subunits in RIA. Current was also seen after applying kainate to *glr-6(ak56)* single mutants and *glr-3(ak57); glr-6(ak56)* double mutants, also consistent with an additional channel subtype in RIA (Figure 2.5B; Supplementary Figure 2.4A,B). Another well-characterized iGluR from *C. elegans* is comprised of GLR-1, GLR-2 as well as the required accessory subunits SOL-1, SOL-2 and STG-2 (Hart et al., 1995; Maricq et al., 1995; Mellem et al., 2002; Zheng et al., 2006; 2004). Expression studies have shown that GLR-2 is expressed in RIA (Brockie et al., 2001).

In order for functional GLR-1,GLR-2 heteromeric channels to form, the accessory subunit SOL-1 is required for channel function, and therefore is a good indicator of where GLR-1 is expressed (Zheng et al., 2004). To determine if RIA expresses SOL-1, we expressed SOL-1 under its native promoter. Expression of SOL-1 fused to YFP shows expression in head neurons. When coexpressed with CFP under the control of the *glr-3* promoter a single cell shows expression in a merged image. Electrophysiological recording from *sol-1(ak63)* mutants or directly from *glr-1(ky176)* mutants (Figure 2.5 B,C; Supplementary Figure 2.4

A,B), showed a loss of a large portion of the current when glutamate is applied. The remaining portion of the current, presumably GLR-3,GLR-6 channels, was sensitive to ConA treatment, as is observed in oocytes (Figure 2.5 B,C; Supplementary Figure 2.4 A,B). These currents, although small, were relatively long-lasting when compared to GLR-1 mediated currents. Consistent with GLR-3, GLR-6 mediated current comprising a small portion of the kainate responsive current in RIA, kainate application to *glr-3(ak57); glr-6(ak56)* double mutants and *glr-6(ak56)* single mutants did not reveal a major reduction in peak current amplitude compared to wildtype (compare *glr-3(ak57); glr-6(ak56)* to wildtype in Figure 2.5 B,C; Supplementary Figure 2.4 A,B). Elimination of three subunits (*glr-1*;*glr-3*;*glr-6*) or all four subunits (*glr-1, glr-2, glr-3, glr-6)* removed all kainate-gated current (Figure 2.5 B,C; Supplementary Figure 2.4 A,B). In order to test the hypothesis that GLR-3 and GLR-6 form functional channels in RIA, transgenic expression of genomic fragments that encode *glr-3* and *glr-6* were injected into the triple (*glr-1*; *glr-3*;*glr-6*) mutant. Using these transgenic worms, the application of kainate onto RIA rescued the ConA sensitive current (Figure 2.5 B,C).

GLR-3, GLR-6 receptors and GLR-1 receptors have distinct expression patterns in the interneuron RIA

In vivo and *in vitro* analysis of GLR-3 and GLR-6 subunits suggest that both are required to form a functional iGluR in RIA, and that receptor is functionally distinct from GLR-1 AMPA receptors. Additionally, the expression of

GLR-3 and GLR-6 subunits compared to GLR-1 in RIA appears to be different. To evaluate how different receptor populations localize within a single neuron, we generated transgenic worms that co-expressed in RIA functional full-length mCherry::GLR-6 and GLR-1::GFP (Figure 2.2I). We noted that GLR-1 puncta were also preferentially localized to the proximal portion of the RIA process, but were more numerous than GLR-6 puncta. We did not find significant overlap in the distribution of the fusion proteins, suggesting that they mediated independent synaptic inputs. To determine what upstream neurons may signal through kainate or AMPA receptors, we took advantage of the known circuitry for thermotactic and chemotactic behaviors.

AIZ signaling occurs specifically through GLR-3, GLR-6 receptors

The serial reconstruction of the nervous system has identified the precise synaptic inputs into RIA (White et al., 1986). This provides information regarding not only the neurons that communicate with one another, but also the location of synaptic contact along the neuronal process. Within the thermotaxis neuronal circuit, three neurons-AWC, AIY and AIZ-synapse directly onto RIA. The chemotaxis circuit important for sensing diacetyl utilizes the chemosensory neuron AWA, in addition to AIY and AIZ. AIY has been shown to release the acetylcholine as a neurotransmitter (Altun-Gultekin et al., 2001). Additionally, the *eat-4* gene has no expression detected in AIY neurons, suggesting that AIY does not use glutamate as a neurotransmitter. Alternatively, the neurons AWC and AIZ have both been shown to use glutamate as a neurotransmitter (Noriyuki et

al., 2011) and therefore may function by signaling to RIA through GLR-3, GLR-6 receptors or GLR-1 AMPA receptors. Interestingly, AWC connects to only one of the two RIA neurons, RIA left. Additionally only two synaptic contacts are made, located adjacent to one another in the process immediately coming out of the cell body. In contrast to the limited AWC synaptic inputs, AIZ provides input at seven synaptic sites on RIA left and five on RIA right. AIZ inputs are located primarily within the hairpin of RIA and within the process between the cell body and the hairpin (Figure 2.6A). AIY synapses are found primarily in the same region of the hairpin. Due to the numerous inputs within the concentrated area of the hairpin and the expression of *eat-4*, we focused on synaptic input from AIZ into RIA. To determine whether signaling from AIZ occurs through synapses containing kainate or AMPA receptors, we took advantage of a split-GFP genetic technique (Feinberg et al., 2008). A typical synapse in the CNS is separated by less than 100nm of extra cellular space between the presynaptic and postsynaptic membranes (Feinberg et al., 2008). Transmembrane proteins expressed by the two cells can span the distance between the membranes. By splitting the GFP molecule and directly linking each half to a transmembrane protein, one on each of the pre- and postsynaptic cells, GFP fluorescence can be reconstituted if the two fragments come in close proximity to one another. Thus, by tagging a presynaptic protein in the upstream neuron and a protein of interest in the postsynaptic neuron, we can evaluate whether synaptic contact is formed between the two. The transmembrane protein neuroligin (NLG-1) is located at synapses both presynaptically and postsynaptically in *C. elegans.* We used

NLG-1 (tagged with split-gfp) expressed in AIZ to evaluate what types of receptors in RIA formed synaptic contacts with AIZ. We hypothesized based on the expression of AMPA and kainate receptors in RIA that we would be able to distinguish distinct AIZ inputs into RIA. Two different possibilities exist: AIZ input to RIA is specific to either AMPA or kainate receptors or that signaling occurs through a mixed population of receptors. If signaling were to occur exclusively through one receptor type, GFP reconstitution would only be seen when that receptor type was tagged with split gfp. Conversely, the excluded receptor type would never show GFP fluorescence. If signaling occurs through both receptor types, GFP fluorescence would be reconstituted when both AMPA or kainate receptor subunits were tagged. To distinguish between these two models, we expressed AIZ::NLG-1::split GFP presynaptically and either GLR-6 or GLR-1 tagged directly with complementary fragments of GFP postsynaptically. Additionally, we coexpressed either full length GLR-6 mCherry (with GLR-1 split GFP) or full length GLR-1 (with GLR-6 split GFP). As predicted, a significant number of GFP puncta were seen representing synaptic contacts between RIA and AIZ within the hairpin region (Figure 2.6B). Additional GFP fluorescence could be seen in the distal region of RIA, presumably resulting from presynaptic expression in additional neurons in addition to AIZ. Due to the lack of a cell specific promoter in AIZ, a promoter was used that while expressed elsewhere, none of the additional neurons provided synaptic input near the hairpin region of RIA. Interestingly, GFP fluorescence was only seen in transgenic lines labeling synapses between GLR-6 and AIZ. Extensive evaluation of transgenic lines

labeling synapses between GLR-1 and AIZ never expressed GFP fluorescence (Figure 2.6C). These results suggest that glutamatergic signaling from AIZ is mediated through synapses containing kainate receptors, and signals independently of GLR-1 AMPA receptors.

glr-3;glr-6 and *glr-1* mutants show defects in chemotaxis and warm thermotaxis

The function of RIA within a behavioral neuronal circuit is largely unknown. Additionally, the function of glutamate receptors is just starting to be unraveled. Differences in current, localization, and input into the two types of glutamate receptors expressed by RIA suggest the possibility of different roles within a single neuron. Worms lacking RIA show defects when navigating a chemical or thermal gradient. To evaluate the possibility of different roles for AMPA and kainate receptors in RIA, we examined *glr-1* and *glr-3, glr-6* mutants during un-stimulated movement and in response to chemical or thermal gradients.

GLR-1 AMPA receptors have been shown to function in the command interneurons and are known to regulate forward and backward movement in the worm (Zheng et al., 1999). Loss of *glr-1* receptors results in a longer forward time, leading to fewer reversals than wildtype under unstimulated conditions. However, worm speed of *glr-1* mutants under standard conditions move at a rate comparable to wildtype. Presently no movement or behavioral defects have been reported in response to the loss of the *glr-3* or *glr-6* genes. We examined *glr-3, glr-6* mutants for defects in normal, unstimulated movement as well as in

response to sensory input. The baseline movement of *glr-3, glr-6* mutants showed no difference in either speed or forward movement in the absence of external stimulation (Supplemental Figure 2.1 C,D). Additionally, no obvious defects were seen in osmotic avoidance, chemotaxis to various stimuli, or thermal nociception. These results showed that *glr-3, glr-6* mutants can maintain normal wildtype sensation, and are not required for the sensing of a variety of different behavioral stimuli.

To determine if *glr-3* and *glr-6* functioned within RIA to control thermotaxis, we analyzed mutant animals ability to thermotax on a linear thermal gradient. Single or double mutants of *glr-3(ak57)* and *glr-6(ak56),* when raised on food at 15 or 20^{o}C, showed no difference in their thermal preference compared to wild type worms (Supplemental Figure 2.5A). When worms were raised at 25^{o}C however, single mutants in *glr-3* or *glr-6* or the double mutant *glr-3,glr-6* did not migrate to 25^{o}C. The inability of either single mutant to thermotax properly is consistent with both subunits forming a heteromeric channel required for thermotaxis. Other thermotaxis mutants *ttx-3* (cryophilic) and *ttx-4* (thermophillic) mutants performed as expected (Hobert, et al., 1997; Okochi et al., 2005). Surprisingly however, we found that under these conditions, *glr-1* mutants showed no defects in thermotaxis despite their expression in RIA (Supplemental Figure 2.5B).

To further investigate the thermotaxis defect in *glr-3, glr-6* mutants, we took advantage of recent insights into *C. elegans* thermotaxis. In depth studies focusing on thermotaxis behavior in response to differing thermal gradients have

suggested that shallow gradients (>.5 degrees/cm) provide conditions ideal for warm thermotaxis (Ramot et al., 2008). We took advantage of the relaxed gradient, in contrast to a steeper gradient used in previous assays, to closely analyze the movement of the worm during warm thermotaxis.

Wildtype movement under relaxed conditions consists of a relatively straight trajectory toward the cultivation temperature and a low reversal rate. As expected, *glr-1* mutants were capable of successfully thermotaxing to the warm region of the plate. Unlike assays performed with a steeper gradient however, *glr-1* mutants did show some thermotaxis defects when closer movement analysis was performed. In addition to the longer forward time typically seen in *glr-1* mutants, worms took significantly longer than wildtype worms to migrate across the plate (Figure 2.7B). As expected, *glr-1* mutants showed a longer forward time during thermotaxis. We further examined movement by evaluating worm head angles during thermotaxis. *glr-1* mutant worms showed an increased travel time in directions away from the warm side of the assay plate compared to wildtype. Presumably this defect results from the lack of reversals found in *glr-1* mutants, limiting the reorientations used by wildtype animals to efficiently adjust to the proper direction. We next evaluated the loss of *glr-3* and *glr-6* on a relaxed temperature gradient. Surprisingly, unlike the results seen on a steeper gradient, we found that *glr-3, glr-6* mutant worms were capable of migrating up the gradient to the appropriate temperature. However, close examination using tracking software showed very different movement between *glr-3, glr-6* mutants and wildtype animals (Supplementary Figure 2.6A). Rather than a relatively

straight trajectory up the gradient as seen with wildtype worms, *glr-3,glr-6* mutants spent a considerable amount of time traveling in incorrect directions and performing more turning and reorientation events (Supplementary Figure 2.6). Consequently, there was considerable difference in the total time it took for mutants to travel across the plate. Importantly, we were able to rescue the *glr-3, glr-6* mutant phenotypes by injecting mutant worms with genomic copies of both genes. Rescue experiments support the hypothesis that the defects seen during thermotaxis behavior are the result of the loss of kainate receptors in RIA. These behavioral experiments suggest that *glr-3, glr-6* mutants are capable of sensing a temperature gradient and that kainate and AMPA receptors contribute differently to warm thermotactic behavior.

Disruptions in chemotactic behavior to diacetyl by animals expressing a caspase in RIA and the movement defects seen during thermotaxis video analysis prompted us to perform a similar analysis on iGluR mutants during chemotaxis assays. Surprisingly, we found very similar results between both *glr-1* and *glr-3, glr-6* mutants during chemotaxis assays as we saw in thermotaxis assays. Similar to warm thermotaxis, *glr-1* mutants exhibited a longer arrival time, increased forward time (decreased reversals) and increased movement in erroneous directions (Figure 2.7A,C,D,E). *glr-3, glr-6* mutants also required longer time to navigate up the gradient, but similar to thermotaxis, showed markedly different movement from *glr-1.* Forward time was again significantly shorter compared to wildtype and incorrect movement direction was much more severe than both wildtype and the defect seen in *glr-1* mutants (Figure 2.7C).

Chemotaxis defects were nearly fully rescued in transgenic worms expressing wildtype copies of *glr-3* and *glr-6.* These experiments suggest that *glr-1* and *glr-3, glr-6* function differently from one another in chemotaxis as well as thermotaxis. Additionally, the similar defects between the two types of taxis behavior suggest that RIA is functioning in a similar manner during two different gradient assays to modulate movement on a gradient.

glr-3, glr-6 mutants perform decreased short reversals and increased long reversals during gradient behavior

To further understand how kainate receptors may be contributing to worm navigation, we re-evaluated the animal movement on a gradient. Typical wildtype movement within a gradient is made up of primarily straight runs interspersed with either forward curving and forward omega turns (lacking a reversal) or short reversals coupled to omega turns in order to facilitate quick reorienting of the animal. Short reversals are comprised of less than three head swings as the worm moves backwards and terminates with the worm reorienting in a new direction. These short movements allow the animal to sample the environment and gradient and adjust their course as needed in order to arrive at the proper stimulus. Rarely, wildtype worms will perform longer reversals (three or more head swings moving in the backward direction); however, these events are rare and seem to occur when the worm has deviated considerably from the proper direction. Previous analysis showed an overall increase in reversal behavior, but the analysis failed to separate long and short reversals as individual behaviors.

Reversal analysis during chemotactic behaviors showed that wildtype worms perform short reversals around 1.5 times per minute and very rarely reorient using a long reversal. Interestingly, separation of reversals by length showed that *glr-3, glr-6* actually performs fewer short reversals compared to wildtype. Additionally, the frequency of long reversals was drastically increased (Figure 2.7F). Conversely, *glr-1* mutants performed very few long or short reversals. These results are consistent with previously reported results for *glr-1* behavior, presumably due to the lack of GLR-1 receptors in the command interneurons (the circuit required for controlling forward and backward movement) (Zheng et al., 1999). To further evaluate what role GLR-1 receptors may have in reversal behavior during gradient taxis, we expressed *glr-1* under a promoter that would express GLR-1 receptors in the command interneurons, but not in RIA. We found no significant change in reversal behavior in worms lacking GLR-1 receptors in RIA compared to that of wildtype animals (Figure 2.7F). These results led us to hypothesize a role specific for kainate receptors in RIA in positively regulating short reversals. We further hypothesized a secondary, parallel pathway responsible for the execution of long reversals in which short reversals act to negatively regulate.

Chemotaxis disruption by the artificial activation of AIZ is blocked by *glr-3* mutants

AMPA and kainate receptors exhibit distinctly different defects when navigating behavioral gradients. Additionally, the reconstitution of split GFP

between the presynaptic neuron AIZ and kainate receptors (not AMPA receptors) led us to hypothesize that signaling from AIZ is required for proper navigation and that improper signaling would disrupt gradient behavior. To test this hypothesis, we expressed a channelrhodospin variant, ChIEF, in the AIZ interneurons using a cre-lox expression system to restrict expression to AIZ (Macosko et al., 2009). ChIEF encodes a light activated channel that is functional only in the presence of the cofactor, all-trans retinal. During chemotaxis assays, single test worms-fed all-trans retinal or control worms were exposed to a 500ms pulse of blue light every 20 seconds for the duration of the experiment. As predicted, the artificial activation of AIZ throughout the assay was sufficient to disrupt chemotaxis in wildtype worms (Figure 2.6D,E). Wildtype worms were no longer capable of navigating the gradient and failed to arrive at the stimulus while light flashes were applied. Worms not raised on all-trans retinal performed normally and arrived at the stimulus despite the application of blue light. The reconstitution of split GFP between AIZ and kainate receptors (not AMPA receptors) suggested that signaling from AIZ to RIA occurred specifically through GLR-3, GLR-6 receptors and not GLR-1 AMPA receptors. We predicted that disrupted chemotaxis due to the artificial activation of AIZ would be blocked in the absence of kainate receptors but not in the absence of AMPA receptors. We performed chemotaxis assays on *glr-3* and *glr-1* mutants raised in the presence and absence of all-trans retinal. In response to pulses of blue light, *glr-3* mutants raised with all-trans retinal were still capable of navigating the odorant gradient and arrived at the stimulus during despite light application. Conversely, *glr-1*

mutants behaved in a similar manner to wildtype and when raised in the presence of all-trans retinal, were incapable of navigating the gradient (Figure 2.6D,E). These findings support the hypothesis that AIZ signals presynaptically to RIA specifically through kainate receptors to modulate gradient navigation.

AIZ activation signals short reversals through kainate receptors

The elimination of receptors made of up *glr-3* and *glr-6* subunits in RIA drastically alters the movement of worms on a chemical or thermal gradient. Movement analysis showed that GLR-3, GLR-6 receptors are required for short reversal behavior as the worm navigates a gradient. Additionally, split gfp flurouesnce and artifical activation of AIZ suggest that signaling from AIZ through kainate receptors is critical for efficient gradient navigation. To determine if AIZ signaling is responsible for the activation of short reversals during gradient navigation, we expressed ChIEF in the AIZ neurons in wildtype worms and compared movement in response to blue light under baseline conditions (no chemical or thermal gradient). Previous work suggested that AIZ activation would stimulate the worm to reverse. As predicted, a 500ms pulse of blue light reproducibly triggered a short reversal (less than three head swings) (Figure 2.6F). A known behavioral response in *C.elegans* is the escape response to ultraviolet light and shorter wavelengths of light. Blue light has been shown to trigger the light response, mediated by the LITE-1 gene (Edwards et al*.,* 2008). A typical light avoidance response is acceleration in the presence of light. However, higher intensities of light have been shown occasionally to induce short

reversals (Fred Hordnli, personal communication). Worms exposed to blue light but lacking all trans retinal showed a spontaneous reversal rate in response to light around 20% of the time, presumably due to LITE-1 mediated effects (Figure 2.6F). Occasionally, AIZ activation would trigger a reorientation in the forward direction, either in the form of a large change in orientation or an omega turn. In response to the GFP expression seen between AIZ and GLR-6 receptor subunits, we expressed ChIEF in AIZ neurons in *glr-3* mutants. We found that *glr-3* mutants suppressed the short reversals seen in wildtype worms. Rather than reversing, *glr-3* mutants continued in a forward direction in response to most blue light pulses. Occasional responses included a reorientation in the forward direction (Figure 2.6F). As a control, we chose to look at *glr-1* mutant worms in response to AIZ activation. *glr-1* expression is found throughout the worm and probably functions both upstream and downstream of RIA, as well as within the neuron itself. GLR-1 receptor function within the command interneurons help regulate reversal frequency, thus *glr-1* mutants suppress reversals. As expected, in response to AIZ activation, *glr-1* mutant worms were unable to reverse. Rather, *glr-1* worms responded with a high probability of reorienting in the forward direction (Figure 2.6F). These results suggest that signaling from AIZ through kainate receptors in RIA triggers the short reversal response during gradient navigation.

Discussion

Here we identify two iGluR subunits, GLR-3 and GLR-6, whose expression is limited to a single pair of cells within the animal. We have demonstrated that GLR-1 AMPARs and GLR-3, GLR-6 kainate receptors function within the RIA interneuron; however, they are found localized to distinct synapses and utilize different channel kinetics. These differences may underlie the differential contribution to temperature and chemosensory gradient navigation we observed in *glr-1 vs. glr-3; glr-6* mutants. Cloning the receptor subunit cDNAs and expressing their corresponding cDNA in *Xenopus* oocytes, were sufficient to reconstitute a functional iGluR. This is the first example of members of an invertebrate kainate subtype iGluR being functionally expressed in a heterologus system. The channel is activated by similar agonists as vertebrate channels, is sensitive to Concanvalin A, and does not require accessory proteins for their function. These findings suggest that *glr-3* and *glr-6* subunits belong to the kainate class of receptor subunits and that the mechanisms of activation and desensitization of iGluRs are conserved across evolution.

In both oocytes and worms, reconstitution of a channel from GLR-3 or GLR-6 requires both the GLR-3 and the GLR-6 channel subunit. This result is different from the most closely related vertebrate subunits GluK1 or GluK2, which are capable of forming homomeric complexes (Egebjerg et al., 1993; Swanson et al., 1998). Evidence from *in vivo* recordings of RIA, along with fact that RIA expresses SOL-1, GLR-1, and GLR-2 demonstrates the presence of an additional iGluR in RIA, besides GLR-3 and GLR-6.

The GLR-1 channel complex requires the accessory channel subunit SOL-1 as well as STG-1 to function in ooctyes. These proteins modulate the desensitization properties of the channel. Interestingly, coexpression of STG-1 or SOL-1 with GLR-3, GLR-6 in oocytes does not significantly change observed currents. This implies these proteins either do not interact with the GLR-3, GLR-6 complex, or no longer perform a modulatory role with this iGluR. The observed differences between *in vivo* recordings and reconstitution in oocytes may suggest that there are additional mechanisms that can modulate GLR-3, GLR-6 channel activity.

Interestingly, we also show the localization of AMPA and kainate receptors in RIA to distinct synapses. This is the first report of the differential localization between different types of iGluRs in invertebrates and supports the hypothesis that different iGluRs or iGluR combinations mediate different behaviors. How does an animal with a nervous system of only 302 neurons integrate information and execute such a wide variety of behaviors? Individual neurons must be required to function in many different facets of behavior. This may be accomplished by neurons participating in wide variety of behaviors as well as an individual neuron contributing to different aspects of the same behavior. How a neuron can differentially regulate signals and translate those signals into appropriate behavioral responses lies within the composition of the synapse. The interneuron RIA receives input from nearly every sensory neuron in the worm as well as a number of neurons of unknown function, suggesting a role in a wide variety of worm behaviors. However it is also likely that RIA functions in

multiple aspects of some behaviors. This may be supported by multiple inputs from a single neuron.

Thermotactic neurons AIY, AIZ and AWC signal through multiple synapses onto the two RIA neurons. The removal of RIA through laser ablation results in the disruption of thermotactic behaviors at all temperatures (Mori et al., 1995). Furthermore, the elimination of AIZ and AWC signaling through the deletion of the *eat-4* gene also causes severe thermotactic disruption. Here we show that the elimination of a subset of glutamate receptors from RIA results in the disruption of a portion of the thermotactic behavior. The removal of kainate receptor subunits GLR-3 and GLR-6 from RIA leads to defective thermotactic behavior when migrating up the gradient to warm temperatures.

We have shown that in assays using steeper gradients, *glr-3, glr-6* mutants no longer thermotax to high temperatures. These data could suggest that kainate receptor mutants are defective in sensing an increasing temperature gradient. However, through closer evaluation using a relaxed temperature gradient, we have shown that *glr-3, glr-6* mutants are capable of sensing and migrating up a temperature gradient. Rather*, glr-3, glr-6* mutants display defects in the movement during warm thermotactic migration. Increased amounts of time spent traveling in inappropriate directions as well as a decreased short reversal rate severely affects the time required for *glr-3, glr-6* worms to travel up the gradient. These movement defects suggest that *glr-3, glr-6* may function in error correcting as the worm compares the immediate external temperature with the memory of the cultivation temperature. Failure of the worm to properly calculate

this value could lead to movement defects while migrating up the gradient. Interestingly, the absence of GLR-1 AMPA receptors results in defects seen only under relaxed gradient conditions. However, the defects in *glr-1* mutants are much less severe than in *glr-3, glr-6* mutants, a fact that may have masked *glr-1* defects in assays using steeper gradients. Like *glr-3, glr-6* mutants, worms lacking *glr-1* receptors have an increased travel time up the gradient, however, not to the same extent. *glr-1* mutants worms also exhibit an increased time traveling in incorrect directions, however, do not show the increased reversal rate seen in *glr-3, glr-6* mutant worms. Similarly, *glr-1* and *glr-3, glr-6* mutants show movement defects navigating up a chemical gradient to the attractive volatile odorant, diacetyl. Interestingly, the movement defects for *glr-1* are very similar on both a thermal and a chemical gradient. This holds true for *glr-3, glr-6* movements defects as well. *glr-1* mutants navigate the gradient less efficiently than wildtype with an increased forward movement time while *glr-3,glr-6* mutants exhibit less efficient navigation due to decreased short reversals and increased long reversals. Rescue of GLR-1 receptors in the command interneurons restores the abilitiy of the worm to reverse, but fails to express GLR-1 receptors in RIA. Worms lacking GLR-1 in RIA exhibit wildtype levels of short reversals, suggesting that AMPA receptors are not involved in short reversal reorientation. Similar phenotypes between the two types of taxis behavior suggest that RIA is functioning in a similar fashion to help control reversals and turning behavior during a range of taxis behaviors.

Consistent with distinct behavioral defects of *glr-1* and *glr-3, glr-6* mutants, we show that input from the interneuron AIZ appears distinct. Presynaptic signals from AIZ, providing a significant number of inputs to RIA, show split-GFP expression with GLR-6 receptor subunits but none with tagged GLR-1 subunits. Split-GFP expression with GLR-6 occurred at predicted inputs along the process based on the reconstruction of the nervous system (White et al., 1986). To further identify the role of AIZ signaling through kainate receptors, we expressed the light activated channel, ChIEF, in AIZ. Artificial activation of AIZ during chemotaxis was sufficient to disrupt behavior, causing worms to fail to find the stimulus. AIZ has also been shown to function in promoting reversals and as predicted, activating AIZ by light stimulation triggered a reproducible short reversal in wildtype worms. Interestingly, activating AIZ in a *glr-3* mutant background acted to suppress short reversals and was sufficient to block the chemotaxis defects due to AIZ over-activation. We also examined AIZ stimulation in *glr-1* mutant background. *glr-1* mutants showed reduced reversals in response to light. Rather, they responded by reorienting reproducible in the forward direction, a light induced behavior also seen in wildtype worms though less frequently than reversals. Additionally, *glr-1* mutants failed to block the chemotaxis disruption due to artificial AIZ stimulation.

Based on these results, we hypothesized that AIZ signals through kainate receptors in RIA to trigger short reversals during gradient navigation. We found that kainate receptor knockouts perform short reversals at a much lower frequency compared to wildtype during gradient behaviors. Additionally, a large

increase in long reversals was found to be a prominent movement defect–a movement seen at low frequencies during wildtype taxis behavior. These results led us to hypothesize a modulatory role for kainate receptors during taxis behaviors that is mediated by AIZ input. AIZ provides excitatory input into RIA through GLR-3, GLR-6 receptors. This input is modulated by the cell and under proper conditions, allows for the trigger of a short reversal. During taxis behaviors, these short reversals allows for quick, efficient sampling of the environment leading to rapid reorientation of the worm. Additionally, however, *glr-3, glr-6* mutant worms exhibit increased long reversals. Here, we hypothesize a secondary, parallel pathway that is only revealed in the absence of short reversals. Long reversals occur rarely and appear to function as a secondary method of reorienting the worm. During taxis behavior, the suppression of long reversals may function to promote short reversals, improving the animal's ability to navigate in a timely manner. Long reversals could function at a time when the animal has strayed significantly from the proper direction within the gradient and could act to provide a major reorientation and resetting of navigating the environment. We speculate that in the absence of the required circuitry for short reversals, long reversal behavior becomes the dominant method for reorientation. Expression, current and functional differences, along with distinct behavioral phenotypes, suggest that both AMPA and kainate receptors function in taxis behaviors in the worm; however, each iGluR works in a distinct manner to properly execute efficient gradient navigation.

Experimental Procedures

General methods and strains

All worms were raised at 20^{o}C under standard conditions unless otherwise indicated. Germ line transgenic strains were generated by injection of the lin-15 rescuing clone pJM23(20ng/ul) as a transformation marker (Huang et al., 1994) or co-expression of *egl-20::*yfp. Transgenic lines included the extra chromosomal arrays and integrated arrays:
akEx164, pCSW44-1(glr-3p::GFP); akIs120, pCSW1248 (glr-6p::mCherry::GLR-6); akEx1120, pDM1259 (glr-6p::RAB-3::GFP); akEx1487, pJG101 (str-2p::split gfp 1-10::NLG-1) pJG69 (glr-6p::split gfp11::NLG-1); pDM1239 (glr-6p::GLR-1::GFP); pJG108 (odr2 2bp::split gfp 1-10::NLG-1); DM1991 (odr2-2bp::LoxPstopLoxP::ChiEF::mCherry::SL2::NLS::GFP::unc-54 3' UTR); DM1284 (glr-1p::mCherry); DM1834 (glr-3p::GFP::GLR-3); pDM42 (glr-6p::GFP); DM2063 (ser-2prom2::ncre); pPB140 (nmr-1::GLR-1::GFP)

Deletion alleles

Imprecise excision of Tc1 was used to create *glr-3(ak57)* (Zwaal et al., 1993). The excision event removed approximately 1.7kb of *glr-3*. The strain used to create Tc1 mediated deletions has increased transposition activity due to the presence of *mut-2(r459).* Rescue of phenotypes associated with *mut-2(r459)* was obtained with a cosmid that covers a 100Kb region near *glr-3(ak57)*, though no lesion responsible for *mut-2(r459)* has been reported (John Collins, personal communication). In order to eliminate *mut-2(r459)* from *glr-3(ak57),* genetic

recombinants based on the reported position for *mut-2(r459)* were used to separate *glr-3(ak57)* from the reported position of *mut-2*. Out crossed worms show none of the high rates of spontaneous mutation and high incidence of males associated with *mut-2(r459).* The *glr-6* mutation was created as for *glr-3(ak57).* All deletion mutants were out crossed to wildtype worms at least eight times. Additional mutant alleles consisted of, *glr-1(ky176), eat-4(ky5), glr-2(ak10), ttx-3(ks5), ttx-4(nj1), mut-2(r459).*

Molecular biology

glr-3 promoter constructs include approximately 5 kilobases 5' to the *glr-3* start codon. *glr-3* and *glr-6* cDNA's were isolated by PCR amplification of cDNA prepared from mixed stage *C. elegans*.

Electrophysiology

Oocyte expression plasmids included pSN5(glr-3 cDNA), pSN14(glr-6 cDNA), pDM350 (sol-1 cDNA), pDM654 (stg-1 cDNA), pDM657 (glr-1 cDNA). Oocyte electrophysiology was conducted as described previously (Strutz-Seebohm et al., 2003; Brockie, et al., 2001). Ion substitution experiments were performed using 10mM Hepes, 10mM NaCl, 3mM CaCl2, 10mM KCl (Base solution). Ion concentrations were adjusted 5-fold by adding 50mM KCl, 15mM CaCl2 or 50mM NaCl. *In vivo* electrophysiology of RIA neurons was performed as described (Brockie et al., 2001). Concanavalin A treatment of neurons was

performed by incubating dissected neuron preparations in 20uM ConA (in extracellular saline) for at least 1 minute prior to pressure application of agonists.

Microscopy

All confocal images were acquired using a Nikon Eclipse Ti microscope equipped with a WaveFX-X1 spinning disk confocal system (Quorum Technologies), Photometrics Cascade II EMCCD cameras, and a Nikon 100x 1.49 NA TIRF objective unless otherwise stated. Image acquisition and image analysis were enabled by Metamorph 7.7.9 (Molecular Devices). Worms were mounted on 10% agarose pads with 2 ul of 30 mM Muscimol. Stacks were acquired using single z plane images with 500 ms exposure time for GFP imaging and 750 ms exposure for mCherry.

Behavioral assays

Thermotaxis assays were performed as in (Mori et al., 1995), and quantified by calculating thermotaxis index ((number of worms on the warm side of the plate – worms on cold side of the plate) / total worms). Thermal gradients were set at .9 degrees/cm and .5 degrees/cm. Chemotaxis assays were performed as described (Bargmann et al., 2003). Diacetyl was diluted to a concentration of 1:1000 using ETOH. Worms were imaged at 3 frames/second using a digital video camera. Individual worm tracks were analyzed using published Matlab software (Albrecht et al., 2011). Long and short reversals were scored manually by using digital movies filmed during taxis behavior. Long

reversals (defined by 3 or more head swings) were scored by determining the length of the reversal in time. Three head swings under taxis conditions lasted on average 3 seconds. For quanitifcation purposes, reversals lasting more than 3 seconds were termed as long reversals. Filmed thermotaxis and chemotaxis assays were performed using a minimum of 7 population assays, with 10 to 15 worms per assay. Time course assays were performed using 50 to 75 worms per plate, on 10 assays performed over several days. ChIEF assays were performed using a 500ms pulse of 488 nm blue light at an intensity of 500 mW/mm^2. Worms were raised overnight using 100mM all-trans retinal and filmed using custom Matlab tracking software (courtesy Jason Wang). A minimum of 10 worms per genotype were assayed. Each worm was exposed to a 500 ms pulse of light every twenty seconds for 3 minutes. Statistical significance was determined using ANOVA, or student's *t*-test. Error bars indicate S.E.M.

Figure 2.1 RIA functions in navigating chemotaxis and thermotaxis gradients
A) Neural circuitry for thermotaxis and chemotaxis to diacetyl. AWA senses the volatile attractant diacetyl; AFD and AWC sense thermal gradients. Both circuits share downstream neurons AIY and AIZ that converge on the interneuron RIA. B) Time course for wildtype worms and worms lacking RIA during warm thermotaxis and chemotaxis to diacetyl. C) Representative rose plots during chemotaxis. Worm head angles taken from individual movie frames using computer software. Red x indicates the location of the stimulus. Wildtype worms show directed movement towards the stimulus while worms lacking RIA spend more time in incorrect directions. D) Average forward time for wildtype worms compared to worms lacking RIA during chemotaxis and thermotaxis. Behavior represents a minimum of 7 population assays; error bars represent standard error of the mean. E) Example tracks from wildtype and worms lacking RIA during chemotaxis. Blue hatch represents starting point; tracks follow the worm up the entire gradient.

A

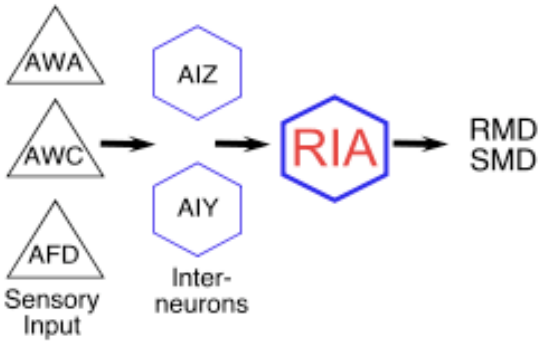
AWA
AWC
AFD
Sensory Input
AIZ
AIY
Inter-neurons
RIA
RMD
SMD

B

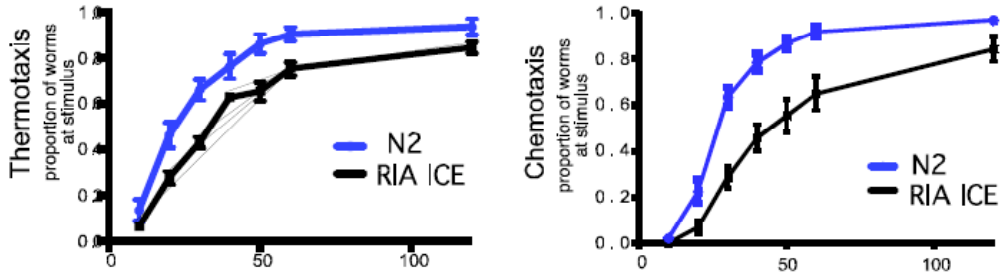
Thermotaxis
proportion of worms at stimulus
N2
RIA ICE
time (minutes)
Chemotaxis
proportion of worms at stimulus
N2
RIA ICE
time (minutes)

C

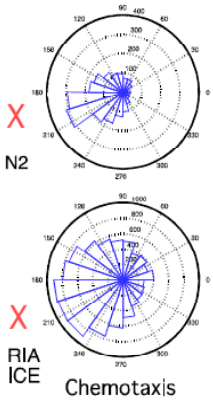
X
N2
X
RIA ICE
Chemotaxis

D

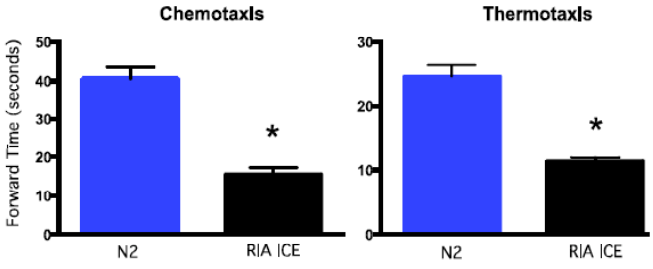
Chemotaxis
Forward Time (seconds)
N2
RIA ICE
Thermotaxis
N2
RIA ICE

E

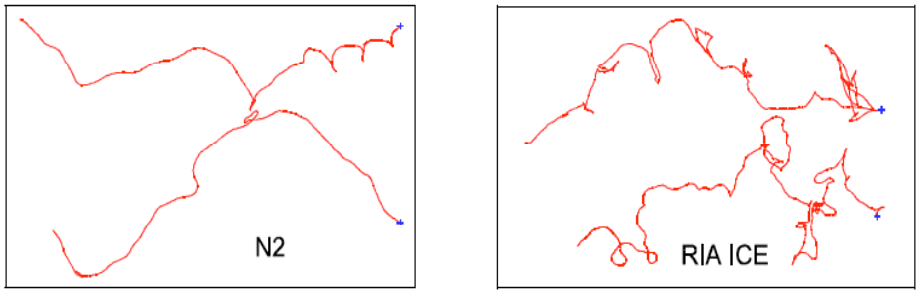
N2
RIA ICE

Figure 2.2 GLR-3 and GLR-6 are expressed exclusively in RIA and localize to distinct synapses from GLR-1 AMPA receptors A) Expression of soluble GFP and mCherry in RIA expressed under GLR-3 and GLR-1 promoters.
Top panel shows full image stack of the nerve ring; lower panels show single plane images of RIA. B) Expression of soluble GFP under the GLR-3 and GLR-6 promoters C) Co-expression of soluble mCherry and GFP under the GLR-3 and GLR-6 promoters. D) Coexpression of full length GLR-6::mCherry and GLR-6::RAB-3. RAB-3 labels the presynaptic region of RIA found distally from the cell body. E) Translational expression of full length GLR-6::mChery::GLR-6 showing limited puncta along the RIA process. F) Translational expression of full length GLR-3::GFP::GLR-3 shows similar puncta compared to GLR-6 expression. G) Translational expression of full length GLR-1 expressed under the GLR-3 promoter. H) Figure representing the morphology of RIA. I) Co-expression of full length GLR-6::mCherry and GLR-1::GFP in RIA. Dashed lines outline axonal process of RIA.

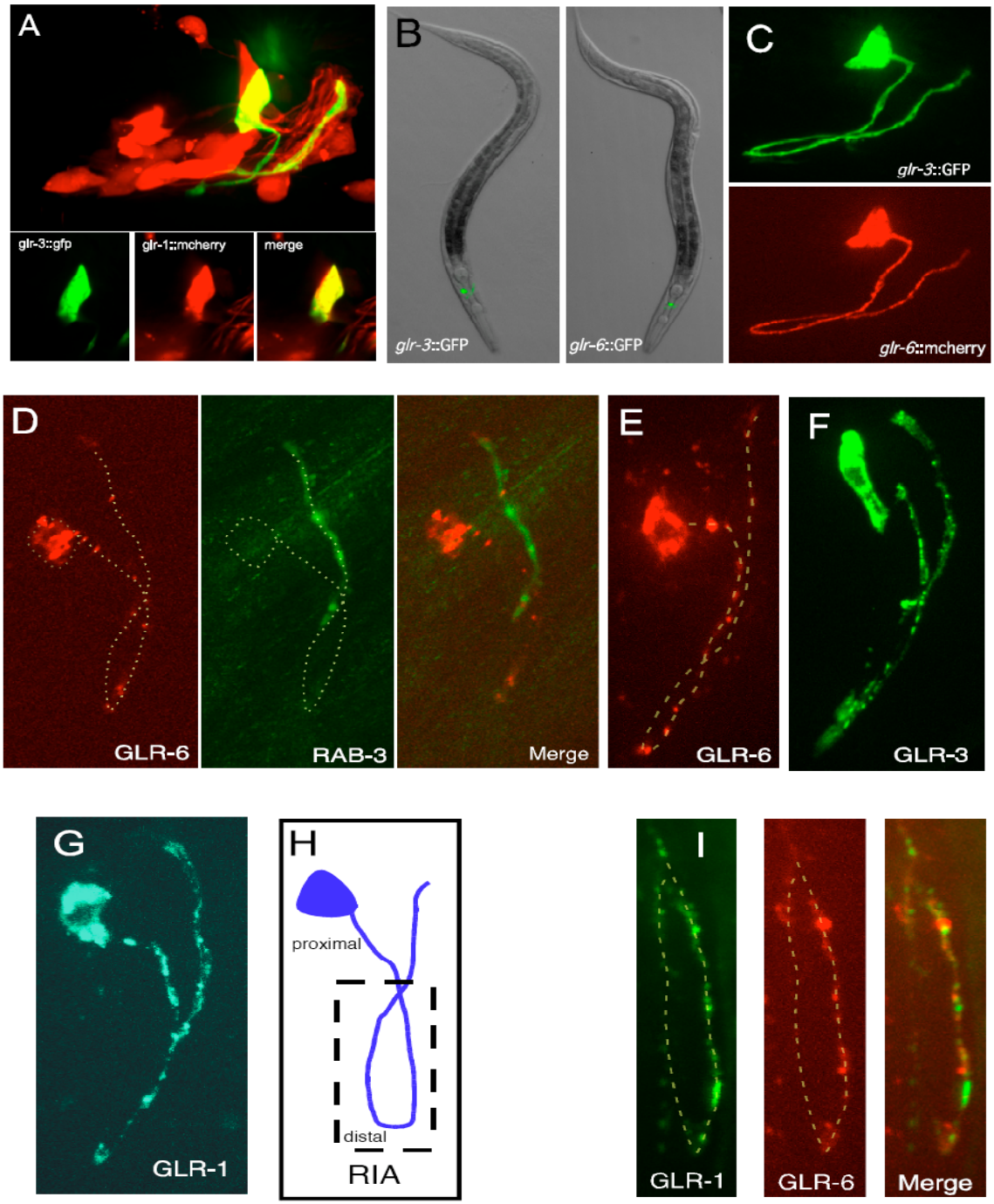
A
glr-3::gfp
glr-1::mcherry
merge
B
glr-3::GFP
glr-6::GFP
C
glr-3::GFP
glr-6::mcherry
D
GLR-6
RAB-3
Merge
E
GLR-6
F
GLR-3
G
GLR-1
H
proximal
distal
RIA
I
GLR-1
GLR-6
Merge

Figure 2.3 *C. elegans* GLR-3 and GLR-6 are distantly related to vertebrate kainate receptor subunits (A) Phylogenetic tree of the amino acid sequences for vertebrate NMDA, AMPA, kainate and delta glutamate receptor subunits in addition to *C. elegans* glr-3 and glr-6 receptor subunits. (B) Amino acid sequences for glr-3 and glr-6 aligned to vertebrate kainate receptor subunits GluK1, GluK2, GluK3, GluK4, GluK5 and vertebrate AMPA subunits GluA1, GluA2, GluA3, and GluA4. Highlighted residue indicates L/Y position, a defining characteristic of AMPA or Kainate receptors. (C) Key residue required for external ion coactivation in kainate receptors. Circles over residues indicate conserved amino acids required for kainate receptor anion binding.

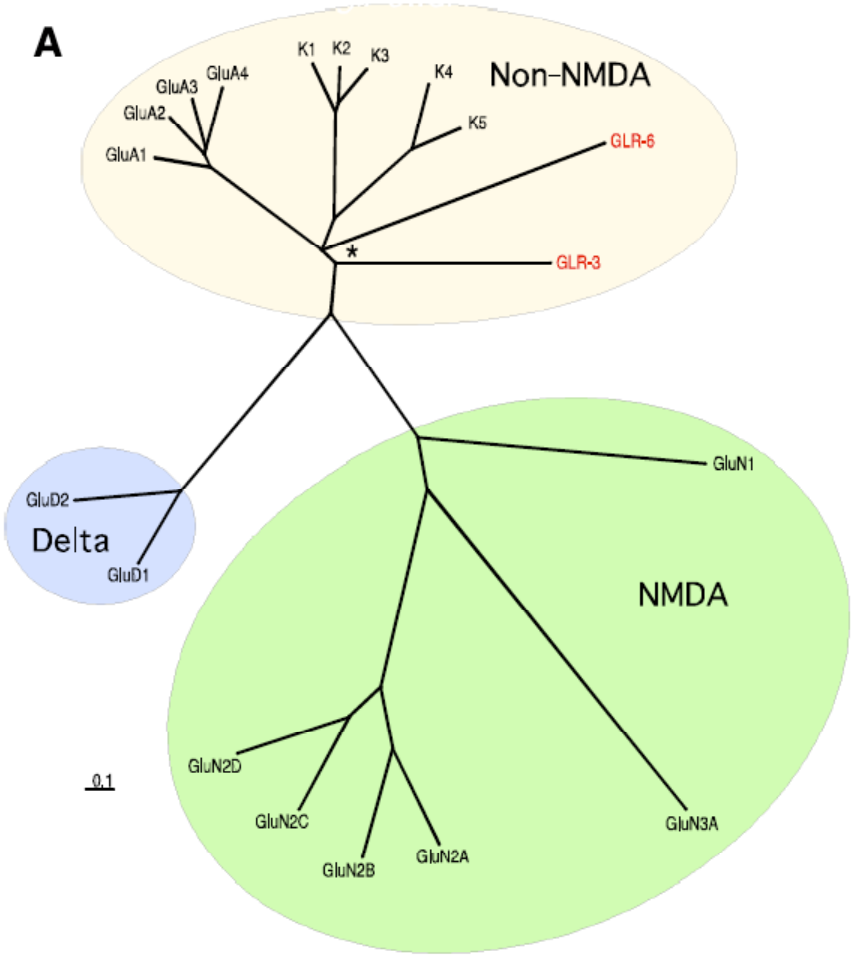

B

	GLR-3	462	ASLTISYGRSEVI
	GLR-6	490	APITVTATRLEVI
KA	GluK2	515	APLAITYVREKVI
KA	GluK3	517	APLTITHVREKAI
KA	GluK1	530	APLTITYVREKVI
KA	GluK4	499	AGLTITAEREKVI
KA	GluK5	498	AAFTITAEREKVI
AMPA	GluA3	501	APLTITLVREEVI
AMPA	GluA4	499	APLTITLVREEVI
AMPA	GluA2	498	APLTITLVREEVI
AMPA	GluA1	491	APLTITLVREEVI

C

	GLR-3	709	GYGIGLPKGSPYRELISTAILRL
	GLR-6	727	GYSIALPKGSKWREKLTRQILDL
KA	GluK2	515	GYGVGTPMGSPYRDKITIALQL
KA	GluK3	517	GYGIGTPMGSPYRDKITIALQL
KA	GluK1	530	GYGVGTPIGSPYRDKITIALQL
KA	GluK4	499	GYGIGMPVGSVFRDEFDLALQL
KA	GluK5	498	GYGIGMPLGSPFRDEITLALQL
AMPA	GluA3	501	GYGVATPKGSALGNAVNLAVLKL
AMPA	GluA4	499	GYGVATPKGSSLGNAVNLAVLKL
AMPA	GluA2	498	GYGIATPKGSSLGNAVNLAVLKL
AMPA	GluA1	491	GYGIATPKGSALRNPVNLAVLKL

Figure 2.4 GLR-3, GLR-6 receptors functionally resemble vertebrate kainate receptors A) Currents measured in response to application of 1mM glutamate before and after ConA treatment when injected with RNA encoding GLR-3, GLR-6 or both. B) Average peak current in response 1mM Glutamate or 100uM kainate before (dark bar) and after (grey bar) ConA treatment. C) Dose response curve to glutamate (open circles) and kainate (closed circles). D) Current voltage relationship for GLR- 3,6(squares) as the concentration of potassium (squares), Calcium (triangles) or sodium (inverted triangles) ions are increased 5 fold above baseline solution containing NMDG (diamonds). E) Currents measured in the response to application of glutamate to oocytes expressing GLR-3,GLR-6 with SOL-1 or STG-1. F) Average peak amplitude of oocytes expressing GLR-3,GLR-6 with SOL-1 or STG-1.

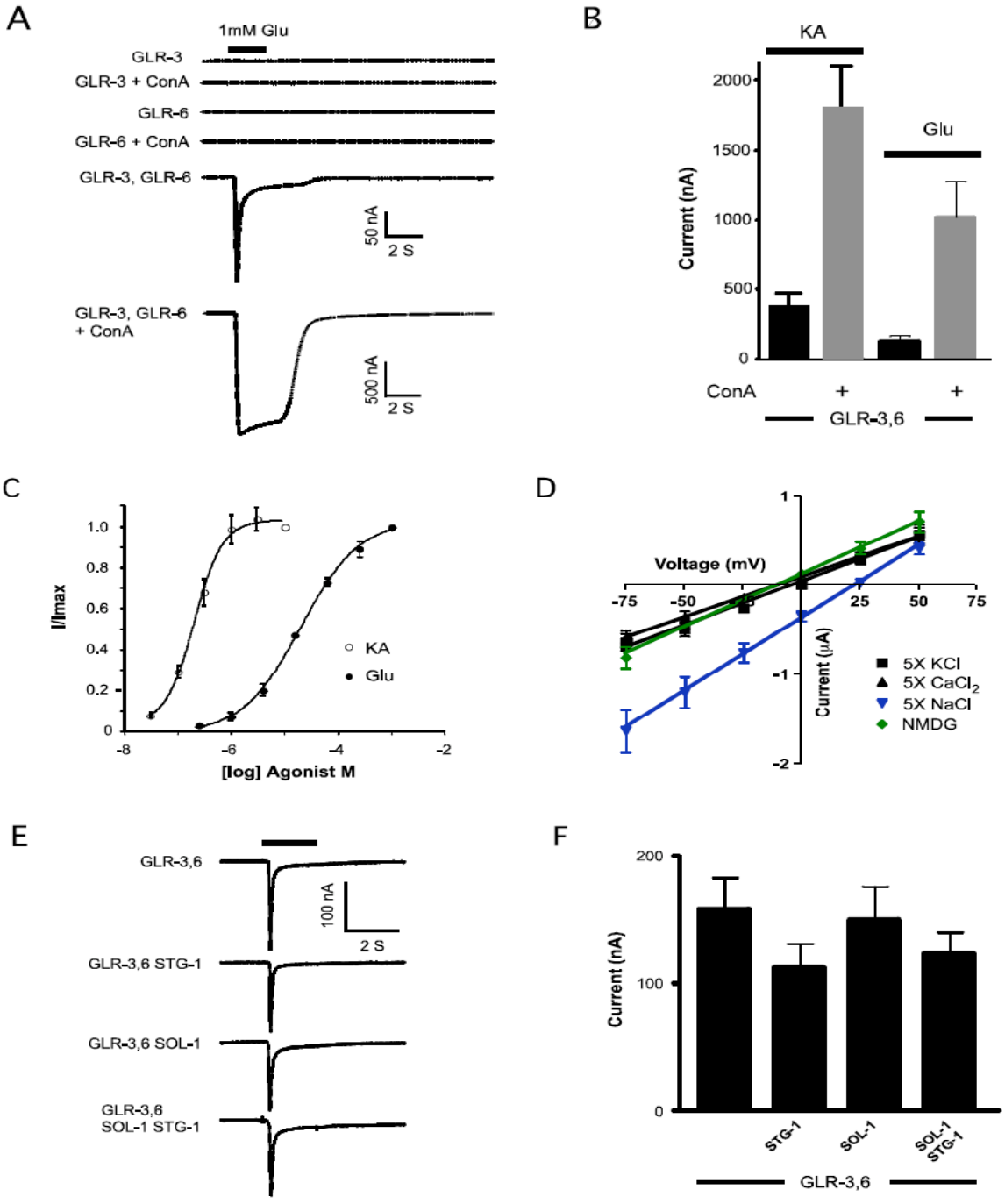
A
1mM Glu
GLR-3
GLR-3 + ConA
GLR-6
GLR-6 + ConA
GLR-3, GLR-6
50 nA
2 S
GLR-3, GLR-6
+ ConA
500 nA
2 S
B
KA
Glu
Current (nA)
2000
1500
1000
500
0
ConA + +
GLR-3,6
C
I/Imax
1.0
0.8
0.6
0.4
0.2
0
-8
-6
-4
-2
[log] Agonist M
KA
Glu
D
Voltage (mV)
-75
-50
25
50
75
1
-1
-2
Current (μA)
5X KCl
5X CaCl2
5X NaCl
NMDG
E
GLR-3,6
100 nA
2 S
GLR-3,6 STG-1
GLR-3,6 SOL-1
GLR-3,6
SOL-1 STG-1
F
Current (nA)
200
100
0
STG-1
SOL-1
SOL-1
STG-1
GLR-3,6

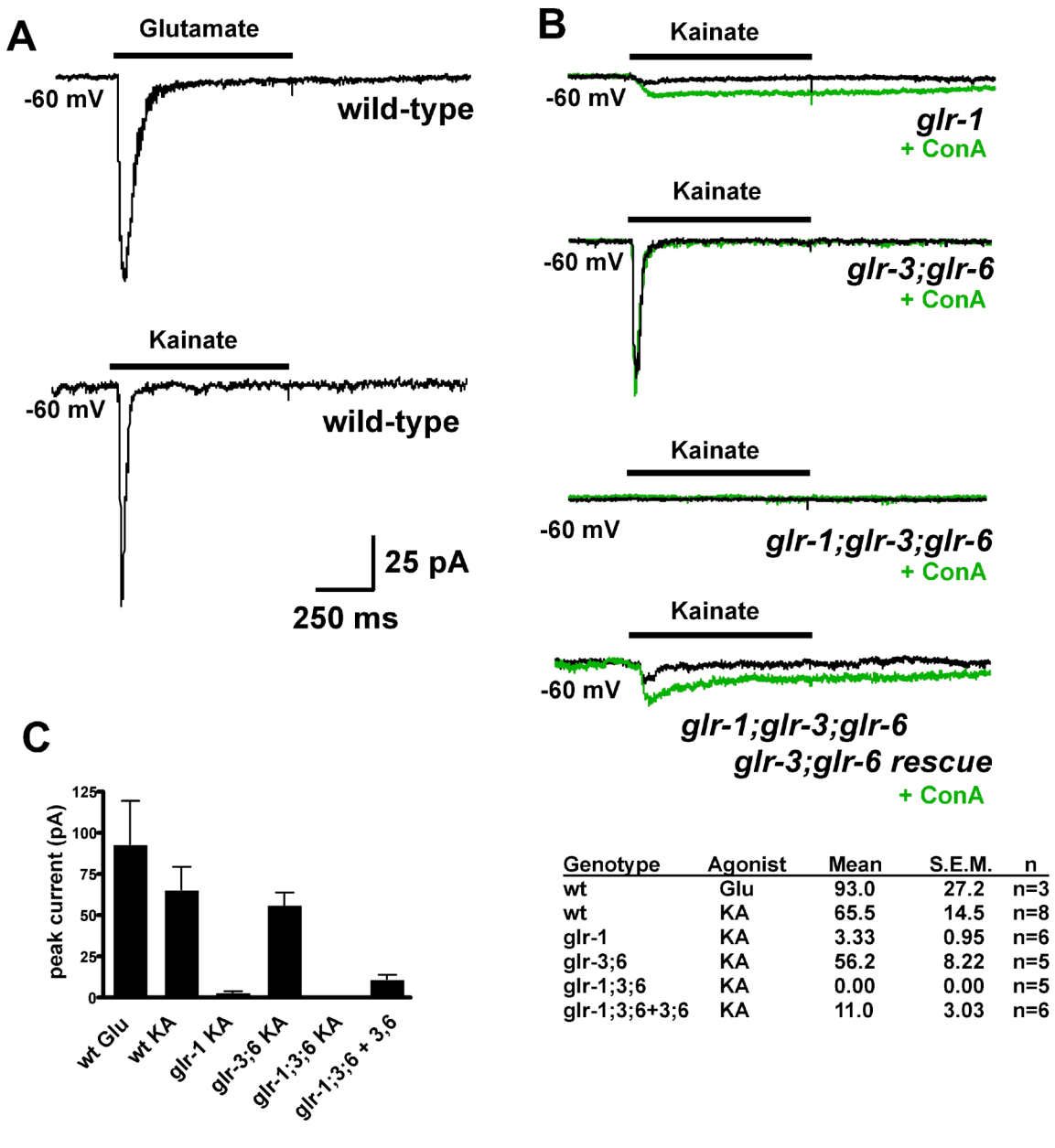

Genotype	Agonist	Mean	S.E.M.	n
wt	Glu	93.0	27.2	n=3
wt	KA	65.5	14.5	n=8
glr-1	KA	3.33	0.95	n=6
glr-3;6	KA	56.2	8.22	n=5
glr-1;3;6	KA	0.00	0.00	n=5
glr-1;3;6+3;6	KA	11.0	3.03	n=6

Figure 2.5 GLR-3 and GLR-6 mediate a portion of iGluR current in RIA A) Wildtype and mutant responses to application of 1mM Glutamate. Green trace indicate response post ConA. B) Wildtype and mutant responses to 100uM kainate, green trace is post ConA treatment. C) Quantification and statistics of A, B.

Figure 2.6 AIZ Input signals through GLR-3, GLR-6 receptors and modifies short reversal behavior. A) Figure depicting AIZ inputs into RIA; inputs are concentrated mainly within the hairpin region of RIA. Blue dots indicate synaptic input or output; red dots are specific inputs from AIZ (White et al*.,* 1986). B) Split gfp expression between GLR-6 subunits and NLG-1 expressed in AIZ; coexpressed with full-length GLR-1::mCherry. Imaging of the hairpin region (shown boxed in A) C) Split GFP expression between GLR-1 sbunuits and NLG-1 expressed in AIZ; coexpressed with full length GLR-6::mCherry. D) Wildtype or mutant behavior in worms expressing ChIEF in AIZ response to blue light with or without the required cofactor all trans retinal during chemotaxis to diacetyl. Quantified as fraction of worms that arrive at the stimulus during light exposure. N=6 worms per genotype E) Tracks from wildtype and *glr-3* mutants raised with retinal, exposed to blue light during chemotaxis. X indicates position of the stimulus. Wildtype worms fail to reach the stimulus while *glr-3* mutants are still capable of navigating the gradient. F) Behavior of wildtype or mutant worms expressing ChIEF in AIZ in response to blue light under nongradient conditions. Measured as percentage of time the worm responded to light exposure with either short or long reversals, or by reorientation. Error bars represent standard error of the mean, n=<75 trials per condition.

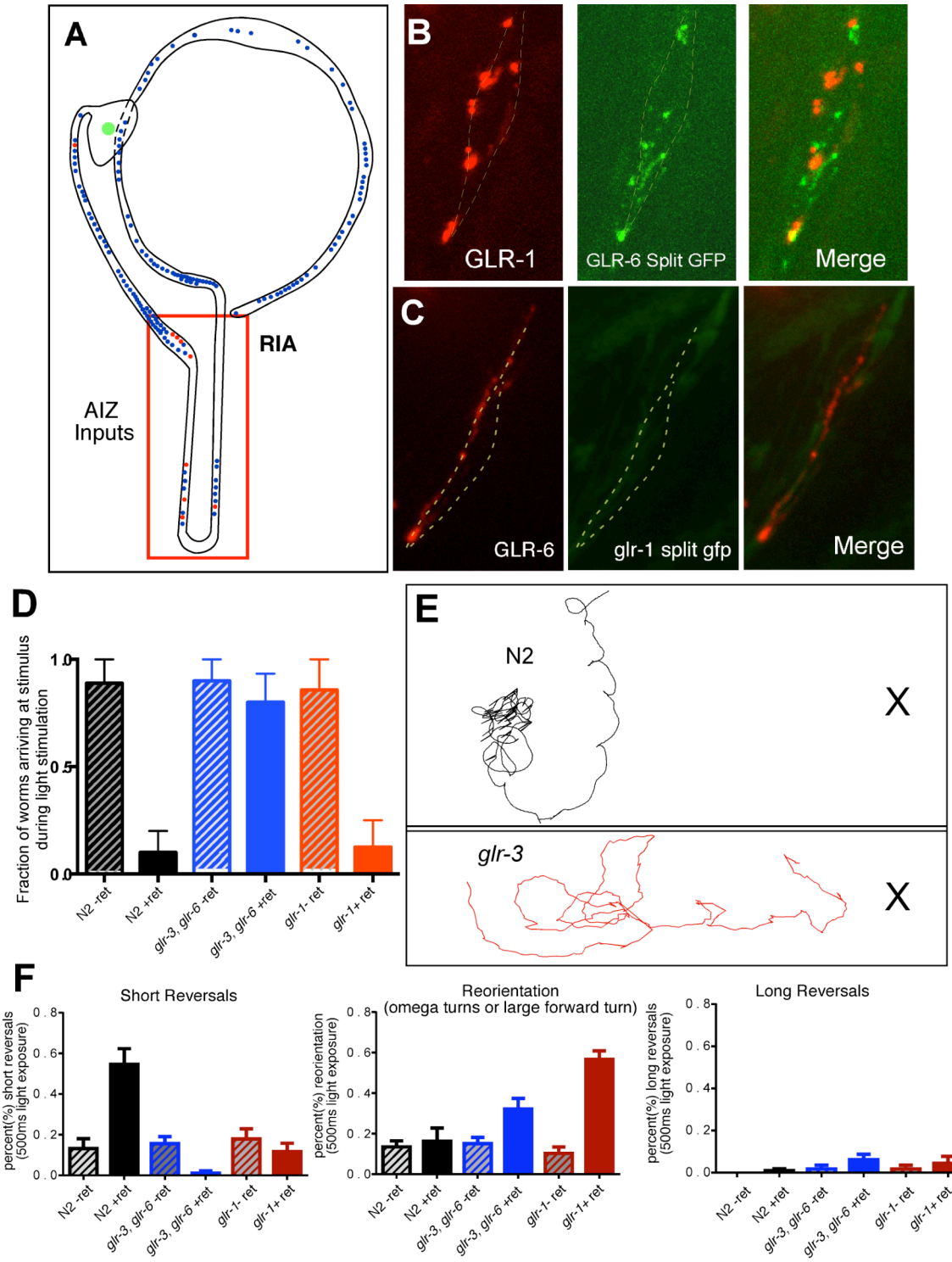
A
RIA
AIZ
Inputs
B
GLR-1
GLR-6 Split GFP
Merge
C
GLR-6
glr-1 split gfp
Merge
D
Fraction of worms arriving at stimulus during light stimulation
1.0
0.5
0.0
N2 -ret
N2 +ret
glr-3, glr-6 -ret
glr-3, glr-6 +ret
glr-1- ret
glr-1+ ret
E
N2
X
glr-3
X
F
Short Reversals
percent(%) short reversals (500ms light exposure)
Reorientation
(omega turns or large forward turn)
percent(%) reorientation (500ms light exposure)
Long Reversals
percent(%) long reversals (500ms light exposure)

Figure 2.7 *glr-1* and *glr-3, glr-6* show different defects in behavioral taxis. A,B) Time course showing the arrival time for wildtype and mutant worms during chemotaxis and thermotaxis. C) Average forward movement (seconds) during chemotaxis to diacetyl. D) Example tracks of wildtype and mutant worms moving across a chemotactic gradient. Blue hatch marks indicate starting position of the worm. E) Rose plots displaying the worm head angle over every frame during a chemotaxis assay. Stimulus position is indicated by red x. F) Mutant and wildtype behavior during chemotaxis, broken down into short and long reversals. Single worms were analyzed from filmed chemotaxis assays and scored by hand. N= <15 worms per genotype. Error bars indicate standard error of the mean.

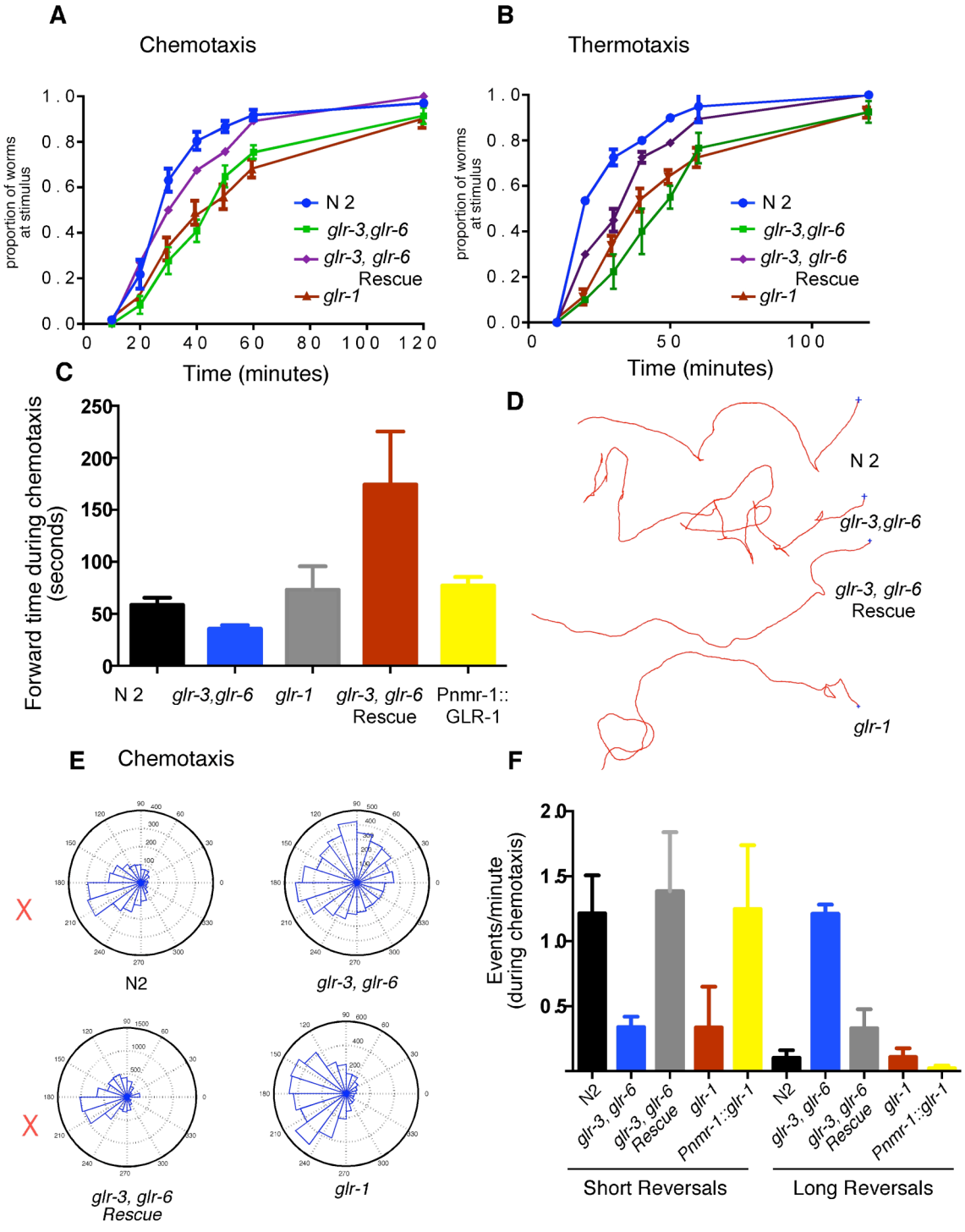
A
Chemotaxis
proportion of worms at stimulus
1.0
0.8
0.6
0.4
0.2
0.0
0
20
40
60
80
100
120
Time (minutes)
N 2
glr-3,glr-6
glr-3, glr-6 Rescue
glr-1
B
Thermotaxis
proportion of worms at stimulus
1.0
0.8
0.6
0.4
0.2
0.0
0
50
100
Time (minutes)
N 2
glr-3,glr-6
glr-3, glr-6 Rescue
glr-1
C
Forward time during chemotaxis (seconds)
250
200
150
100
50
0
N 2
glr-3,glr-6
glr-1
glr-3, glr-6 Rescue
Pnmr-1:: GLR-1
D
N 2
glr-3,glr-6
glr-3, glr-6 Rescue
glr-1
E
Chemotaxis
X
N2
glr-3, glr-6
X
glr-3, glr-6 Rescue
glr-1
F
Events/minute (during chemotaxis)
2.0
1.5
1.0
0.5
N2
glr-3, glr-6
glr-3, glr-6 Rescue
glr-1
Pnmr-1::glr-1
N2
glr-3, glr-6
glr-3, glr-6 Rescue
glr-1
Pnmr-1::glr-1
Short Reversals
Long Reversals

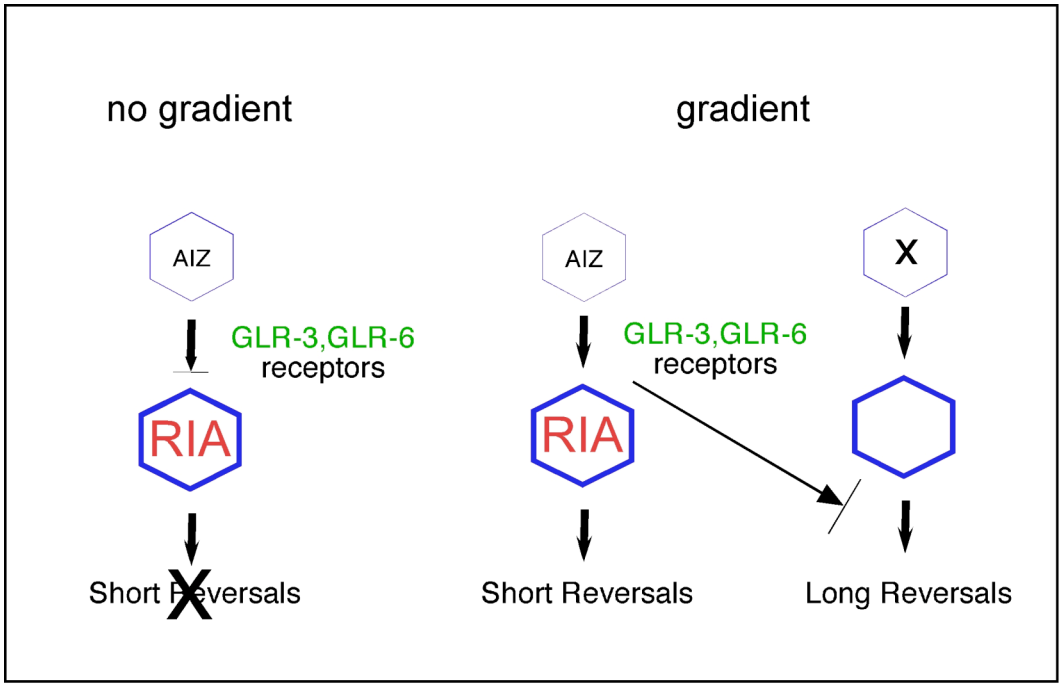

Figure 2.8 Model for kainate receptor function during gradient behaviors. Kainate receptor signaling through RIA during gradient behaviors is turned on through signaling from upstream neuron AIZ. AIZ signaling triggers short reversals, allowing for rapid reorientation during gradient navigation. A second, parallel pathway is revealed in the absence of short reversals, where typically rare long reversals become a prominent movement. Under nongradient conditions, this signaling does not occur.

Supplementary Figure 2.1 Worms lacking RIA neurons as well as glutamate receptor mutants exhibit normal behavior under baseline conditions. A) Behavior of wildtype and worms expressing the caspase ICE in RIA on worms with no stimulation. Assays include a minimum of seven population assays, each with 12-15 worms. Analyzed using matlab software. Error bars represent standard error of the mean. B) Time course for wildtype worms and *eat-4* mutants during standard population chemotaxis assays. N=<7 assays with 40-60 worms each. C) Average forward and backward time for wildtype and mutant worms. Single worms were tracked using custom software for 7-10 minutes. N=15 worms. D) Average speed for wildtype and mutant worms under no stimulation conditions. Worms were filmed and analyzed using matlab software. Error bars represent standard error of the mean.

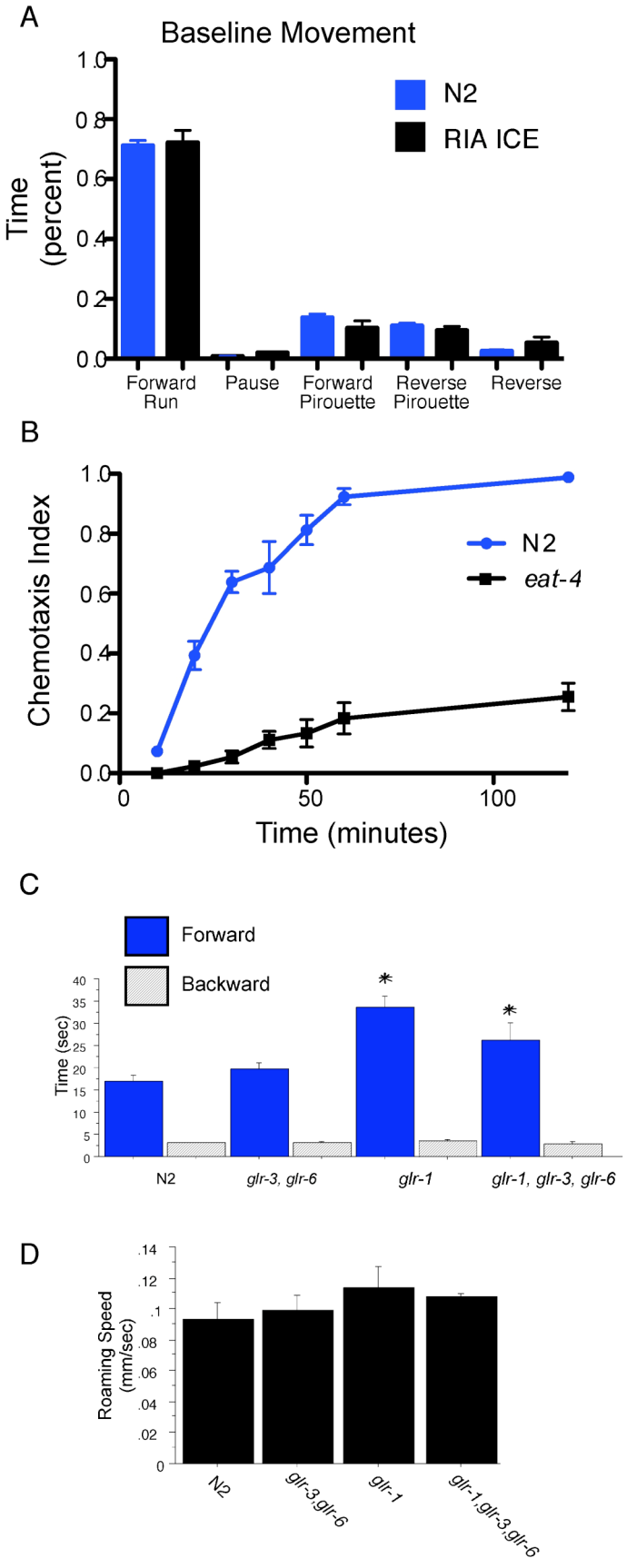
A
Baseline Movement
N2
RIA ICE
Time (percent)
1.0
0.8
0.6
0.4
0.2
0.0
Forward Run
Pause
Forward Pirouette
Reverse Pirouette
Reverse
B
Chemotaxis Index
N2
eat-4
0
50
100
Time (minutes)
C
Forward
Backward
Time (sec)
N2
glr-3, glr-6
glr-1
glr-1, glr-3, glr-6
D
Roaming Speed (mm/sec)
N2
glr-3,glr-6
glr-1
glr-1,glr-3,glr-6

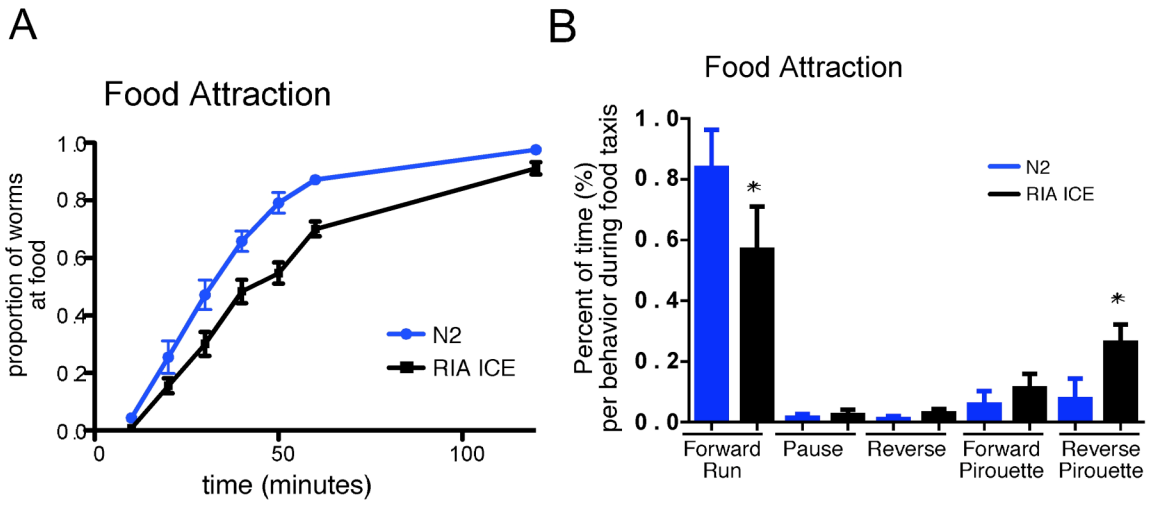

Supplemental Figure 2.2 RIA Lacking worms show minor defects in food migration. A) Time course of wildtype and mutant worms lacking RIA navigating to a food source. B) Behavior during food navigation broken down into different behaviors and quantified by the percentage of time performed over the course of the assay.

A

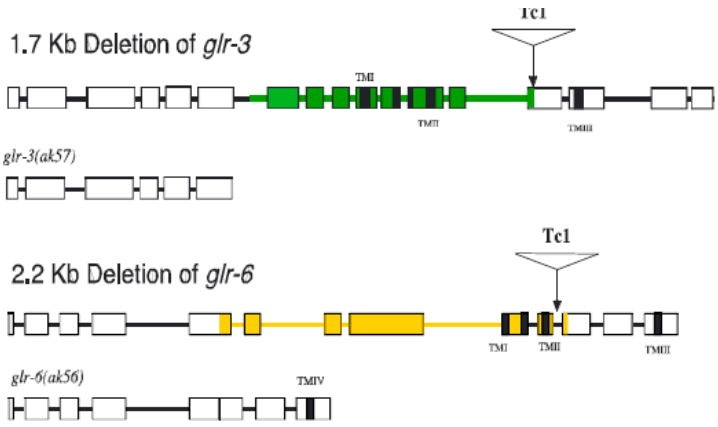

B

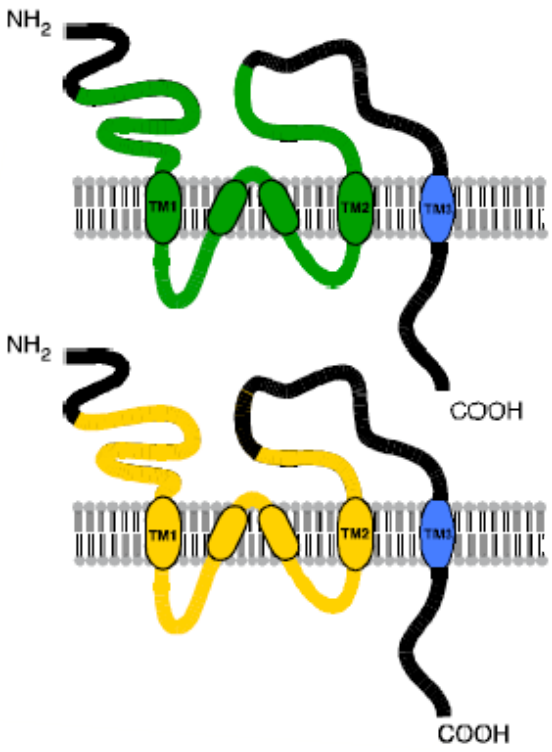

Supplementary Figure 2.3 Knockout Alleles of *glr-3* and *glr-6* genes. A) *glr-3* and *glr-6* deletion mutations; green and yellow areas indicate portions of DNA removed after imprecise excision. Boxes are exons. Tc1 indicates position of Tc1 transposon insertion. B) Figure indicating the deleted region of GLR-3 and GLR-6 receptor subunits, yellow and green areas indicate deleted regions.

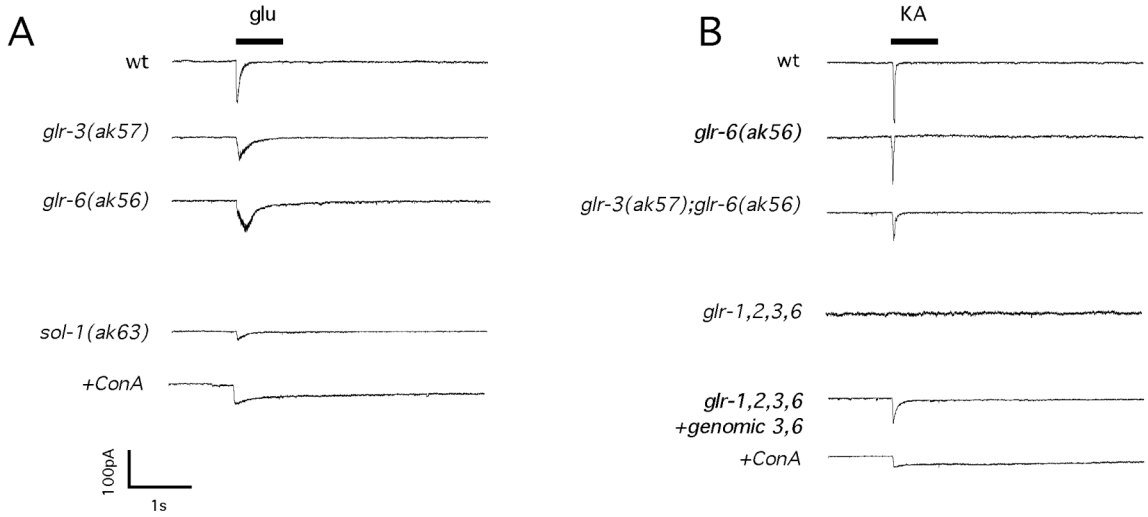

Supplementary Figure 2.4 GLR-3 and GLR-6 mediate a portion of iGluR current in RIA. A) Wildtype and mutant responses to application of 1mM Glutamate. Final trace indicates response post ConA treatment. B) Wildtype and mutant responses to 100uM Kainate, final trace is post ConA treatment.

A B

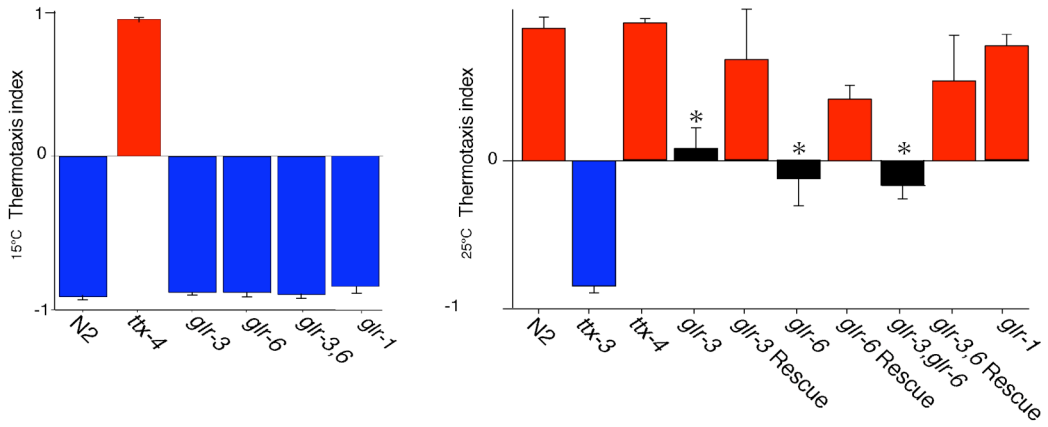

Supplementary Figure 2.5 *glr-3*, *glr-6* mutants show distinct defects from *glr-1* in warm thermotaxis. A,B) Thermotaxis to cold (15 degrees) and warm (25 degrees) using a steep temperature gradient. Quantified as thermotaxis index. N= <10 assays per genotype; error bars represent standard error of the mean.

Supplemental Figure 2.6 Thermotaxis defects in RIA null and *glr-3, glr-6* mutant worms. A) Worm behavior filmed, tracked and analyzed. Animal movement in wildtype and mutant worms are broken down into different behaviors and quantified by the percentage of time performed. B) Representative rose plots plotting head angles for the duration of the assay. C) Example tracks of worms moving up a thermal gradient. Time course assays include a minimum of seven population assays, each assay uses 40-60 animals. Error bars represent standard error of the mean.

A

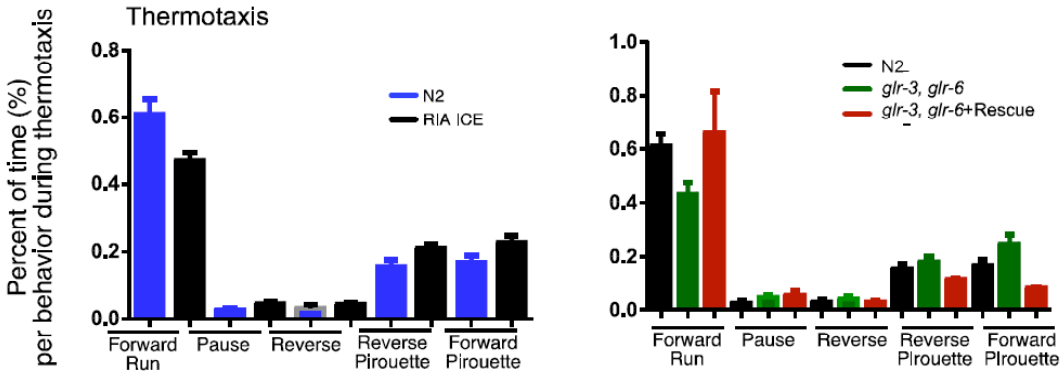
Thermotaxis
Percent of time (%) per behavior during thermotaxis
N2
RIA ICE
Forward Run
Pause
Reverse
Reverse Pirouette
Forward Pirouette
N2
glr-3, glr-6
glr-3, glr-6+Rescue
Forward Run
Pause
Reverse
Reverse Pirouette
Forward Pirouette

B

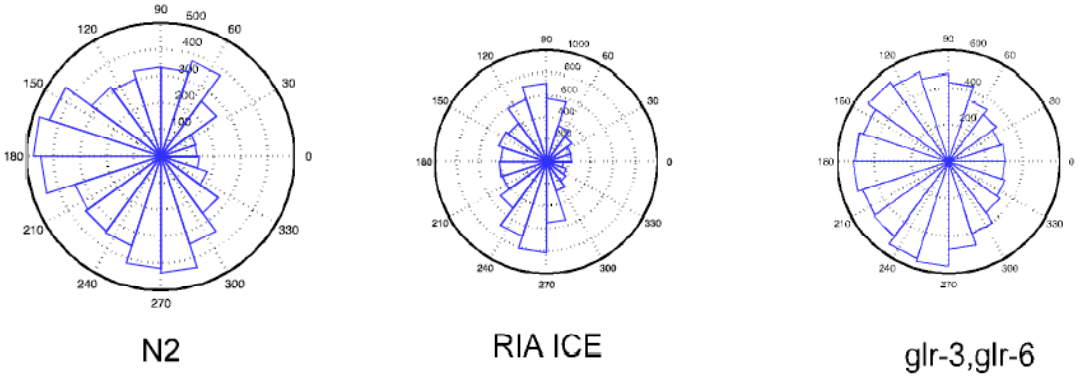
N2
RIA ICE
glr-3,glr-6

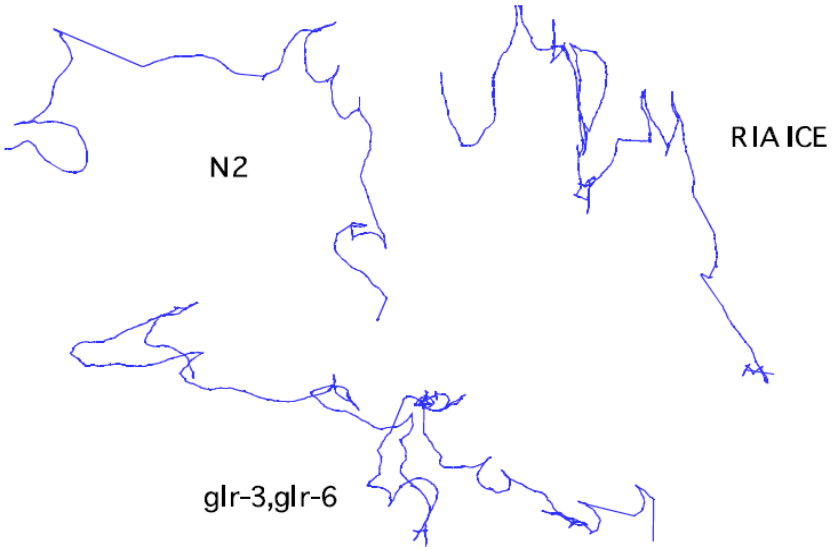
N2
RIA ICE
glr-3,glr-6

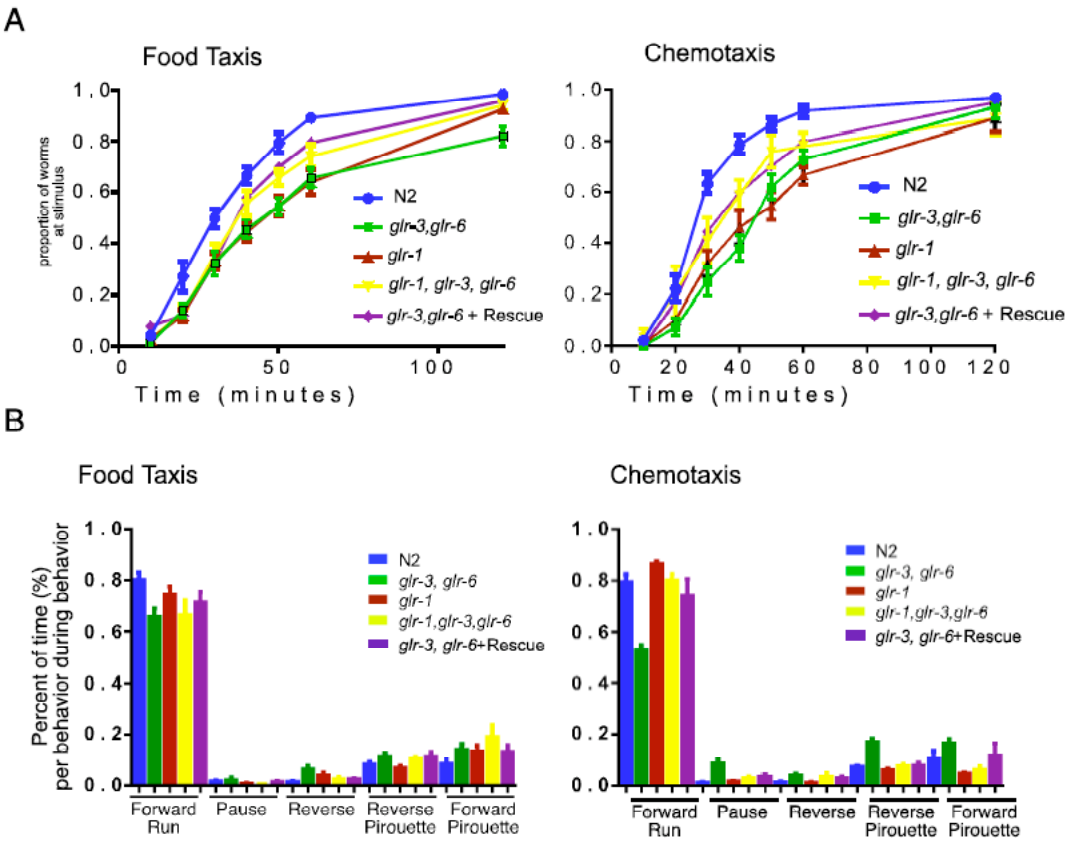

Supplemental Figure 2.7 iGluR mutants show defects during taxis behaviors A) Time course of wildtype and mutant worms during chemotaxis to diacetyl and food. B) Animal movement during taxis behaviors broken down into individual types of movement. Time course assays include a minimum of seven population assays; each assay uses 40-60 animals. Behavior analysis was performed by filming a minimum of seven assays including 12-15 worms each. Error bars represent standard error of the mean.

References

Albrecht, D.R. & Bargmann, C.I. (2011) *Nat Meth* 8,599-605.

Altun-Gultekin, Z., Andachi, Y., Tsalik, E.L., Pilgrim, D., Kohara, Y., & Hobert, O. (2001) *Develop* 128, 1951-1969.

Bellocchio, E. E., Reimer, R. J., Fremeau, R. T., Jr. & Edwards, R. H. (2000) *Science* 289, 957-60.

Berger, A.J., Hart, A.C., Kaplan, J.M. (1998) *J Neurosci* 18:2871-80.

Biron, D., Wasserman, S., Thomas, J.H., Samuel, A.D., & Sengupta, P. (2008) *Proc Natl Acad Sci USA* 105, 11002-11007.

Bowie, D. (2010) *J Physiol* 1, 67-81.

Brockie, P. J., Madsen, D. M., Zheng, Y., Mellem, J. & Maricq, A. V. (2001) *J Neurosci* 21, 1510-22. 18.

Brockie, P. J., Mellem, J. E., Hills, T., Madsen, D. M. & Maricq, A. V. (2001) *Neuron* 31, 617-30.

Clark, D., Biron, D., Sengupta, P., Samuel A. (2006) *J Neurophysiol* 97, 1903-1910.

Colon-Ramos, D.A., Margeta, M.A., Shen, K. (2007) *Science* 318, 103-6.

Dingledine et al. (2010) *Pharm Rev* 62, 405-496.

Dingledine, R., Borges, K., Bowie, D. & Traynelis, S. F. (1999) *Pharmacol Rev* 51, 7-61.

Edwards, S.L., Charlie, N.K., Milfort, M.C., Brown, B.S., Gravlin, C.N., Kneckt, J.E., Miller, K.G. (2008) *PLOS Biol* 6(8).

Egebjerg, J. & Heinemann, S. F. (1993) *Proc Natl Acad Sci U S A* 90, 755-9.

Egebjerg, J., Bettler, B., Hermans-Borgmeyer, I. & Heinemann, S. (1991) *Nature* 351, 745-8.

Everts, I., Petroski, R., Kizelsztein, P., Teichberg, V. I., Heinemann, S. F. & Hollmann, M. (1999) *J Neurosci* 19, 916-27.

Feinberg, E.H., Vanhoven, M.K., Bendesky, A., Wang, G., Fetter, R.D., Shen, S., & Bargmann, C.I. (2008) *Neuron* 57, 353-363.
Gray, J.M., Hill, J.J., Bargmann, C.I. (2005) *PNAS* 102 9:3184-3191.

Hart, A. C., Sims, S. & Kaplan, J. M. (1995) *Nature* 378, 82-5.

Hedgecock, E. M. & Russell, R. L. (1975) *Proc Natl Acad Sci U S A* 72, 4061-5.

Hobert, O., Mori, I., Yamashita, Y., Honda, H., Ohshima, Y., Liu, Y. & Ruvkun, G. (1997) *Neuron* 19, 345-57.

Hollmann, M. (1999) *J Neurosci* 19, 916-27.

Huang, L. S., Tzou, P. & Sternberg, P. W. (1994) *Mol Biol Cell* 5, 395-411.

Ikeda, D.D., Duan, Y., Matsuki, M., Kunitomo, H., Hutter, H., Hedgecock, E.M., Iino, Y. (2008) *Proc Natl Acad Sci USA* 105, 5260-5.

Kuhara, A., Okumura, M., Kimata, T., Tanizawa, Y., Takano, R., Kimura, K. Inada, H., Matsumoto, K. Mori, I. (2008) *Science* 320, 803-807.

Lee, R. Y., Sawin, E. R., Chalfie, M., Horvitz, H. R. & Avery, L. (1999) *J Neurosci* 19, 159-67.

Lerma, J., Paternain, A.V., Rodriguez-Moreno, A., & Lopez-Garcia, J. (2001) *Physiol Rev* 81, 971-998.

Macosko, E.Z., Pokala, N., Feinberg, E.H., Chalasani, S.H., Butcher, R.A., Bargmann, C.I. (2009) *Nature* 458:1171-76.

Maricq, A. V., Peckol, E., Driscoll, M. & Bargmann, C. I. (1995) *Nature* 378, 78-81.

Mellem, J. E., Brockie, P. J., Zheng, Y., Madsen, D. M. & Maricq, A. V. (2002) *Neuron* 36, 933-44.

Mori, I. & Ohshima, Y. (1995) *Nature* 376, 344-8.

Noriyuki, O., Atsushi, K., Fumiya, N., Yoshifumi, O., & Mori, I. (2011) *EMBO J* 10.1038.

Okochi, Y., Kimura, K. D., Ohta, A. & Mori, I. (2005) *EMBO J* 24, 2127-37.

Ohnishi, N., Kuhara, A., Nakamura, F., Okochi, Y., Mori, I. (2011) *EMBO J* 30:1376-1388.

Paternain, A.V., Cohen, A., Stern-Bach, Y., Lerma, J. (2003) *J Neurosci* 23, 8641-8.
Plested, A.J.R. & Mayer, M.L. (2007) *Neuron* 53, 829-841.

Ramot, D., Macinnis, B.L., Lee, H.C., Goodman, M.B. (2008) *J Neurosci* 28, 12546-57.

Stern-Bach, Y., Russo, S., Neuman, M. & Rosenmund, C. (1998) *Neuron* 21, 907-18.

Stetak, A., Horndli, F., Maricq, A.V., Van Den Heuvel, S., Hajnal, A. (2009) *PLoS One* 4:6.

Swanson, G. T., Green, T. & Heinemann, S. F. (1998) *Mol Pharmacol* 53, 942-9.

Tsalik, E.L. & Hobert, O. *Devel Neuro*. (2003) 56 2:178-197.

Wakabayashi, T., Kitagawa, I., Shingai, R. (2004). *Neurosci Res*. 50 1:103-111.

Walker, C. S., Maricq, A. V. & Hollmann, M. (2003) *J Biol Chem* 278, 44691-701.

Walker, C.S., Brockie, P.J., Madsen, D.M., Francis, M.M., Zheng, Y., Koduri, S., Mellem, J.E., Strutz-Seebohm, N. & Maricq, A.V. (2006) *Proc Natl Acad Sci USA* 103, 10891-6.

Wang, R., Walker, C.S., Brockie, P.J., Francis, M.M., Mellem, J.E., Madsen, D.M., Maricq, A.V. (2008) *Neuron* 59, 997-1008.

White, J. G., Southgate, E., Thomson, J. N. & Brenner, S. (1986) *Phil Trans R Soc Lond* B 314, 1-340.

Yamada, Y., Ohshima, Y. (2003) *J Exp Biol* 206:2581-2593.

Zhang, Y., Lu, H., & Bargmann, C.I., (2005) *Nature* 438, 179-84.

Zheng, Y., Brockie, P. J., Mellem, J. E., Madsen, D. M. & Maricq, A. V. (1999) *Neuron* 24, 347-61.

Zheng, Y., Brockie, P. J., Mellem, J. E., Madsen, D. M., Walker, C. S., Francis, M. M. & Maricq, A. V. (2006) *Proc Natl Acad Sci U S A*.

Zheng, Y., Mellem, J. E., Brockie, P. J., Madsen, D. M. & Maricq, A. V. (2004) *Nature* 427, 451-7.

Zwaal, R. R., Broeks, A., van Meurs, J., Groenen, J. T. & Plasterk, R. H. (1993) *Proc Natl Acad Sci U S A* 90, 7431-5.

CHAPTER 3

IDENTIFYING NOVEL KAINATE SPECIFIC ACCESSORY PROTEINS USING GAIN-OF-FUNCTION RECEPTOR SUBUNITS

Abstract

Kainate receptors and their accessory molecules have remained an enigma despite recent advances in the field of ionotropic glutamate receptors. What proteins function in the synthesis, trafficking, insertion and function of kainate receptors remain largely unknown. Gain of function point mutations in different classes if iGluRs have resulted in leaky or constitutively open ion channels (Scannevin et al., 2000; Dong et al., 1997; Daw et al., 2000; Osten et al., 2000; Puchalski et al., 1994; Lipsky et al., 2003). Introducing a gain of function point mutation into kainate receptor subunits in *C. elegans* results in morphological defects of the RIA neuronal process. Additionally, electrophysiological recordings *in vivo* and *in vitro* show altered channels kinetics in activated kainate receptors. The drastic morphological and electrophysiological defects caused by the expression of gain-of-function receptors provide a unique genetic opportunity to screen for kainate-specific molecules within a single interneuron, RIA. Here we show the design and

execution of a small-scale forward genetic screen that takes advantage of axonal morphological defects caused by gain-of-function kainate receptors.

Introduction

In the field of vertebrate neurobiology, the role of kainate receptors has remained elusive and poorly understood relative to other glutamate receptor subtypes. In particular few accessory or modulatory proteins known to function with kainate receptors have been discovered. Little is known about the proteins necessary for the synthesis, trafficking, localization and insertion of kainate receptors. Discrepancies in kainate receptor kinetics between native and heterologously expressed receptors suggest the existence of modulatory proteins. This idea is supported by the identification of two vertebrate auxiliary proteins, NETO1 and NETO2, which alter the kinetics of kainate receptors (Zhang et al., 2009). However, the identification of kainate-specific molecules in vertebrates has proved to be difficult. Thus far, no kainate-specific proteins have been identified in invertebrates. Yet the restricted expression of kainate receptors to the single interneuron RIA provides a unique opportunity to focus on kainate specific molecules in a concise area of an already simplified nervous system.

Defects in glutamatergic signaling have been implicated in a variety of neurological disorders. Glutamate excitotoxicity is a signaling defect with far-reaching consequences leading to a range of problems including ischemia as well as chronic neurodegenerative disorders such as Parkinson's, multiple

sclerosis, amyotrophic lateral sclerosis and others (Montastruc et al., 1997; Ulas et al., 1994).

Glutamatergic excitotoxicity is characterized by excessive glutamate resulting in neuronal dysfunction and degeneration due to excessive stimulation. Increased levels of glutamate can occur when there is ineffective clearance of glutamate around the synaptic cleft, following traumatic brain injury, or the over activation of glutamate receptors. (Manev et al., 1989). Reminiscent of excitotoxicity, a spontaneous alanine to threonine point mutation found in a highly conserved region of the vertebrate delta2 receptor resulted in a constitutively active channel leading to neuronal death by apoptosis (Zuo et al., 1997) (Figure 3.1A). In *C. elegans*, the analogous alanine to threonine mutation in the AMPA receptor GLR-1 leads to behavioral and electrophysiological defects (Zheng et al., 1999). GLR-1 receptors are expressed and function within the command interneurons in the worm nervous system, a neuronal circuit that controls the animals' forward and backward movement. Behaviorally, the A/T gain of function point mutation leads to a hyperreversal movement defect. Here we show that the analogous A/T mutation in kainate receptor subunits leads to excessive channel signaling resulting in behavioral defects and leading to the disruption of RIA neuronal processes. Dominant morphological defects in the axon provided a phenotype that could be utilized to look for novel, kainate specific molecules in a forward genetic screen. Here we report the small-scale forward genetic screen performed using activated kainate channels and the initial description of two

proteins that suppress the morphological and electrophysiological defects associated with those channels.

Results

Expression of GLR-6 A/T induces behavioral and neuronal defects

Originally identified as a mutation in the vertebrate delta receptor (Zuo et al., 1997), the disruption of iGluR function by an alanine to threonine point mutation has been utilized as a tool to study the *C. elegans* AMPA receptor GLR-1. The analysis of GLR-1 A/T induced phenotypes and electrophysiological defects consistent with over activation of the channel. We hypothesized that if GLR-3, GLR-6 receptors are activated by glutamate in response to sensory signaling to control worm movement, mutations causing over activation of the receptor would be expected to cause phenotypes in the absence of input. In order to induce inappropriate glutamate signaling in RIA, we introduced the analogous alanine to threonine point mutation into GLR-3 and GLR-6 receptor subunits (Figure 3.1B). In transgenic worms, the expression of GLR-6A/T in a *glr-6(ak56)* mutant resulted in the animal raising its nose at an increased frequency. During normal movement, wildtype worms will occasionally lift their noses slightly off the agar surface. Rarely, this movement is exaggerated, resulting in the raising of the entire head of the worm. General observation of GLR-6 A/T transgenic worms showed an increased frequency in small nose-up movements as well as an increase in large nose lifts. Additionally, transgenic worms expressing GLR-6 A/T, GLR-3 A/T or those expressing both gain of

function subunits showed defects in temperature thermotaxis, a behavior that requires proper RIA function (Figure 3.2).

To further investigate the effect of gain of function kainate receptors in RIA, we used confocal microscopy to examine the neuronal morphology of RIA in transgenic worms. Wildtype RIA morphology is consistent and reproducible in *C. elegans*. The cell body of RIA is triangular in shape, extending a process ventrally to the ventral neuropil before making a hairpin loop back to the nerve ring (Figure 3.1C). Worms expressing GLR-6 A/T in a *glr-6(ak56)* background as well as a soluble GFP marker in RIA were used to visualize the cell body and neuronal process of RIA, an interneuron found in the head of the worm. RIA neurons that express either GLR-6 A/T or GLR-3 A/T receptors exhibit a markedly different morphology similar to neurons undergoing apoptotic death. Cell bodies in these neurons are distinctively rounded. Additionally, rather than the smooth, wildtype neuronal process typically seen in RIA, an interrupted "string of pearls" appearance characterized the axon fragments (Figure 3.1D). In transgenic worms expressing both GLR-3 and GLR-6 gain of function receptor subunits, GFP fluorescence was eliminated, suggesting that RIA neurons in these worms may have undergone complete apoptosis and engulfment. Interestingly, transgenic worms expressing the gain of function AMPA receptor GLR-1 in RIA displayed no defects in RIA process morphology. As a result of gain of function channels expressed in RIA, behavioral defects as well as dramatic visual phenotypes indicate that inappropriate glutamatergic signaling through kainate receptors have severe consequences on RIA neurons.

Gain of function mutations in kainate receptor subunits alter channel kinetics

In order to determine the effect of gain of function mutations on kainate receptor channel function, we performed both *in vivo* and *in vitro* electrophysiological analyses. Using the heterologouos expression system *Xenopus laevis*, cRNAs for receptor subunits were injected into oocytes and used for electrophysiological analyses. The expression of wildtype GLR-3 and GLR-6 cDNAs followed by application of glutamate results in a fast inward current that rapidly desensitizes. However, the expression of GLR-3 A/T with wildtype GLR-6 cDNAs or wildtype GLR-3 with GLR-6 A/T cDNAs in oocytes leads to a decreased rate and extent of current desensitization. Consistent with a decreased desensitization rate, mutant channels showed an increase in peak current amplitude. (Figure 3.3). The expression of both GLR-3 A/T and GLR-6 A/T resulted in a small but nondesensitizing response to glutamate application (Figure 3.3). To directly evaluate the effect of activated kainate receptors in RIA, electrophysiological recordings of worms expressing GLR-6 A/T were performed in response to kainate application. Wildtype recordings from RIA result in a fast, inward, rapidly desensitizing current composed of a major component, contributed by GLR-1 receptors, and a minor component from GLR-3, GLR-6 receptors (Figure 3.4A). Recordings from transgenic worms expressing GLR-6 A/T in a *glr-6(ak56)* background produced a rapid inward current, contributed by GLR-1 AMPA receptors and a long-lasting, nondesensitizing current resulting from activated kainate receptors not seen in wildtype responses (Figure 3.4B).

Activated kainate receptor suppressor screen

In an effort to identify novel kainate receptor cofactors, we took advantage of the profound morphological change seen in the RIA neuronal process of GLR-6 A/T transgenic worms. Visual neuronal defects provided a reproducible physical phenotype that could be used in a forward genetic screen to identify mutant suppressor genes. Dominant molecules provide a powerful platform for performing genetic screens. These screens allow for the identification of molecules required to function in genetic pathways. Due to the nature of the dominantly activated molecule, loss of function mutations in genes required for the molecules' function will result in the restoration of a more normal phenotype. The disruption of any upstream steps involved in kainate receptor synthesis, trafficking, localization or function will prevent dominantly active kainate receptors from function in RIA and thus suppress the morphological and electrophysiological defects. Many different reagents have been used to induce mutations for genetic screens, each prone to creating specific types of genetic perturbations. Chemical mutagenesis in *C. elegans* has primarily relied on ethyl methanesulfonate (EMS) to produce missense mutations for genetic screens. While EMS is capable of inducing mutation at a high frequency, it is limited in that the molecular lesions it produces are primarily G/C to A/T transitions (reviewed Anderson, 1995). To extend the type of molecular lesions and therefore increase the probability of finding novel kainate-interacting molecules, we used N-ethyl-N-nitrosourea (ENU) to induce a different spectrum of mutations. ENU most often produces A/T to T/A transversions and A/T to G/C transitions and can lead to

high allelic variability including gain-of-function or loss-of-function mutations (De Stasio et al., 2001). We performed a small-scale genetic screen of 2,688 haploid genomes to identify mutated worms that reversed the activated GLR-6 phenotype, thus resulting in a wildtype neuronal processes in RIA. Neuronal screening was performed by mounting and imaging individual worms using confocal microscopy. This method allowed for the screening of an individual neuron, RIA, for suppressors of activated kainate receptors expressed exclusively within that neuron.

sup1 and *sup2* suppress RIA morphological and electrophysiological defects

The visual screening of mutated worms expressing activated kainate channels resulted in the discovery of two independent specific suppressors. Worms expressing suppressor genes in the GLR-6 A/T, *glr-6(ak56)* background exhibited RIA neuronal processes more similar to wildtype than the screening strain. Two mutants identified, named *sup1* and *sup2,* showed a neuron morphology similar to wildtype but with different levels of suppression. Neuronal morphology in *sup1* mutants closely resembled wildtype RIA neurons. Unlike the rounded cell body seen in lines expressing the activated GLR-6 receptors, *sup1* RIA neurons have a triangular cell body similar to wildtype. Additionally, the neuronal process is intact with proper morphology. *sup1* mutant neurons however do not have the typical smooth appearance seen in wildtype. Rather, the process appears to be thickened and flattened in areas, becoming more

prominent toward the distal region (Figure 3.5A). In contrast to *sup1,* the cell body morphology in *sup2* mutants retained the circular phenotype seen in gain-of-function mutants. The neuronal process, however, closely resembled that of *sup1* mutants. *sup2* mutant neurons showed proper morphology and interestingly also showed the thickening and flattening seen in *sup1* mutants. This phenotype appeared to be more pronounced in *sup2* mutants than *sup1* mutants, and could be seen along a large portion of the process, rather than just the distal region (Figure 3.5B).

To verify kainate receptor specificity we performed a secondary screen looking for the suppression of GLR-6A/T electrophysiological defects (Figure 3.4C). Two suppressors of the morphological defect, *sup1* and *sup2*, were found to also shown suppression of the prolonged, nondesensitizing channel current. Electrophysiological suppression suggests that the molecules mutated in *sup1* and *sup2* mutants function specifically with GLR-6 containing kainate receptors.

Discussion

The role and functionality of kainate receptors is dependent on the accessory proteins that function in all stages of forming and regulating an operational kainate receptor. These proteins have just recently begun to be discovered in the vertebrate system; however, the complexities of the nervous system have hindered the discovery of novel kainate receptor-specific molecules. The unique advantages of *C.elegans* provide a distinctive opportunity for kainate receptor study. The only two kainate receptor subunits, GLR-3 AND GLR-6,

found in *C. elegans* show exclusive expression in the interneuron RIA. Thus, the study of kainate receptors and the identification of kainate specific molecules can focus on a single neuron within a simplified nervous system. Additionally, the expression of kainate receptors within RIA neurons is limited to a number of discrete puncta along the neuronal process (see Chapter 2). The severely limited expression of kainate receptors in the worm allows clean genetic studies as well as simplified molecular analysis.

The expression of GLR-6 A/T interestingly showed a morphological defect in the neuronal process of RIA. RIA morphology became reminiscent of apoptotic cells following glutamatergic excitotoxicity. The alanine to threonine point mutation expressed singlely in either the GLR-3 or GLR-6 kainate receptor subunit resulted in a similar phenotype. However, the expression of both activated receptor subunits produced a more severe phenotype. This may be due to a synergistic effect of the mutations present in both subunits thus exhibiting an enhanced phenotype. The expression of soluble GFP in addition to the receptor subunits allows visualization of the cell body and neuronal process of RIA. Doubly expressed gain of function subunits resulted in the elimination of visual GFP. This result, in conjunction with the nondesensitizing current seen in *Xenopus* oocytes expressing both gain of function subunits, are consistent with a stronger channel defect when both mutations are present. The elimination of RIA GFP expression by these channels could occur for several different reasons. One possibility is the over-activation of kainate receptors could lead to the death of RIA in early developmental stages prior to GFP expression. Alternatively, the

lack of GFP could result from the complete apoptosis and engulfment of RIA. Interestingly, the analogous point mutation in GLR-1 AMPA receptors fails to induce excitotoxicity and apoptosis in RIA as well as other neurons that natively express GLR-1. GLR-1 A/T receptors produce a drastic behavioral phenotype in *C. elegans*. Rather than moving forward for significant amounts of time with short backward movements like wildtype worms, GLR-1 A/T transgenic worms have equal forward and backward movements producing a lurching phenotype. Additional studies of the GLR-1 A/T channel have revealed that these receptors function by causing an increase in affinity for glutamate and a decreased desensitization rate of the channel (Kohda et al., 2000; Klein et al., 2004; Taverna et al., 2000; Schwarz et al., 2001). Further investigation into how the GLR-6 A/T mutation changes the kinetics of kainate receptors may provide insight into how the same point mutation AMPA and kainate receptors can produce drastically different outcomes.

What specific differences between AMPA and kainate receptors in *C. elegans* results in kainate receptor induced excitotoxicity but not AMPA receptor induced? AMPA receptor expression in RIA is found at significantly more synapses relative to the expression of kainate receptors. Additionally, GLR-1 AMPA receptors mediate the vast majority of glutamate-induced current within RIA (see Chapter 2). These results suggest that kainate receptors function differently than AMPA receptors, either by inherent channel properties or by accessory protein modulation to allow excitotoxic consequences in the presence of activating mutations.

How do kainate receptors form functional receptors at the synapse, and by what means do they achieve their unique channel kinetics? These questions remain largely unanswered in vertebrates and are completely unknown in the invertebrate iGluR field. The identification of kainate-specific molecules in vertebrates has been hindered by the complexity of the nervous system. By utilizing the simple nervous system of *C. elegans,* the identification of molecules can be more easily achieved. Due to high conservation across species in the field of iGluRs, novel molecules found in *C. elegans* will likely contribute to vertebrate receptor understanding.

The mutation of many genes that do not function specifically with kainate receptors could potentially suppress the RIA morphological defect. The morphological similarities of RIA expressing activated kainate receptors to neurons undergoing apoptotic death suggest that molecules functioning in the cell death pathway could be found as suppressors. However, two independent worm lines were recovered from mutagenesis showing neuronal processes similar to wildtype as well as suppression of the electrophysiological defect. Named *sup1* and *sup2* due to suppression of the phenotype, these mutated genes displayed different levels of suppression. *sup2* showed suppression along the neuronal process but retained the rounded cell body seen in animals expressing dominant kainate receptors. Alternatively, in *sup1* mutants the wild type cell body shape is restored. Both suppressors showed some degree of non-uniform edges along the process not typically seen in to that degree in wildtype RIA neurons. In addition to suppressing the morphological defects in RIA, both

mutants showed suppression of the electrophysiological defect. These secondary results suggest that the mutations are specific to kainate receptors, and eliminate nonspecific molecules such as those involved in the cell death pathway. Such mutants would be expected to suppress the morphological defects but have no effect on the gain-of-function channel kinetics.

The mapping, cloning and characterization of *sup1* and *sup2* may lead to the identification of novel kainate-specific molecules or may provide insight into new roles for previously identified proteins. This work will provide a greater understanding of kainate receptors and their accessory molecules as well as adding insight into the function of kainate iGluRs across species.

Experimental Procedures

General methods and strains

All worms were raised at 20^{o}C under standard conditions unless otherwise indicated (Brenner et al., 1974). Germline transgenic strains were generated by injection of the lin-15 rescuing clone pJM23(40ng/ul) as a transformation marker (Huang et al., 1994). Transgenic lines included the extra chromosomal arrays: akEx164, pCSW44-1(glr-3p::GFP); akEx272, pJG14, pCSW88-2(genomic glr-6A620T)

Electrophysiology

Oocyte expression plasmids included pSN5(glr-3 cDNA), pSN14(glr-6 cDNA), pCSW85(GLR-6A620T), pJG10(GLR-3A619T). Oocyte electrophysiology was conducted as described previously (Strutz-Seebohm et al., 2003). *In vivo* electrophysiology of RIA neurons was performed as described (Brockie et al., 2001) Concanavalin A treatment of neurons was performed by incubating neuron preparation in 10uM ConA for at least 1 minute incubation before agonist application.

Microscopy

Screening of worms was performed by anesthizing worms using 100uM sodium azide. Worms were mounted and imaged using a Nikon Eclipse Ti-E microscope and a Nikon 100x 1.49NA TIRF objective. All images were acquired using Metamorph with a Photometrics Cascade II EMCCD camera and a Yokogawa CSU10 confocal head.

Mutagenesis and Screening

Mutagenesis was performed following standard mutagenesis protocols. L4 worms were exposed to .05M ENU for four hours at room temperature. Twenty-four hours post mutatgenesis, worms were transferred every 6 hours to new plates and allowed to lay eggs. F1 worms were picked clonally and a population of offspring mounted and screened for suppression.

Behavioral assays

Thermotaxis assays were performed as previously described (Mori & Ohshima, 1995) using a temperature gradient of either .8 degrees/cm or .5 degrees/cm. Worms were imaged at .5 frame/second using a digital video camera. Individual worm tracks were analyzed using custom Matlab software (Samuels lab) Osmotic avoidance assays were performed following standard procedure (Hilliard et al., 2002). Thermal nociception assays were performed as outlined (Wittenburg et al., 1999) and chemotaxis to diacytl was performed at a 1:10 dilution and followed standard behavioral protocol found in (Bargmann et al., 1991).

Figure 3.1 Activating mutations in GLR-6 cause neuronal morphological defects in RIA. A)Topology of an individual iGluR subunit with position of A/T indicated. B) Conserved alanine observed in the region near MIII in vertebrate kainate receptors subunits as well as GLR-3 and GLR-6 C) Wildtype morphology of the interneuron RIA imaged by expressing soluble GFP under the RIA specific promoter *glr-3.* D) RIA imaged from transgenic worms expressing GLR-6 A/T co-expressed with soluble GFP.

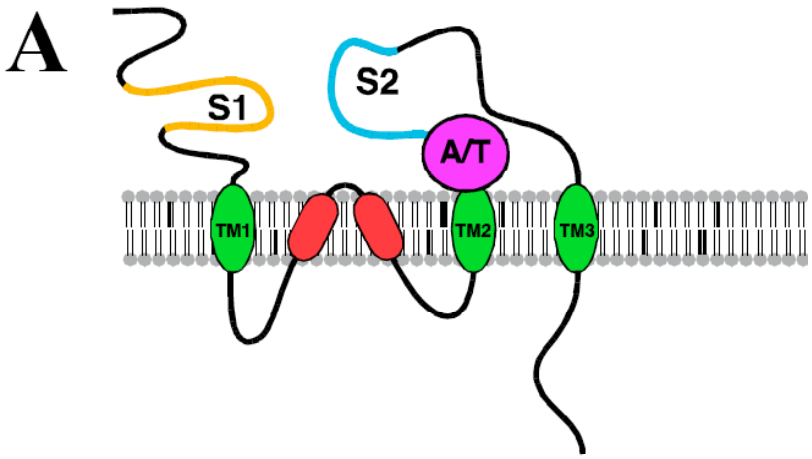
A
S1
S2
A/T
TM1
TM2
TM3

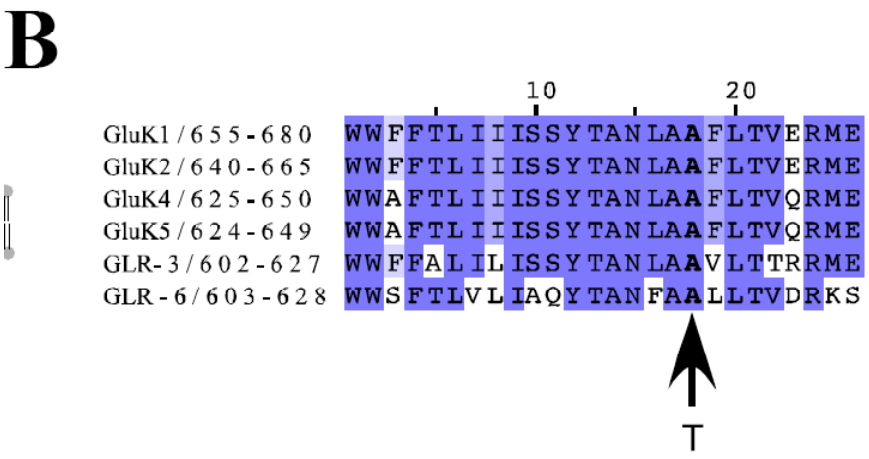
B
10
20
GluK1/655-680 WWFFTLIIISSYTANLAAFLTVERME
GluK2/640-665 WWFFTLIIISSYTANLAAFLTVERME
GluK4/625-650 WWAFTLIIISSYTANLAAFLTVQRME
GluK5/624-649 WWAFTLIIISSYTANLAAFLTVQRME
GLR-3/602-627 WWFFALILISSYTANLAAVLTTRRME
GLR-6/603-628 WWSFTLVLIAQYTANFAALLTVDRKS
T

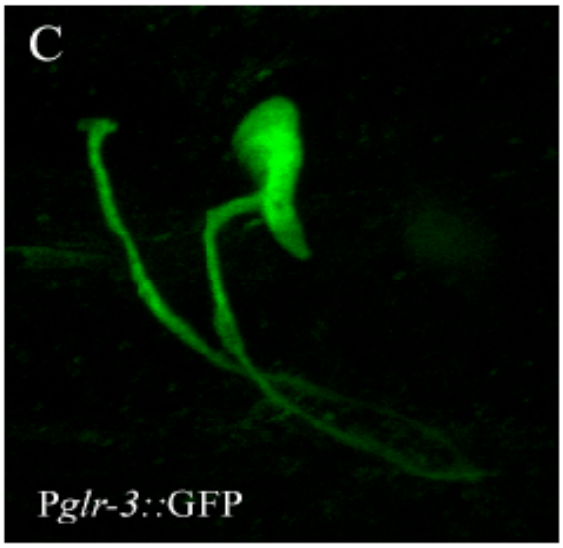
C
Pglr-3::GFP

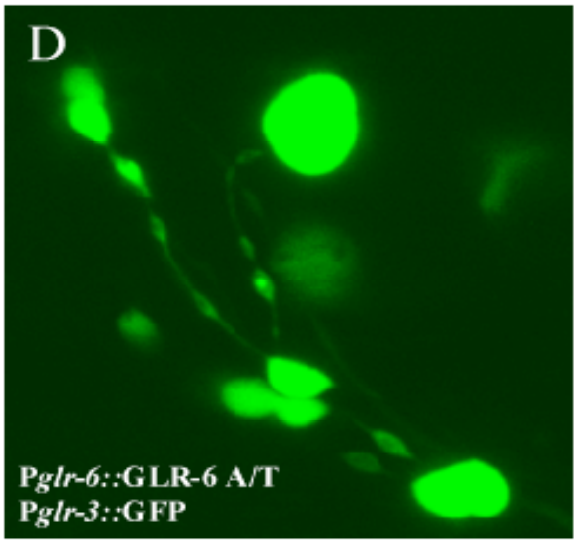
D
Pglr-6::GLR-6 A/T
Pglr-3::GFP

Figure 3.2 Gain of function kainate receptors are defective in thermotactic behavior. A) Behavior of worms expressing either single GLR-6 A/T, GLR-3 A/T or double GLR-6 A/T, GLR-3 A/T receptor subunits during thermotaxis. Behavior represents <7 population assays using 10-15 worms per assay. Error bars represent standard error of the mean. B) Example traces from worms expressing gain of function kainate receptor subunits during thermotaxis. Blue hatch mark indicates starting position; track represents worm movement up the thermal gradient.

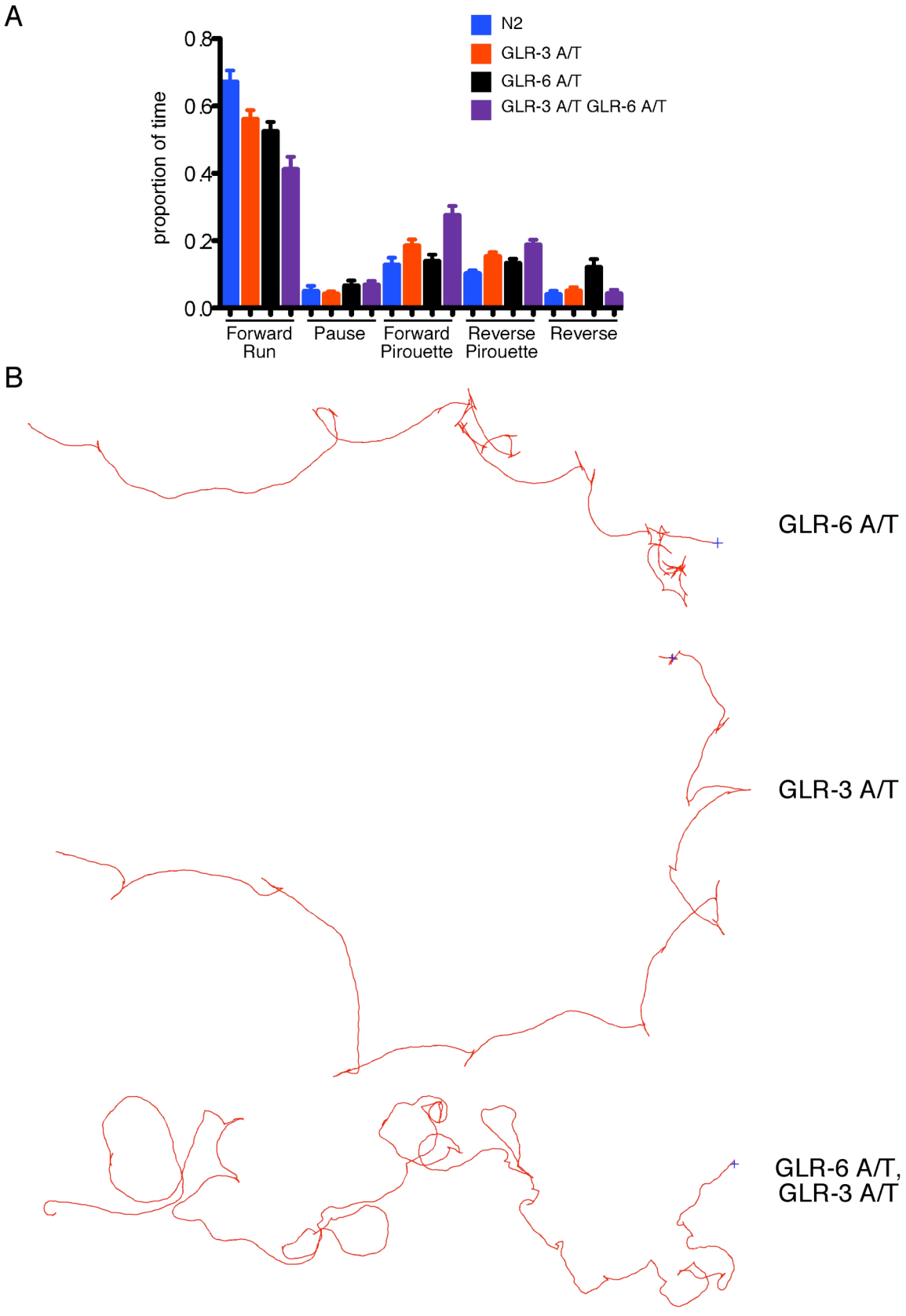
A
N2
GLR-3 A/T
GLR-6 A/T
GLR-3 A/T GLR-6 A/T
proportion of time
0.8
0.6
0.4
0.2
0.0
Forward Run
Pause
Forward Pirouette
Reverse Pirouette
Reverse
B
GLR-6 A/T
GLR-3 A/T
GLR-6 A/T, GLR-3 A/T

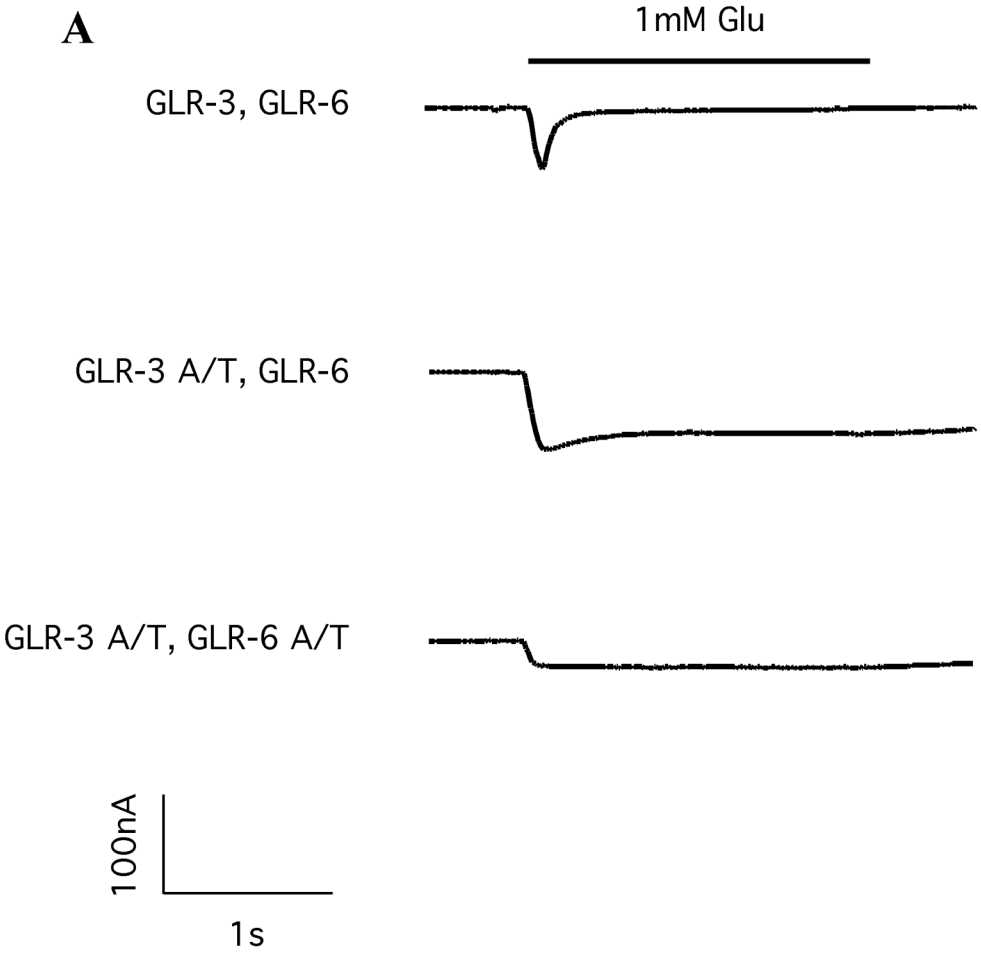

Figure 3.3 Gain of function mutations in kainate receptor subunits alter channel kinetics. A) Recordings from *Xenopus* oocytes containing combinations of activated and wildtype GLR-3 and GLR-6 subunits. Currents were recorded in response to 1 mM glutamate application. Coexpression of GLR-3 A/T and GLR-6 A/T results in a synergistic defect, producing a small, nondesensitizing current.

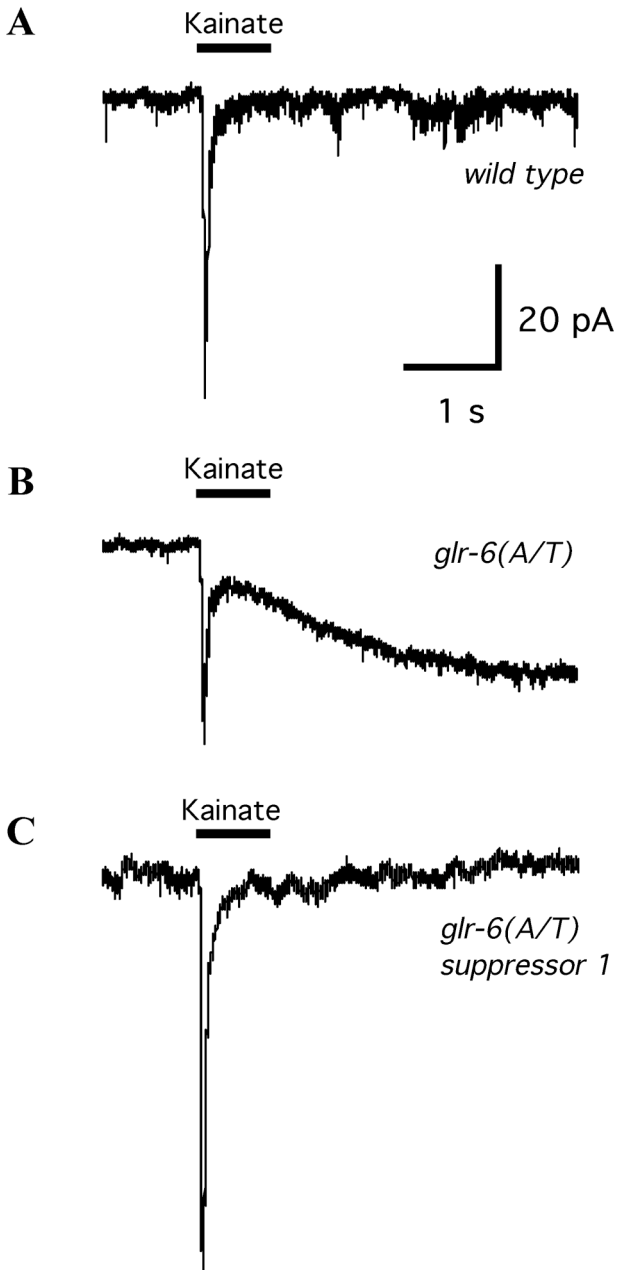

Figure 3.4 *sup1* mutants suppress activated kainate receptor defects.
A) Whole-cell response to 100uM kainate in RIA of wildtype worms.
B) Response to kainate in worms expressing GLR-6 A/T activated receptors.
C) Suppression of GLR-6 A/T electrophysiological defects by *sup1* mutants.
Activated kainate receptors produce a long-lasting, nondesensitizing current that can be suppressed by *sup1*.

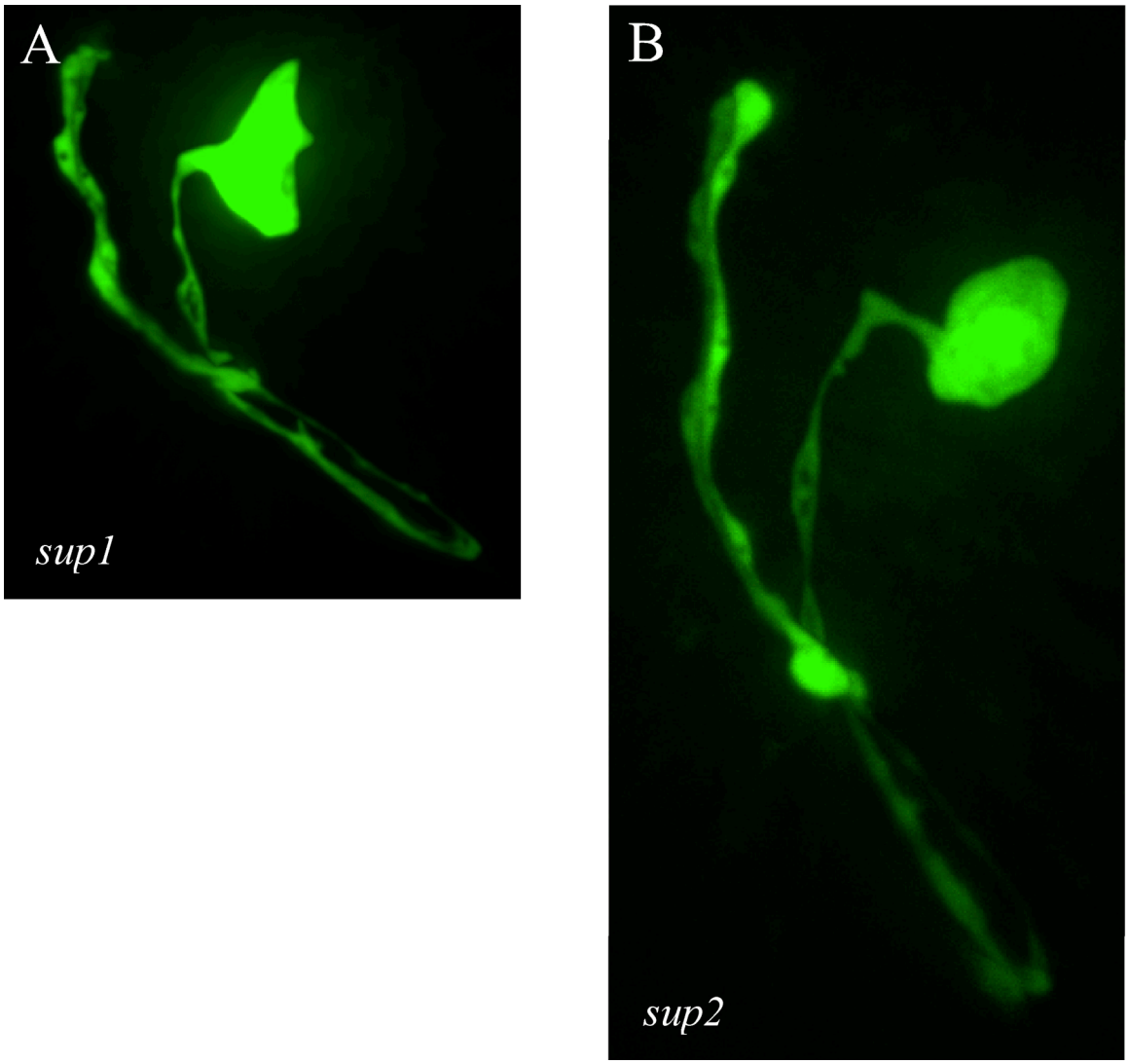

Figure 3.5 *sup1* and *sup2* mutants suppress neuronal morphological defects in RIA. A,B) Confocal images of RIA neuronal processes in two suppressor lines. *sup1* and *sup2* mutants suppress gain-of-function morphological defects to varying degrees.

References

Anderson P. (1995) *Methods Cell Biol* 48, 31–58.

Bargmann, C.I., & Horvitz, H.R. (1991) *Neuron* 7, 729-42.

Brenner, S. (1974) *Genetics* 77, 71-94.

Brockie, P. J., Mellem, J. E., Hills, T., Madsen, D. M. & Maricq, A. V. (2001) *Neuron* 31, 617-30.

Daw, M. I., Chittajallu, R., Bortolotto, Z. A., Dev, K. K., Duprat, F., Henley, J. M., Collingridge, G. L. & Isaac, J. T. (2000) *Neuron* 28, 873-86.

De Stasio, E.A., Dorman S. (2001) *Mutat Res* 495, 81-8.

Dong, H., O'Brien, R. J., Fung, E. T., Lanahan, A. A., Worley, P. F. & Huganir, R. L. (1997) *Nature* 386, 279-84.

Hilliard, M. A., Bargmann, C. I. & Bazzicalupo, P. (2002) *Curr Biol* 12, 730-4.

Huang, L. S., Tzou, P. & Sternberg, P. W. (1994) *Mol Biol Cell* 5, 395-411.

Klein, R. M. & Howe, J. R. (2004) *J Neurosci* 24, 4941-51.

Kohda, K., Wang, Y. & Yuzaki, M. (2000) *Nat Neurosci* 3, 315-22.

Lipsky, R. H. & Goldman, D. (2003) *Ann N Y Acad Sci* 1003, 22-35.

Kim, K.S., Straub, C., Burlingame, A.L., Hower, R.J., & Tomita, S. (2009) *Neuron* 61, 385-396.

Manev, H., Favaron, M., Guidotti, A., & Costa, E. (1989) *Mol Pharm* 36, 106-112.

Maricq, A. V. & Hollmann, M. (2003) *J Biol Chem* 278, 44691-701.

Montastruc, J.L., Rascol, O., & Senard, J.M. (1997) *Neurosci Biobehav Rev* 21, 477-80.

Mori, I. & Ohshima, Y. (1995) *Nature* 376, 344-8.

Osten, P., Khatri, L., Perez, J. L., Kohr, G., Giese, G., Daly, C., Schulz, T. W., Wensky, A., Lee, L. M. & Ziff, E. B. (2000) *Neuron* 27, 313-25.

Puchalski, R. B., Louis, J. C., Brose, N., Traynelis, S. F., Egebjerg, J.,

Kukekov,V., Wenthold, R. J., Rogers, S. W., Lin, F., Moran, T. & et al. (1994) *Neuron* 13, 13-47.

Scannevin, R. H. & Huganir, R. L. (2000) *Nat Rev Neurosci* 1, 133-41.

Schwarz, M. K., Pawlak, V., Osten, P., Mack, V., Seeburg, P. H. & Kohr, G. (2001) *Eur J Neurosci* 14, 861-8.

Strutz-Seebohm, N., Werner, M., Madsen, D. M., Seebohm, G., Zheng, Y., C.S. Walker, A.V. Maricq & M. Hollmann. (2003) *J Biol Chem* 278, 44691-701.

Taverna, F., Xiong, Z. G., Brandes, L., Roder, J. C., Salter, M. W. & MacDonald, J. F. (2000) *J Biol Chem* 275, 8475-9.

Ulas, J., Weihmuller, F.B., Brunner, L.C., Joyce, J.N., Marshall, J.F., & Cotman, C.W. (1994) *J Neurosci* 14, 6317-24.

Walker, C. S., Maricq, A.V., & Hollmann, M. (2003) *J Biol Chem* 278:44691-701.

Wittenburg, N., & Baumeister, R. (1999) *Proc Natl Sci Acad USA* 96, 10477-10482.

Zhang, W., St-Gelais, F., Grabner, C.P., Trinidad, J.C., Sumioka, A., Morimoto-Tomita, M., Kim, K.S., Straub, C., Burlingame, A.L., Howe, J.R. & Tomita, S. (2009) *Neuron* 61:385-396.

Zheng, Y., Brockie, P. J., Mellem, J. E., Madsen, D. M. & Maricq, A. V. (1999) *Neuron* 24, 347-61.

Zuo, J., De Jager, P. L., Takahashi, K. A., Jiang, W., Linden, D. J. & Heintz, N. (1997) *Nature* 388, 769-73.

CHAPTER 4

SUMMARY AND CONCLUSIONS

Introduction

A fundamental problem in the field of neuroscience is to unravel how sensory experience is translated into behavior. To truly understand how this occurs, an understanding of the molecules, cells and circuits that direct behavior must be achieved. Additionally, understanding how these components work together from the level of individual molecules up to the behavioral output is essential. The complexity of the vertebrate nervous system highlights the difficulties in achieving this kind of understanding. However, studies using model systems have shown that the function of nervous system is conserved across evolution, greatly developing our understanding of behavior and the nervous system. From these studies, it became clear that excitatory neurotransmission within the central nervous system functions through the use of ionotropic glutamate receptors (iGluRs). iGluRs are widely expressed throughout the central nervous system and play important roles in learning and memory (Chen and Tonegawa, 1997). Additionally, the disruption of iGluR function results in a wide range of pathological conditions such as stroke and epilepsy (Meldrum., 1994; Mody, 1998). The properties of iGluR channel function have been

studied through both heterologous expression systems as well as *in vivo* electrophysiology work in mice and insects; however, the neuronal complexity and lack of powerful genetic techniques in these organisms has hindered understanding iGluR function and at the level of behavior.

Here we have taken advantage of the simple nervous system of *C. elegans* to use a systems approach in understanding iGluR function in gradient taxis. In this work we have: 1) Characterized GLR-3, GLR-6 channels as functional kainate type receptors, 2) Determined the functional and behavioral roles of *C. elegans* kainate receptor subunits as well as the distinct differences between AMPA and kainate type receptors, and 3) Identified a strategy allowing for the isolation of kainate receptor accessory proteins using gain-of-function receptor subunits.

Navigating thermal and chemical gradients in *C. elegans* remain as some of the most interesting behaviors in the worm. Thermotaxis is a critical behavior for all cold-blooded animals. This behavior allows them to move relative to a temperature source to maintain a favorable internal temperature. Thermotaxis behavior in *C. elegans* is interesting in that worms can learn and remember the cultivation temperature and track back to that temperature when place on a thermal gradient. The thermotactic circuit was identified as a pair of sensory neurons, AFD and AWC, a pair of interneurons, AIZ and AIY, and a third level interneuron pair, RIA, responsible for integrating and directing output for the circuit (Mori and Ohshima, 1995, Clark et al., 2006; Biron et al., 2008; Kuhara et al., 2008). Of the five known cells required for this circuit, RIA remains the key

neuron for integrating all incoming thermal information and determining which direction will lead to the previous cultivation temperature. *eat-4* expression has indicated that three of the four remaining neurons (AFD, AWC and AIZ) in the circuit use glutamate as a neurotransmitter (Noriyuki et al., 2011). These results suggest that glutamate signaling is essential for the proper function of the thermotaxis circuit, and that RIA must express glutamate receptors to receive glutamatergic signaling.

Chemotaxis to different chemicals also functions as a key behavior in animal survival. Navigating gradients enables the worm to avoid toxic substances or locate food sources, making it critical that it be performed efficiently. Worm behavior allows for the discrimination and chemotaxis to a wide variety of stimuli. One of these, attractive navigation to the volatile odorant diacetyl, is mediated specifically by the chemosensory neuron AWA (Bargmann et al., 1993). Downstream signaling from AWA occurs among other neurons, through the interneurons AIY and AIZ, where the signal then converges onto RIA. While the neurotransmitter required for AWA signaling is unknown, these inner layers of circuitry are conserved between the thermotaxis and chemotaxis pathways, supporting the idea that interneuron signaling in chemotaxis may also require glutamatergic signaling to function properly.

GLR-3, GLR-6 Channels Function as Kainate Type Receptors

To understand the role of iGluRs in RIA, we looked at the reported expression patterns of glutamate receptor subunits in the worm (Brockie et al.,

2001a). Two receptor subunits, GLR-3 and GLR-6, were reported to show exclusive expression with the interneuron RIA. This unique expression pattern suggested the formation of a heteromeric receptor made up of GLR-3 and GLR-6 subunits. Expressing GLR-3 and GLR-6 cRNAinto *Xenopus* oocytes, we showed the formation of a functional heteromeric receptor. Additionally, we characterized the channel as one similar to vertebrate kainate receptors based on kainate sensitivity, ConA channel modification, and lack of requirement for accessory proteins for function. These results indicated very different channel function from *C. elegans* GLR-1 AMPA receptors that show less sensitivity to kainate as well as a small ConA effect. Most striking is the absolute requirement of GLR-1 receptors for accessory proteins SOL-1 and STG-1, clearly placing GLR-3, GLR-6 receptors in a different receptor class than GLR-1. *In vivo* recordings of GLR-3, GLR-6 receptors in RIA also indicated a channel activated to a high degree by kainate that is modifiable by ConA, as well as identifying the expression of GLR-1 AMPA receptors within RIA. Interestingly, we show here that GLR-1 receptors mediate the vast majority of the glutamate gated current in RIA relative to the small current contributed by GLR-3, GLR-6 receptors. This work represents the first reconstitution of an invertebrate kainate receptor in a heterologous system as well as the first characterization of an invertebrate kainate channel.

GLR-1 AMPA and GLR-3, GLR-6 Kainate Receptors in RIA are Functionally Different

To further characterize the function of GLR-1 AMPA and GLR-3, GLR-6 kainate receptors in RIA, we looked at the distribution of receptors within the neuronal process. For the first time reported, we looked at the distribution of AMPA and kainate receptors within a single neuronal process. Interestingly, the localization of tagged subunits shows very little overlap between AMPA and kainate subunits, suggesting the two receptor classes are expressed at separate synapses. In addition to the kinetic differences discussed previously, separate localization between receptor types suggests unique roles for each receptor type. The limited expression of iGluRs within RIA and their localization to distinct sites along the process suggested that we might be able to identify the sites of input into individual synapses. The reconstruction of the nervous system by White et al. has identified the sites of synaptic input into RIA. Two neurons within the thermotactic circuit use glutamate as a neurotransmitter as well as provide input directly to RIA. AWC provides input to only two synapses near the cell body of RIA while AIZ expresses significantly more inputs along the process down into the hairpin loop. Here we show that synaptic input from AIZ signals primarily through the limited number of GLR-3, GLR-6 containing synapses. Despite the significantly higher number of synapses containing GLR-1 in RIA, no expression was seen in split-GFP expression studies between AIZ and GLR-1 subunits. These results suggest the specific signaling to either kainate or AMPA receptors may mediate specific behaviors.

To study the role of kainate and AMPA receptors in thermotactic and chemotactic behavior, we used genetic deletions of *glr-1, glr-3* and *glr-6.* Both AMPA and kainate receptor mutants were capable of performing cryophilic thermotaxis in a manner similar to wildtype. Conversely, when thermotaxis toward warm temperatures was performed, kainate receptor single and double mutants were unable to properly execute the behavior. Interestingly, *glr-1* mutant worms appeared to show no defects in warm thermotaxis. Insight into *C. elegans* thermotactic behavior has shown that worm behavior is affected by the steepness of the temperature gradient (Ramot et al., 2008). We took advantage of a relaxed gradient to further examine the thermotactic behaviors of *glr-1* and *glr-3, glr-6* mutants. Here we show that *glr-3, glr-6* mutants are competent to sense and migrate up a temperature gradient. However, kainate receptor mutants show defects in the mode of travel as they migrate up the gradient. Increased long reversals and fewer short reversals severely impair the efficiency and proper navigation up both thermal and chemical gradients. Alternatively, *glr-1* mutants show more subtle movement defects when traveling up gradients. Further analysis of movement tracks during thermotaxis and chemotaxis showed similarities between the two taxis behaviors. As predicted, *glr-1* mutants exhibited decreased reversals; however, they did show increased movement in improper directions in both types of gradient behavior. Rescue of *glr-1* in command interneurons, but not within RIA itself showed wildtype levels of both long and short reversals. Interestingly, *glr-1* mutants show a much less severe phenotype compared to *glr-3, glr-6* mutants despite a much higher expression

level, as well as contributing the majority of the glutamate-gated current in RIA. These results suggest that GLR-1 receptors function in a different facet than kainate receptors in RIA.

Activated Kainate Receptors in the Interneuron RIA

In order to understand how kainate receptors function within RIA, we took advantage of a previously discovered gain of function mutant (Zuo et al.,1997). Expression of gain of function glutamate receptors, despite the type of mutated subunit, leads to severe behavioral defects in the affected animals. These mutations are thought to lead to constitutively leaky or over active receptors. The analogous mutation when placed into *C. elegans* kainate subunits also leads to behavioral defects, however in an unprecedented manner, also leads to a neuronal phenotype reminiscent of apoptotic death. What differences exist within kainate receptors that allow for this type of defect to occur? A direct comparison to *C. elegans* gain of function AMPA receptor GLR-1 A/T in the same neuron, RIA, shows no indication of morphological defects. As a highly conserved group of subunits, kainate receptor subunits have been evolutionarily conserved within *C. elegans* to a single neuron. Clearly distinctive kinetics and functional properties separate these subunits from those of other subtypes. Utilizing activated gain of function mutations for the purposes of forward genetic screens provides a powerful tool for selectively isolating kainate-specific molecules. However, further research and insight into the nature of the gain of function mutation and what differences facilitate such drastic functional properties

between AMPA and kainate receptors will provide valuable information in the field of iGluRs. The elusive role of kainate receptors in vertebrates can be bridged through further study of receptor mutations such as the GLR-6 and GLR-3 A/T receptor subunits.

Concluding Remarks

This work represents the first characterization of kainate receptors in invertebrates and identifies a role in fine-tuned behavioral responses. This previously unknown role for kainate receptors will provide insight into novel roles for vertebrate kainate receptors. Furthermore, the identification of novel kainate-specific molecules through the study of gain of function receptors described here could lead to the discovery of molecules important in the synthesis, trafficking, insertion or function of kainate iGluRs. The highly localized expression of GLR-3 and GLR-6 receptors to a single cell highlights the evolutionary importance of these two subunits and kainate receptors. Further study and insight into the molecular mechanisms used by these receptors to modify behavior will provide valuable information as to the elusive role of kainate receptors in vertebrates. The expression of AMPA receptors within the same cell provides a unique opportunity to directly compare the function of AMPA and kainate receptors. Understanding the localization, channel properties, and roles in behavior of two separate types of receptors within a single cell helps get us enticingly closer to fully understand how molecules, cells and circuits function together to achieve behavior.

References

Biron, D., Wasserman, S., Thomas, J., Samuel, A., Sengupta, P. (2008) *Proc Natl Acad Sci* 105,11002-11007.

Brockie, P. J., Mellem, J. E., Hills, T., Madsen, D. M. & Maricq, A. V. (2001) *Neuron* 31, 617-30.

Chen, C., & Tonegawa, S. (1997) *Annu Rev Neurosci* 20, 157-84.

Clark, D., Biron, D., Sengupta, P., Samuel A. (2006) *J Neurophysiol* 97, 1903-1910.

Kuhara, A., Okumura, M., Kimata, T., Tanizawa, Y., Takano, R., Kimura, K. Inada, H., Matsumoto, K. Mori, I. (2008) *Science* 320, 803-807.

Meldrum, B.S. (1994) *Neurology* 44, S14-23.

Mody, I. (1998) *Int Rev Neurobiol* 42, 199-226.

Mori, I. & Ohshima, Y. (1995) *Nature* 376, 344-8.

Noriyuki, O., Atsushi, K., Fumiya, N., Yoshifumi, O., & Mori, I. (2011) *EMBO J* 10.1038.

Ramot, D., Macinnis, B.L., Lee, H.C., Goodman, M.B. (2008) *J Neurosci* 28, 12546-57.

White, J. G., Southgate, E., Thomson, J. N. & Brenner, S. (1986) *Phil Trans R Soc Lond* B 314, 1-340.

Zuo, J., De Jager, P. L., Takahashi, K. A., Jiang, W., Linden, D. J. & Heintz, N. (1997) *Nature* 388, 769-73.

APPENDIX A

AWC SIGNALING THROUGH KAINATE RECEPTORS

Summary and Results

As one of contributing neurons to the thermotaxis circuit with a known expression profile including *eat-4*, we looked at AWC as a possible connection to RIA. Interestingly, AWC connects to only one of the two RIA neurons. Additionally only two synaptic contacts are made, located adjacent to one another in the process immediately coming out of the cell body (Figure A.1A) (White et al., 1986). To evaluate the localization of GLR-6 with respect to presynaptic sites in AWC, we coexpressed mCherry::GLR-6 and the presynaptic protein RAB-3::GFP in AWC. One RAB-3 puncta was seen reproducibility nearly colocalizing with GLR-6 in the region of predicted AWC input (Figure A.1B) To further verify the signaling of AWC through synapses containing kainate receptors, we took advantage of a split-GFP genetic technique (Feinberg et al., 2008). A typical synapse in the CNS is separated by less than 100nm of extra cellular space between the presynaptic and postsynaptic membranes. Transmembrane proteins expressed by the two cells can span the distance between the membranes. By splitting the GFP molecule and directly linking each

half to transmembrane proteins, one on each of the pre- and postsynaptic cells, GFP fluorescence can be reconstituted if the two fragments come in close proximity to one another. The transmembrane protein neuroligin (NLG-1) is located at synapses both presynaptically and postsynaptically in *C. elegans.* We expressed RIA::NLG-1and AWC::NLG-1 proteins tagged with complementary fragments of GFP in transgenic worms coexpressing full length GLR-6::mCherry. Reconstitution of GFP identified the two synapses formed between AWC and RIA in the expected location. Similar to imaging RAB-3, one of the two GFP puncta from reconstituted GFP was found to be colocalized with GFR-6 puncta (Figure A.1C,D), further supporting the idea that a portion of AWC signaling to RIA uses kainate receptors. AWC signaling to RIA through synapses containing kainate receptors addresses only one GLR-6 puncta found throughout the process. This severely limited input provides potential problems with revealing the underlying function of a single synapse. In an attempt to find other input signals into the remaining GLR-6 synapses, we looked at the other thermotactic neuron, AIZ. Increased synaptic input from AIZ led us to pursue the behavior regulated from AIZ rather than AWC. However, the synaptic connection between RIA and AWC through kainate receptors remains a possible pathway for continuing to unravel the circuitry and behavioral computations of RIA.

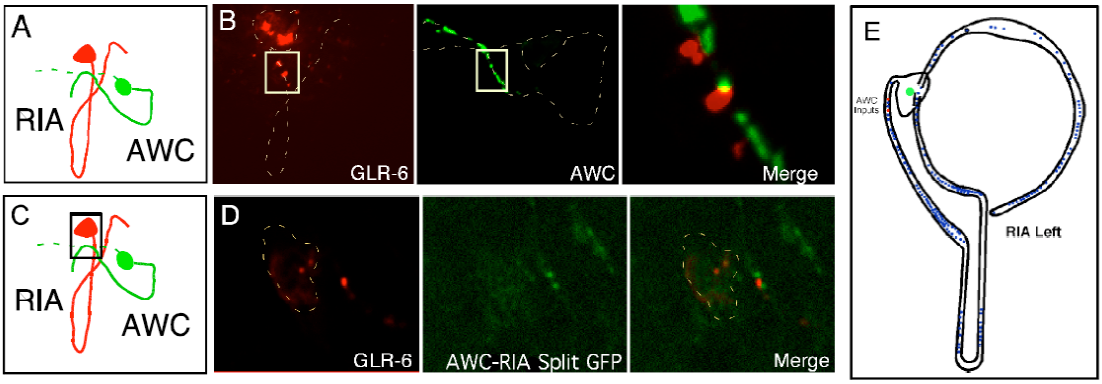

Figure A.1 AWC synapses through kainate receptors in RIA. A) Figure displaying the relationship between RIA and AWC neurons. B) Full length GLR-6::mCherry coexpressed with AWC::RAB-3; merged box shows zoomed in view of signal overlap. C) Cartoon indicating zoomed area of the process immediately exiting the cell body. D) Full length GLR-6::mCherry co-expressed with RIA::NLG-1 and AWC::NLG-1, each tagged with complimentary pieces of split gfp. E) Figure representing predicted AWC inputs into RIA by White et al., 1986. Red dots indicate AWC input; blue dots represent other inputs and outputs.

References

Feinberg, E.H., Vanhoven, M.K., Bendesky, A., Wang, G., Fetter, R.D., Shen, S., & Bargmann, C.I. (2008) *Neuron* 57, 353-363.

White, J. G., Southgate, E., Thomson, J. N. & Brenner, S. (1986) *Phil Trans R Soc Lond* B 314, 1-340.

APPENDIX B

GLUTAMATE RECEPTOR EXPRESSION IN THE INTERNEURON RIA

Summary and Results

To understand the role of iGluRs within the interneuron RIA, we expressed full-length fusion proteins expressing either GFP or mCherry labels (see Chapter 2). Surprisingly, we found very limited puncta from both the expression of GLR-3 and GLR-6 subunits. This limited expression appears to be reproducible and fairly stereotypical, with puncta dispersed from the cell body, down through the hairpin loop and a few extending out into the far distal regions. In contrast, GLR-1 receptors are found much more abundantly throughout the entire process. GLR-1 expression also appears to be reproducible; however, the higher overall signal makes the puncta less defined. RIA input is also predicted to differ between the right and left neurons (White et al., 1986). Thus we would predict that the synapse locations and their components would differ between the two neurons. The axonal morphology of RIA provides challenges when orientating and imaging the axonal process, making it difficult to directly look at precise puncta position relative to other animals in a quantifiable fashion. However, consistent imaging of the animals in the same orientation (rolled onto their side)

allows for a consistent, qualitative pattern to be seen. Here, we show a panel of RIA neurons expressing different receptors to illustrate the differences in expression levels and patterns.

GLR-6

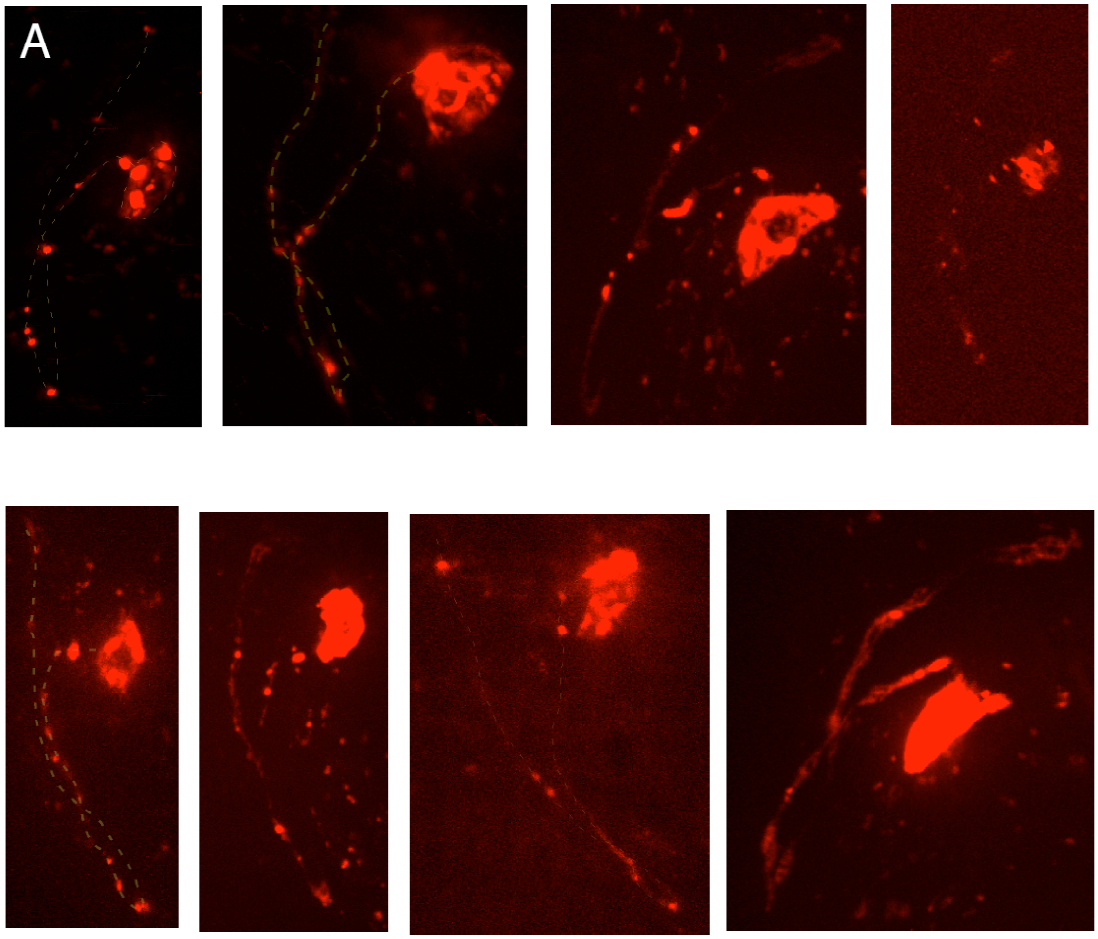

Figure B.1 GLR-6 expression in RIA. Representative images of full length glr-6::mcherry::GLR-6. Multipe images of individual worms expressing full length GLR-6 in RIA; dotted outlines have been added to clarify some processes.

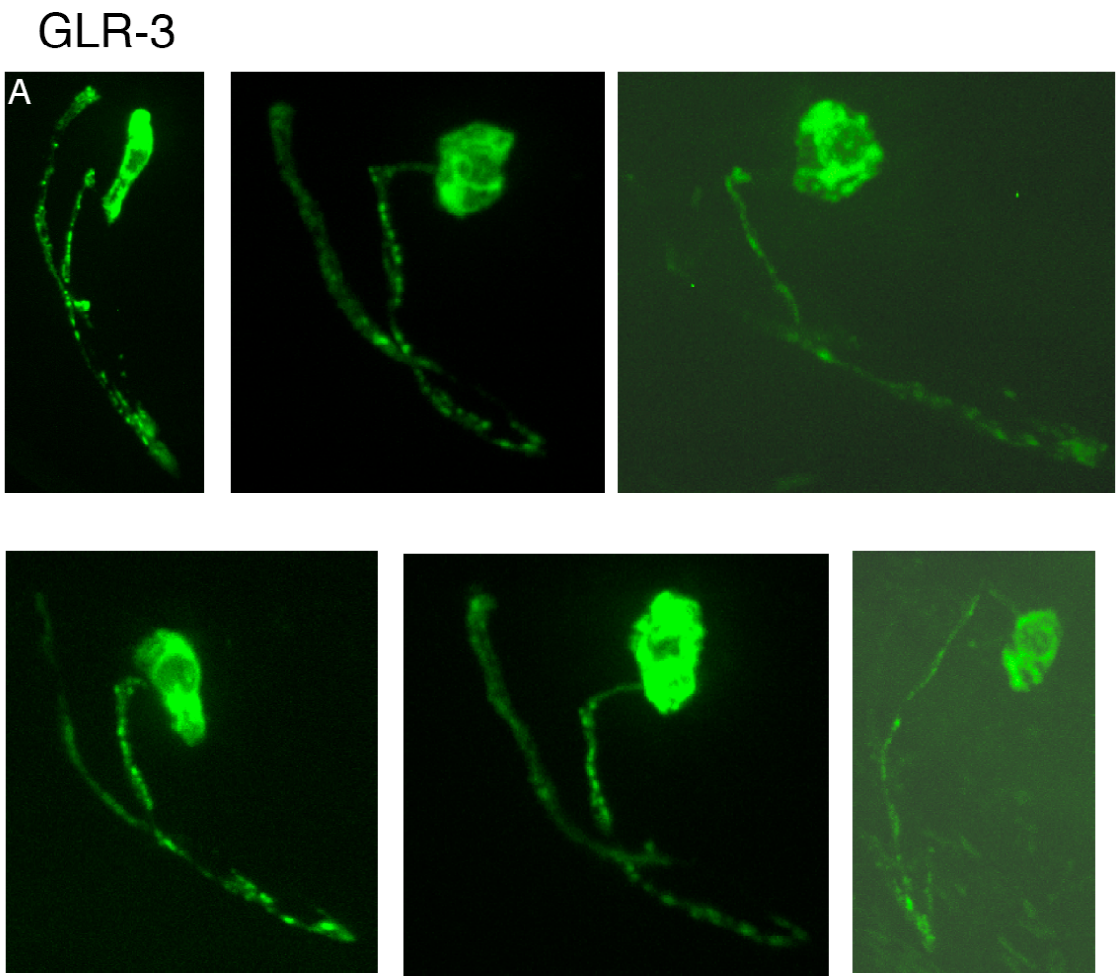

Figure B.2 GLR-3 expression in RIA. Representative images of full length Pglr-3::GFP::GLR-3. Multiple images of individual worms expressing full length GLR-3 in RIA.

GLR-1

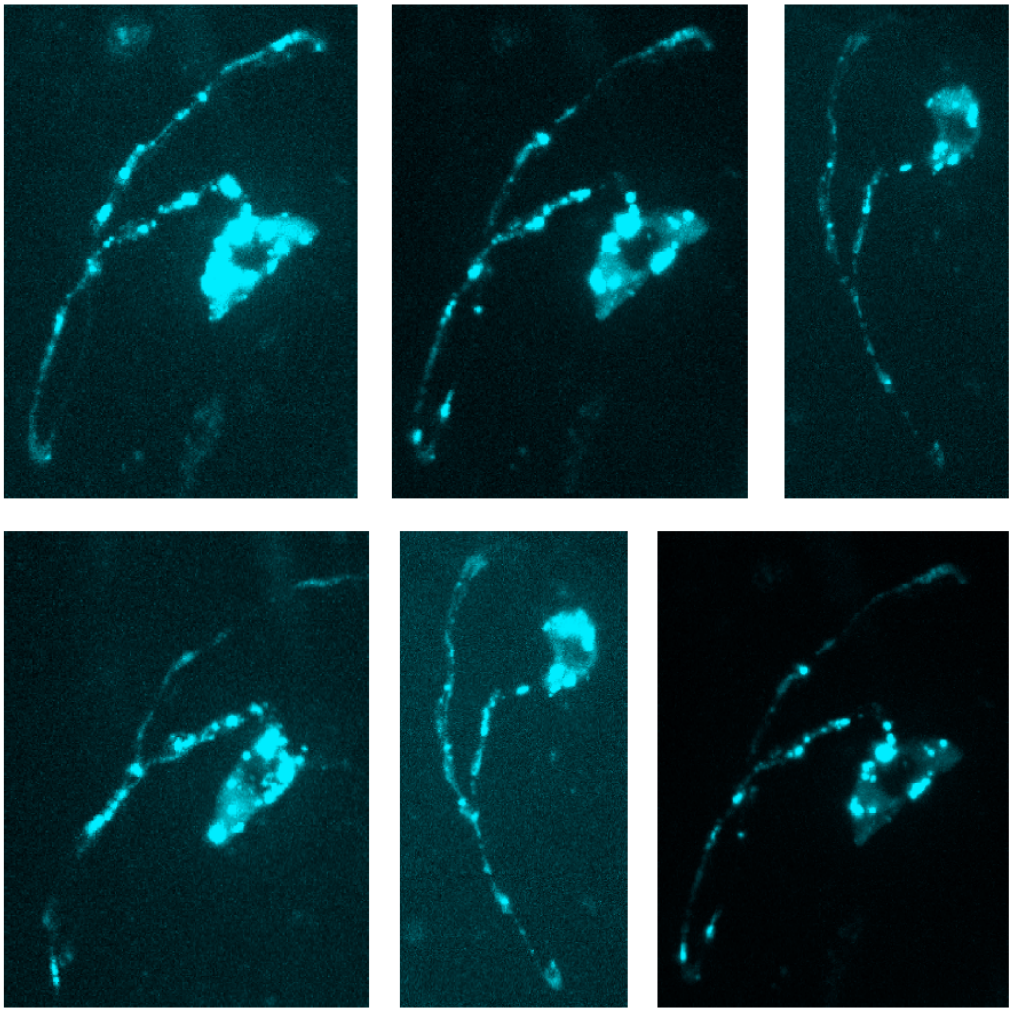

Figure B.3 GLR-1 expression in RIA. Representative images of full length Pglr-3::teal::GLR-1. Multiple images of individual worms expressing full length GLR-1 in RIA.

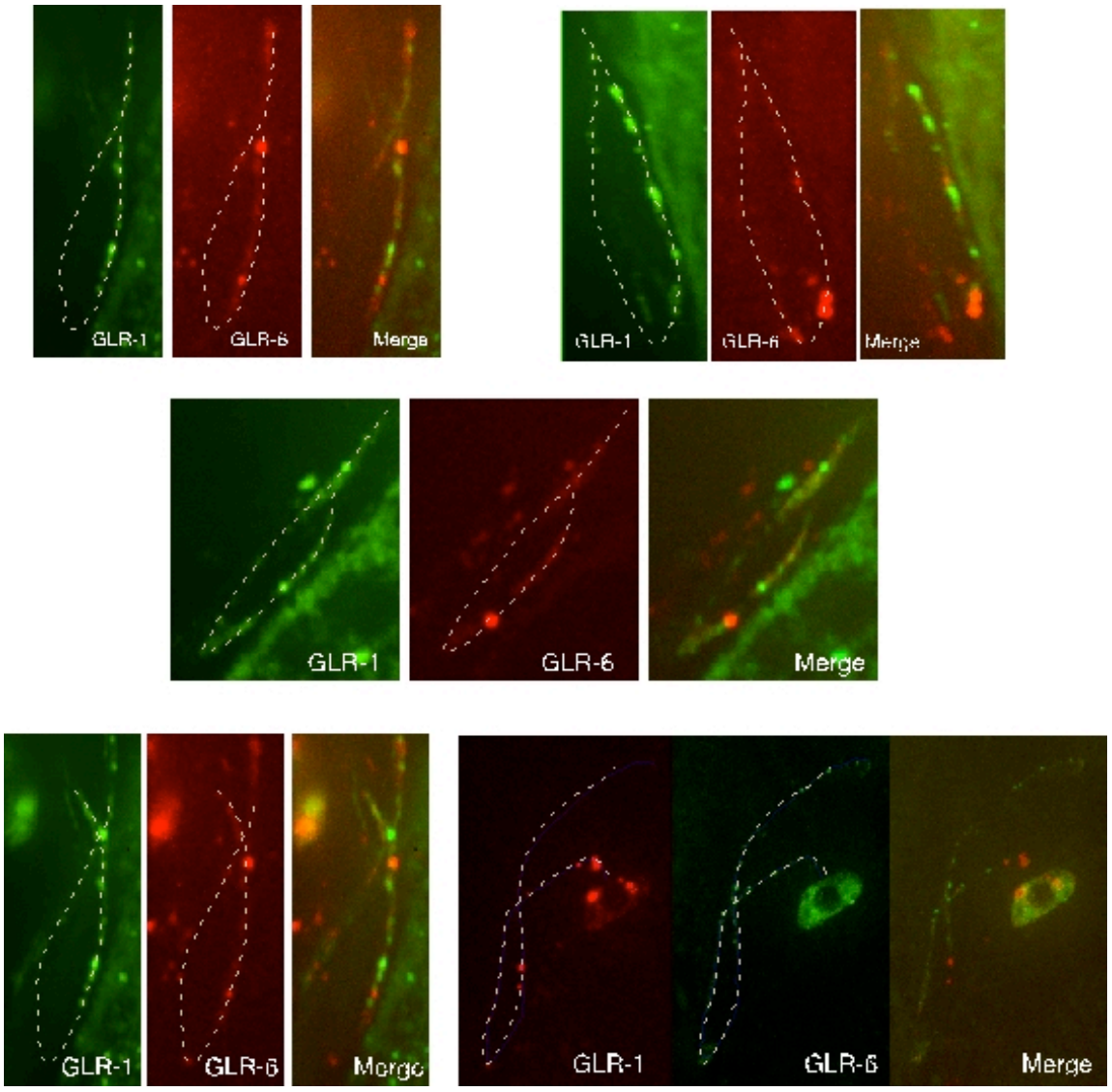

Figure B.4 Coexpression of GLR-6 and GLR-1 in RIA. Representative images of GLR-1 and GLR-6 Puncta in RIA. Images of transgenic lines coexpressing full length GLR-1::GFP and GLR-6::mCherry. Images are of the hairpin region of RIA with the exception of bottom right panel, which shows the full RIA process.

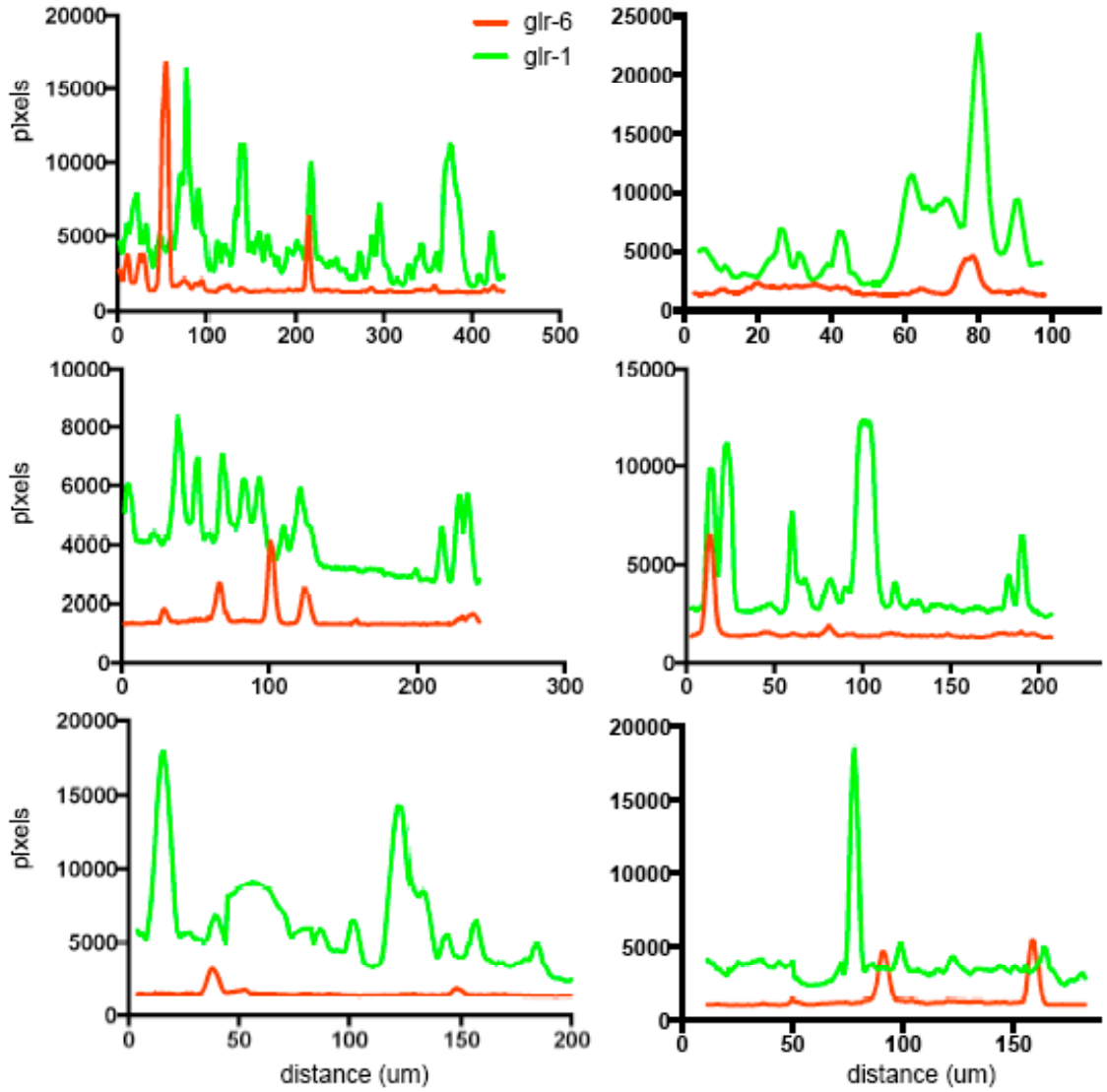

Figure B.5 Analysis of GLR-1 and GLR-6 localization and expression
Representative graphs of line scan analysis from transgenic worms co-expressing GLR-1 and GLR-6 in RIA. Green traces represent GLR-1 puncta, red traces represent GLR-6 puncta. Graphs show pixel intensity over time. Individual line scans taken from the hairpin region of RIA. Lengths vary between animals due to age, size and orientation. GLR-1 GFP expression shows consistently higher expression than GLR-6. Nonoverlapping peaks between the two signals are evident as well as areas of possible colocalization.

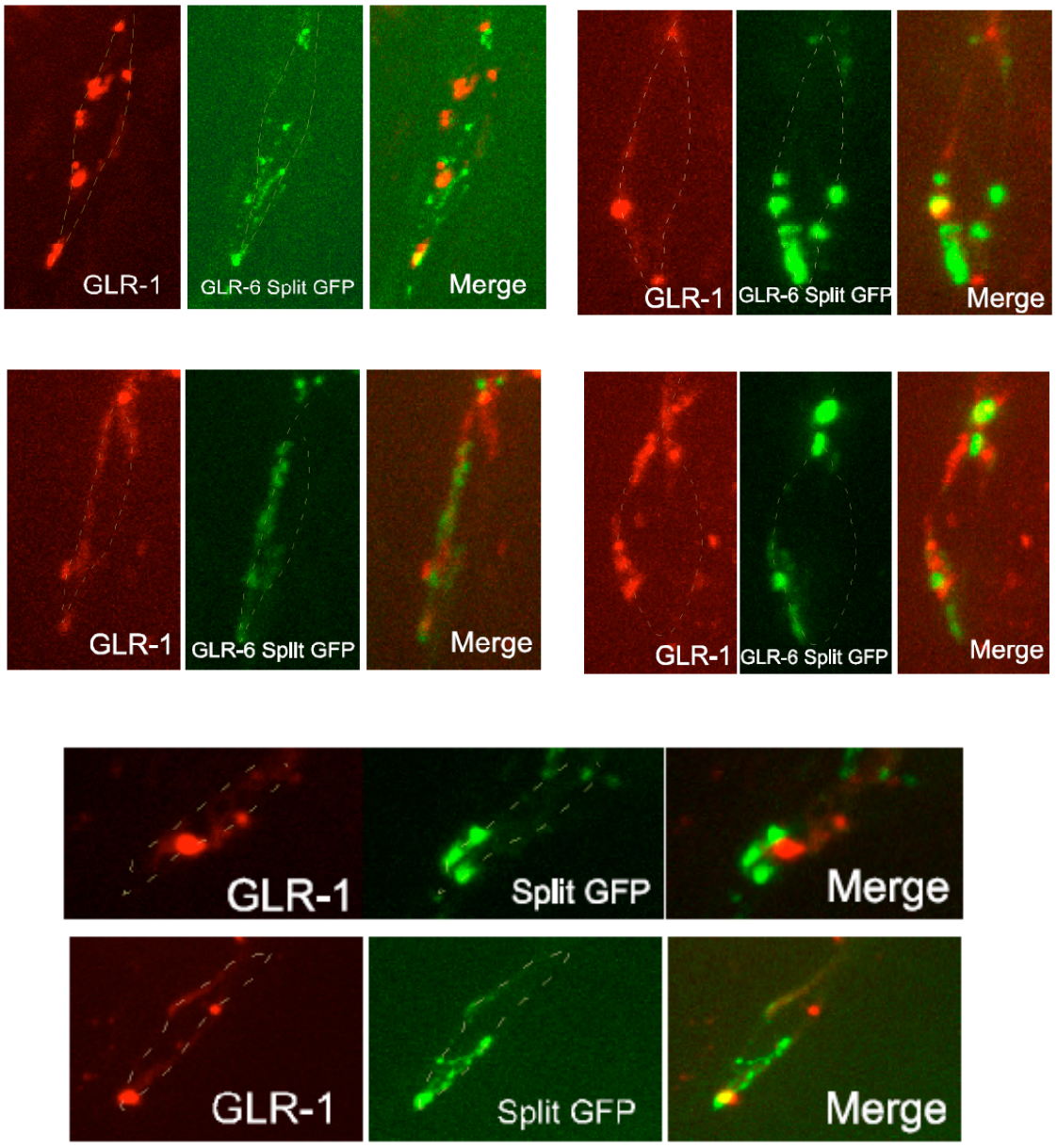

Figure B.6 Split GFP puncta between AIZ and GLR-6 subunits. Representative images from transgenic strains expressing split GFP between AIZ and GLR-6 subunits, coexpressed withfull length GLR-1::mCherry. Puncta in hairpin region of RIA shown where expected AIZ inputs are made into RIA.

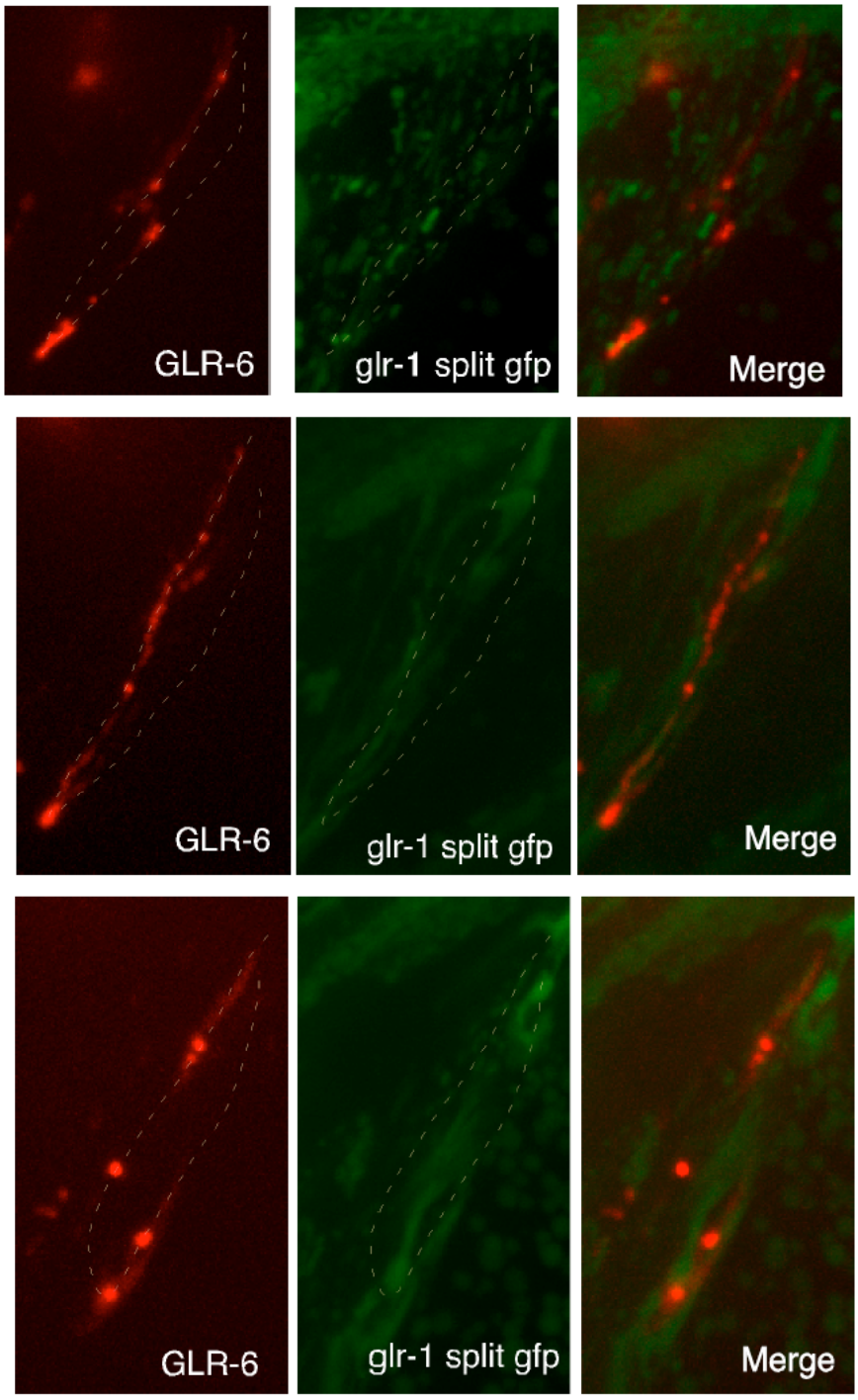

Figure B.7 Split GFP expression between GLR-1 subunits and AIZ. A) Representative image showing the lack of GFP expression seen between GLR-1 subunits and AIZ using a spit-GFP approach. Animals co-express full length GLR-6::mCherry. Images show hairpin region of RIA. N=<45 independent lines examined for gfp reconstitution between AIZ and GLR-1 receptors.

References

White, J. G., Southgate, E., Thomson, J. N. & Brenner, S. (1986) *Phil Trans R Soc Lond* B 314, 1-340.